Atmospheric Greenhouse Gas Measurements

Automn School – 3/11/2022

Jean-Daniel Paris – jdparis@lsce.ipsl.fr

Atmospheric GHG measurement

- Why measuring atmospheric GHG composition?
- Stable isotopes
- Ppm vs umolmol-1
- GC/MS
- Optical methods: NDIR, CRDS
- calibration and the WMO scale
- 14C
- Mobile measurements
- Ground base remote sensing

Atmospheric GHG measurement

- Why measuring atmospheric GHG composition?
- Stable isotopes
- Ppm vs umolmol-1
- GC/MS
- Optical methods: NDIR, CRDS
- calibration and the WMO scale
- 14C
- Mobile measurements
- Ground base remote sensing

Svante Arrhenius

Doubling of CO2 = +5°C global T
Arrhenius, 1896

LONDON, EDINBURGH, AND DUBLIN
PHILOSOPHICAL MAGAZINE
AND
JOURNAL OF SCIENCE.

[FIFTH SERIES.]

APRIL 1896.

XXXI. *On the Influence of Carbonic Acid in the Air upon the Temperature of the Ground.* *By* Prof. SVANTE ARRHENIUS *.

I. *Introduction : Observations of* Langley *on Atmospherical Absorption.*

A GREAT deal has been written on the influence of the absorption of the atmosphere upon the climate. Tyndall † in particular has pointed out the enormous importance of this question. To him it was chiefly the diurnal and annual variations of the temperature that were lessened by this circumstance. Another side of the question, that has long attracted the attention of physicists, is this : Is the mean temperature of the ground in any way influenced by the presence of heat-absorbing gases in the atmosphere? Fourier‡ maintained that the atmosphere acts like the glass of a hot-house, because it lets through the light rays of the sun but retains the dark rays from the ground. This idea was elaborated by Pouillet § ; and Langley was by some of his researches led to the view, that "the temperature of the earth under direct sunshine, even though our atmosphere were present as now, would probably fall to −200° C., if that atmosphere did not possess the quality of selective

* Extract from a paper presented to the Royal Swedish Academy of Sciences, 11th December, 1895. Communicated by the Author.
† 'Heat a Mode of Motion,' 2nd ed. p. 405 (Lond., 1865).
‡ *Mém. de l'Ac. R. d. Sci. de l'Inst. de France*, t. vii. 1827.
§ *Comptes rendus*, t. vii. p. 41 (1838).

Are there meaningful variations in atmospheric CO_2?

harles Keeling and CO_2

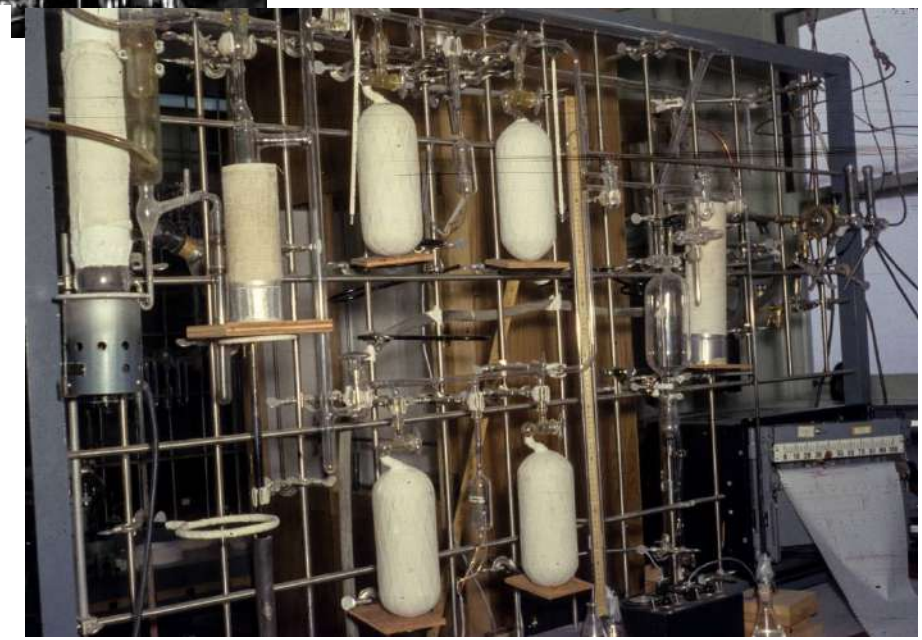

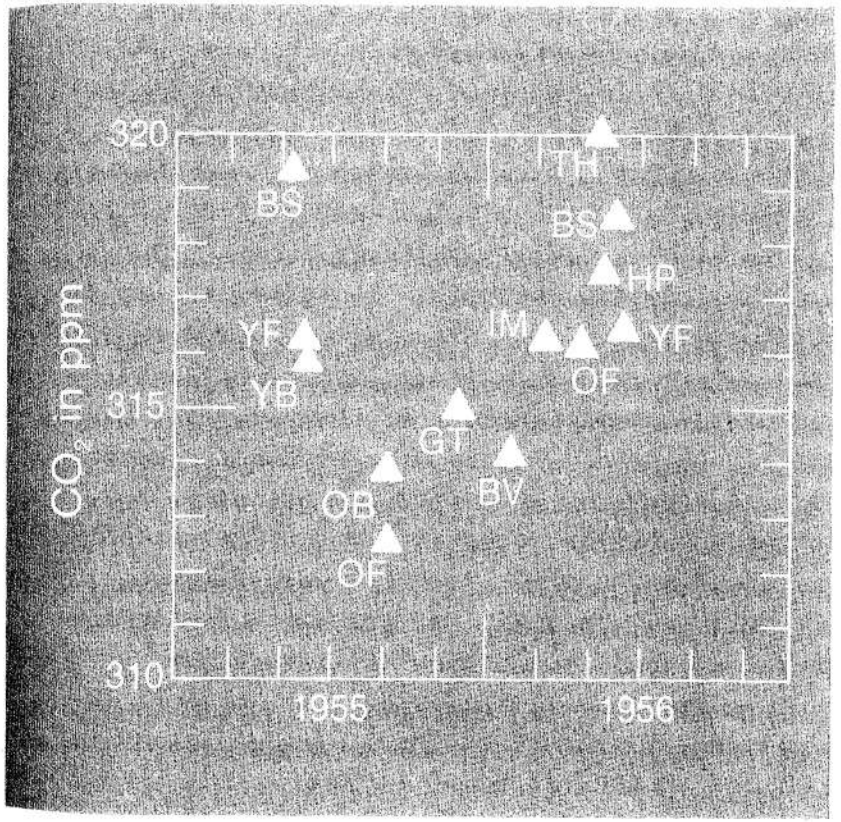

Figure 4. Minimum concentrations of atmospheric CO_2 at various sites near the west coast of the United States during 1955 and 1956. Concentrations were determined manometrically from liquid nitrogen temperature condensates. Sites are identified as follows: BS, Big Sur; YF, Yosemite forest; YB, Yosemite barren ground; OF, Olympic forest; OB, Olympic beach; GT, Gulf of Tehuantepec; BV, Borrego Valley; IM, Inyo Mountains; OP, Organ Pipe; HP, Howard Pocket; TH, Telephone Hill.

Mauna Loa, Hawaii, 1958…

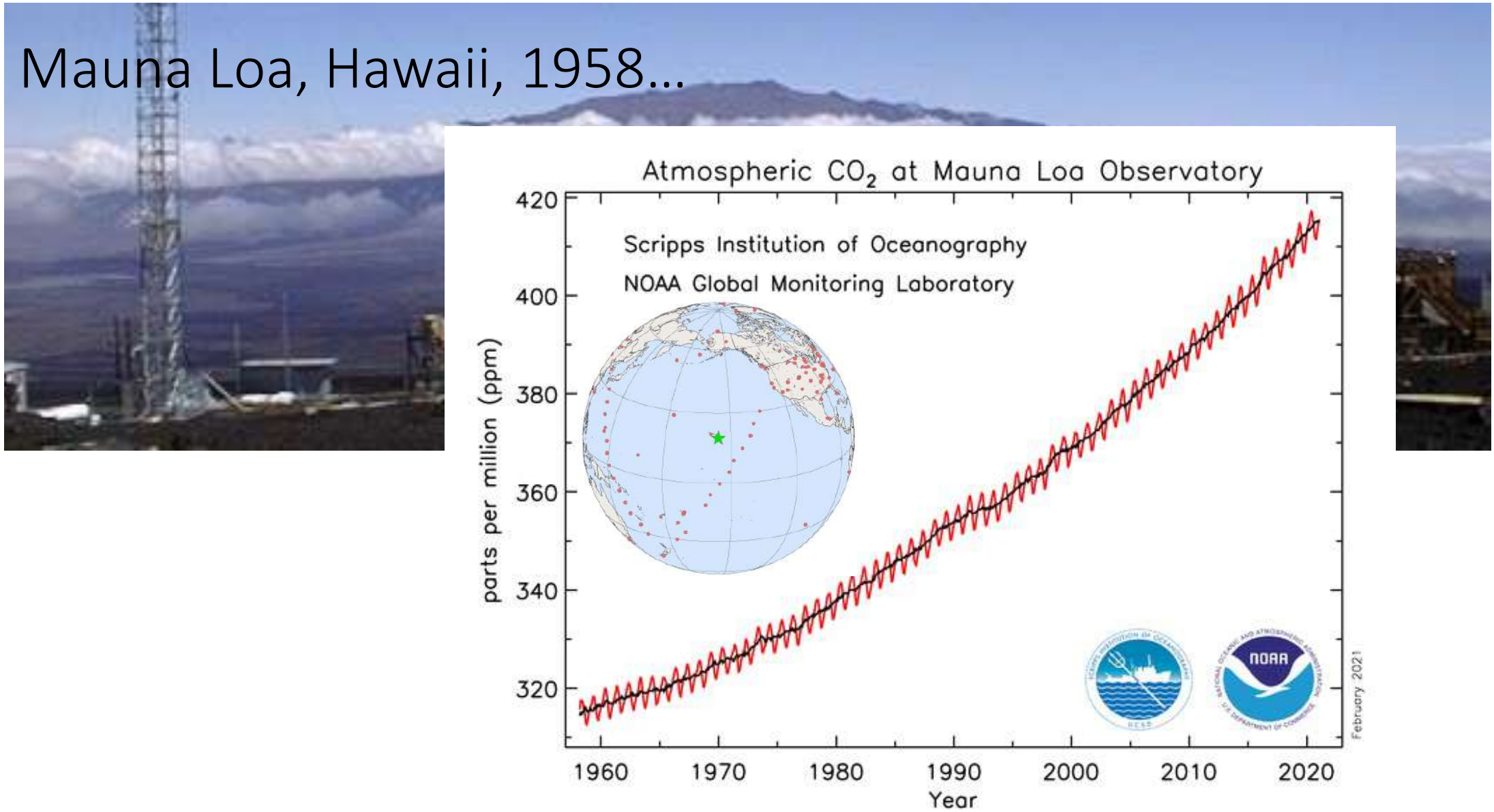

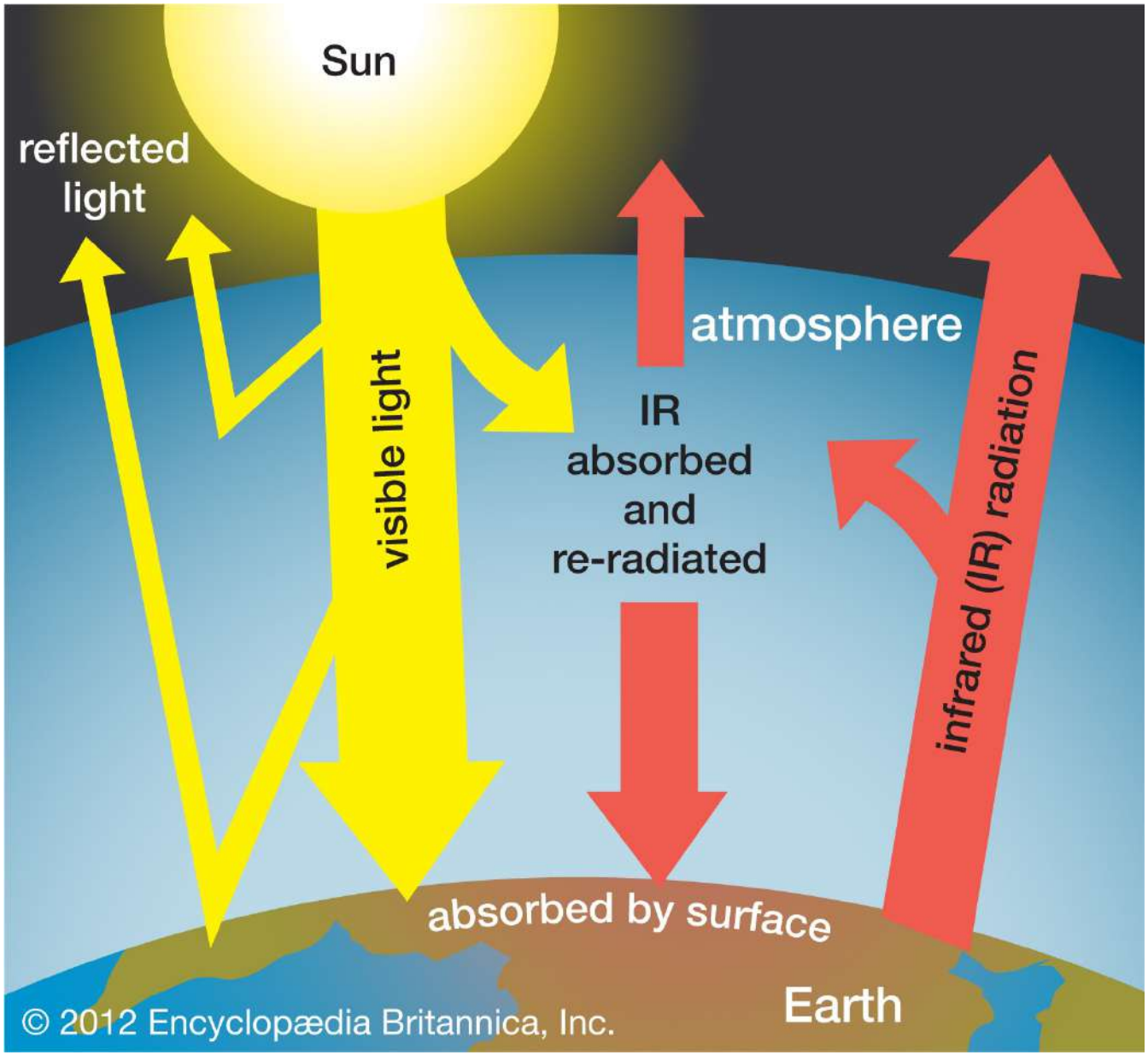
Sun
reflected light
visible light
atmosphere
IR absorbed and re-radiated
infrared (IR) radiation
absorbed by surface
Earth
© 2012 Encyclopædia Britannica, Inc.

britannica

Observed warming is driven by emissions from human activities, with greenhouse gas warming partly masked by aerosol cooling

Figure SPM.2

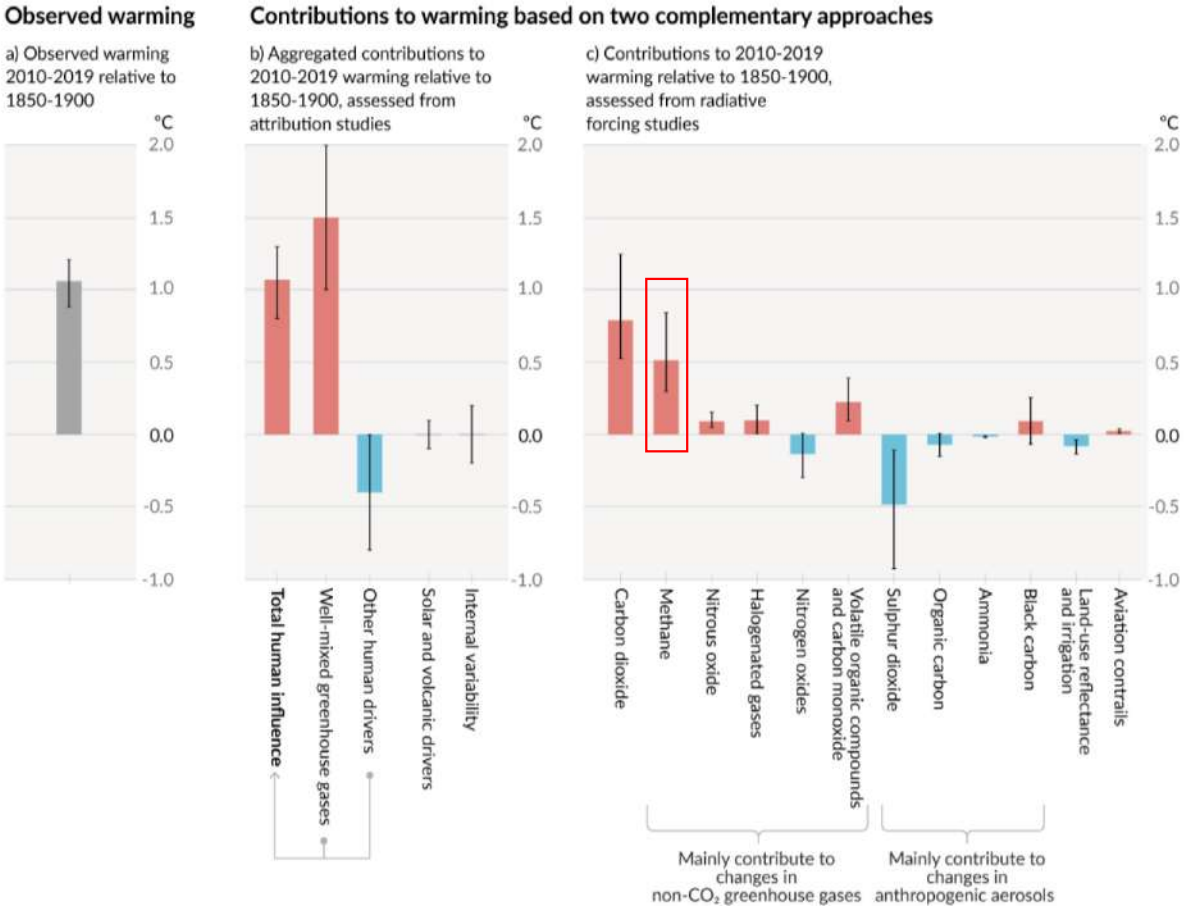

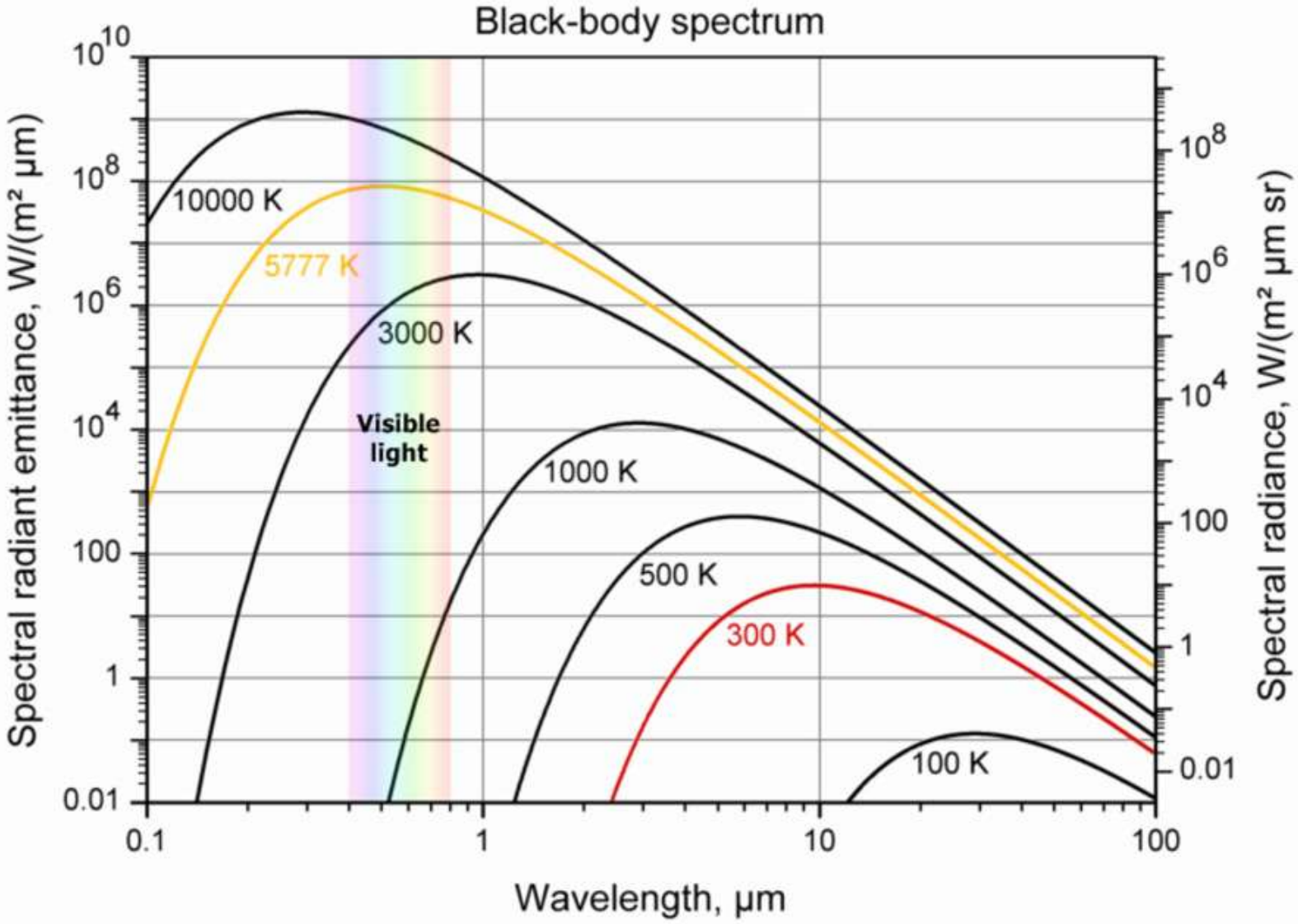
Black-body spectrum
Spectral radiant emittance, W/(m² μm)
Spectral radiance, W/(m² μm sr)
Wavelength, μm
10000 K
5777 K
3000 K
1000 K
500 K
300 K
100 K
Visible light
10^10
10^8
10^6
10^4
100
1
0.01
0.1
1
10
100

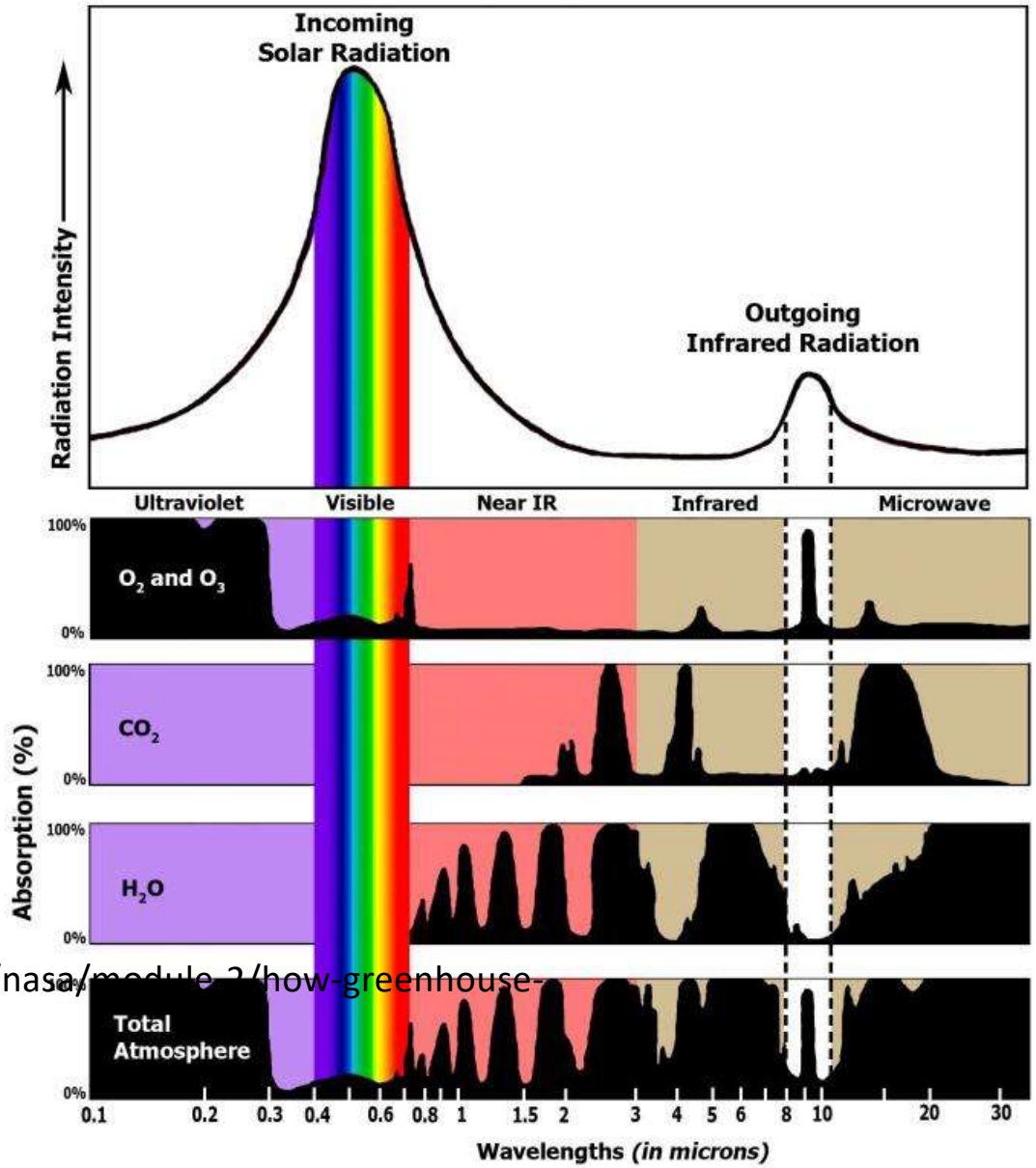

http://www.ces.fau.edu/nasa/module-2/how-greenhouse-effect-works.php

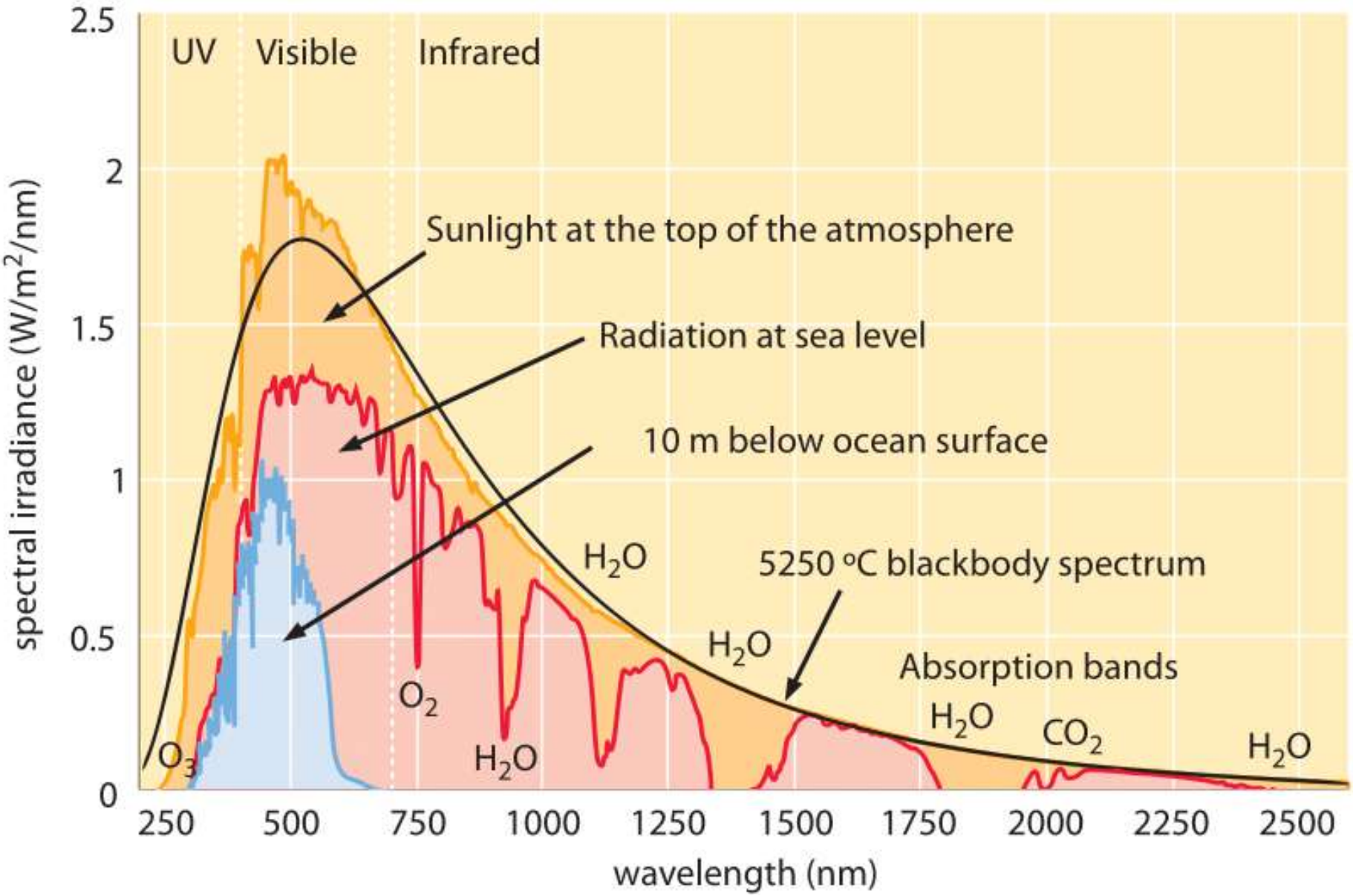
UV
Visible
Infrared
Sunlight at the top of the atmosphere
Radiation at sea level
10 m below ocean surface
5250 °C blackbody spectrum
Absorption bands
O_3
O_2
H_2O
H_2O
H_2O
H_2O
CO_2
H_2O
spectral irradiance ($W/m^2/nm$)
2.5
2
1.5
1
0.5
0
250
500
750
1000
1250
1500
1750
2000
2250
2500
wavelength (nm)

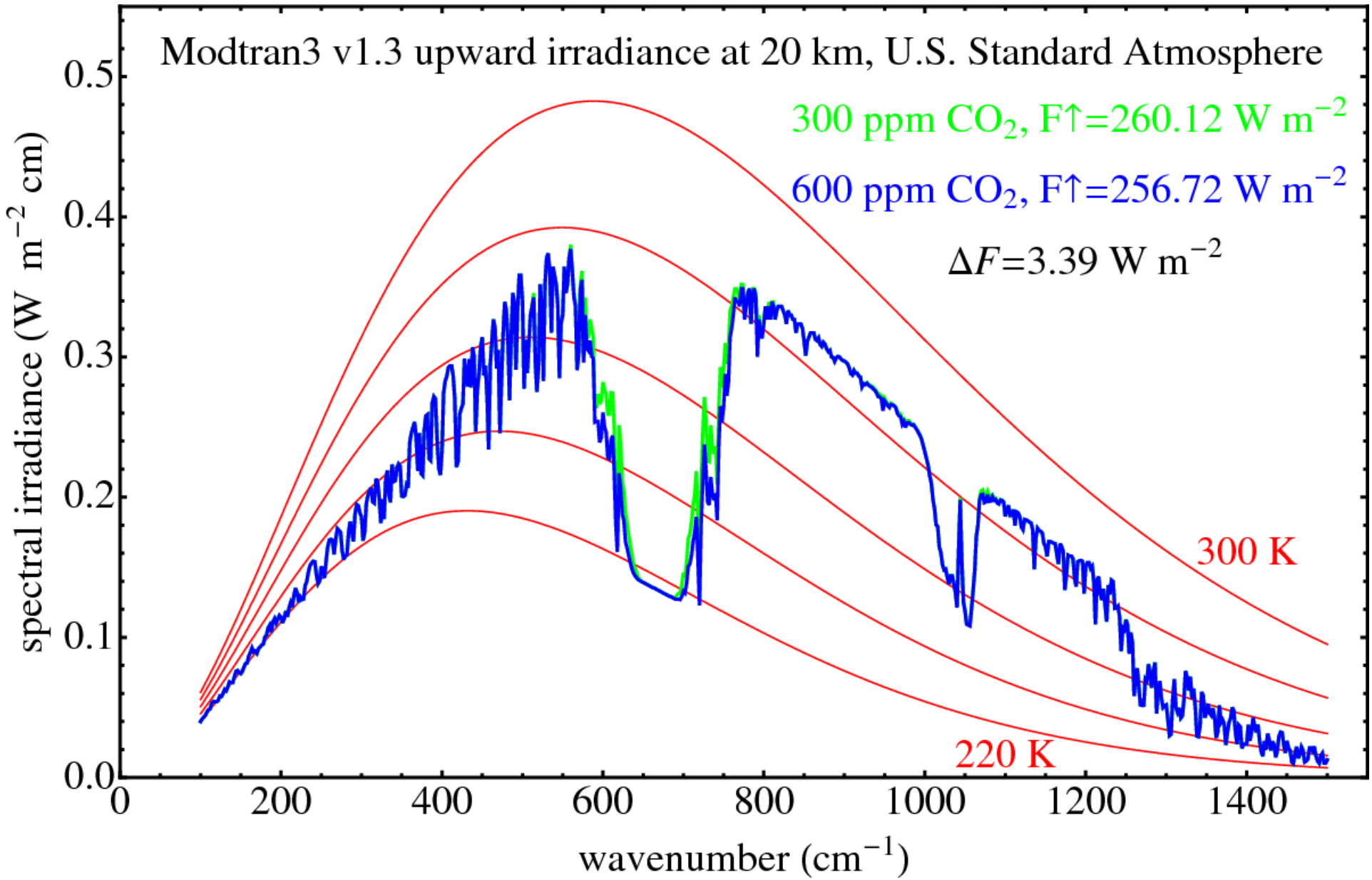
Modtran3 v1.3 upward irradiance at 20 km, U.S. Standard Atmosphere
300 ppm CO2, F↑=260.12 W m−2
600 ppm CO2, F↑=256.72 W m−2
ΔF=3.39 W m−2
300 K
220 K
spectral irradiance (W m−2 cm)
wavenumber (cm−1)
0.0
0.1
0.2
0.3
0.4
0.5
0
200
400
600
800
1000
1200
1400

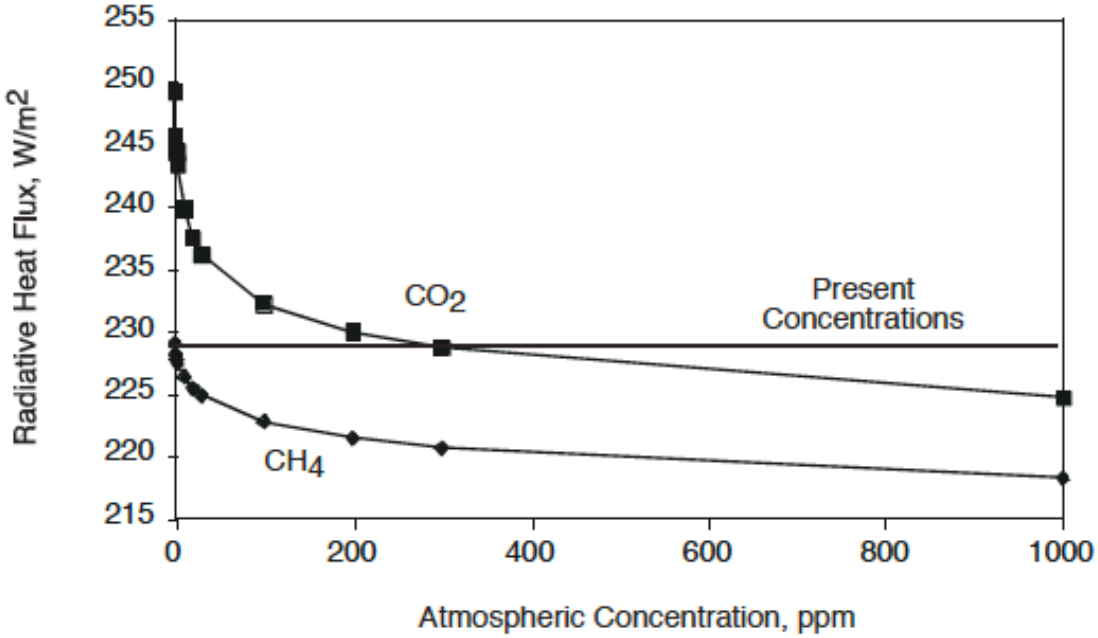

Fig. 1. Radiative impacts of atmospheric methane and CO_2 concentrations: the outgoing longwave radiation flux over midlatitude winter conditions, from the Modtran model (Rothman, 1992), with a web interface at http://geosci.uchicago.edu/~archer/cgimodels/radiation.html. The sensitivities to methane and CO_2 are fundamentally similar, but because methane is present at lower concentration, the atmosphere is at a steeper part of the curve where a single molecule of methane would have approximately twenty times the radiative impact of a single molecule of CO_2. The leveling off of this curve is due to saturation of absorption bands.

Concordia, Antartica

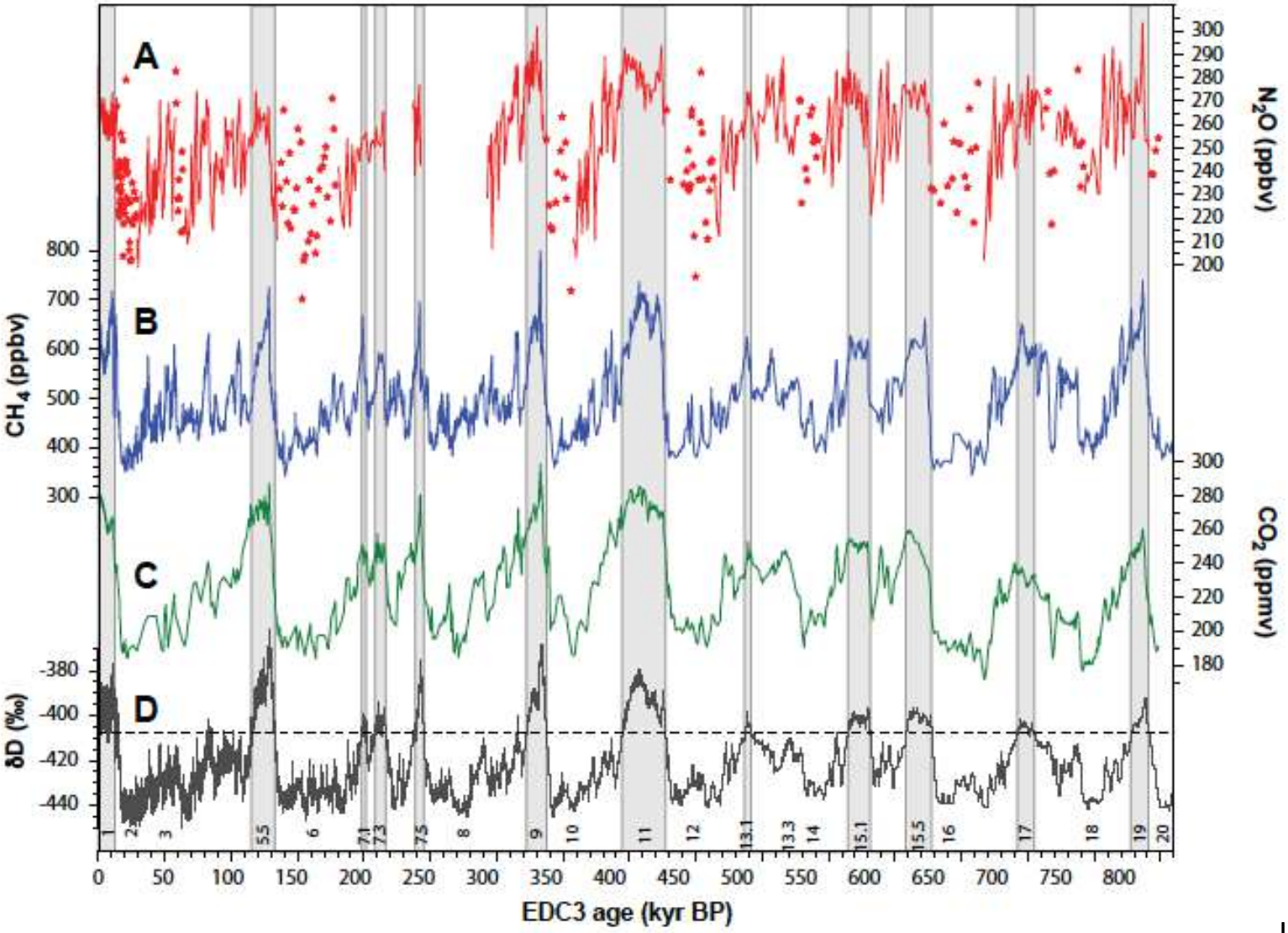

Jouzel et al., 2013

Perturbation of the global carbon cycle caused by anthropogenic activities, averaged globally for the decade 2010–2019 ($GtCO_2$/yr)

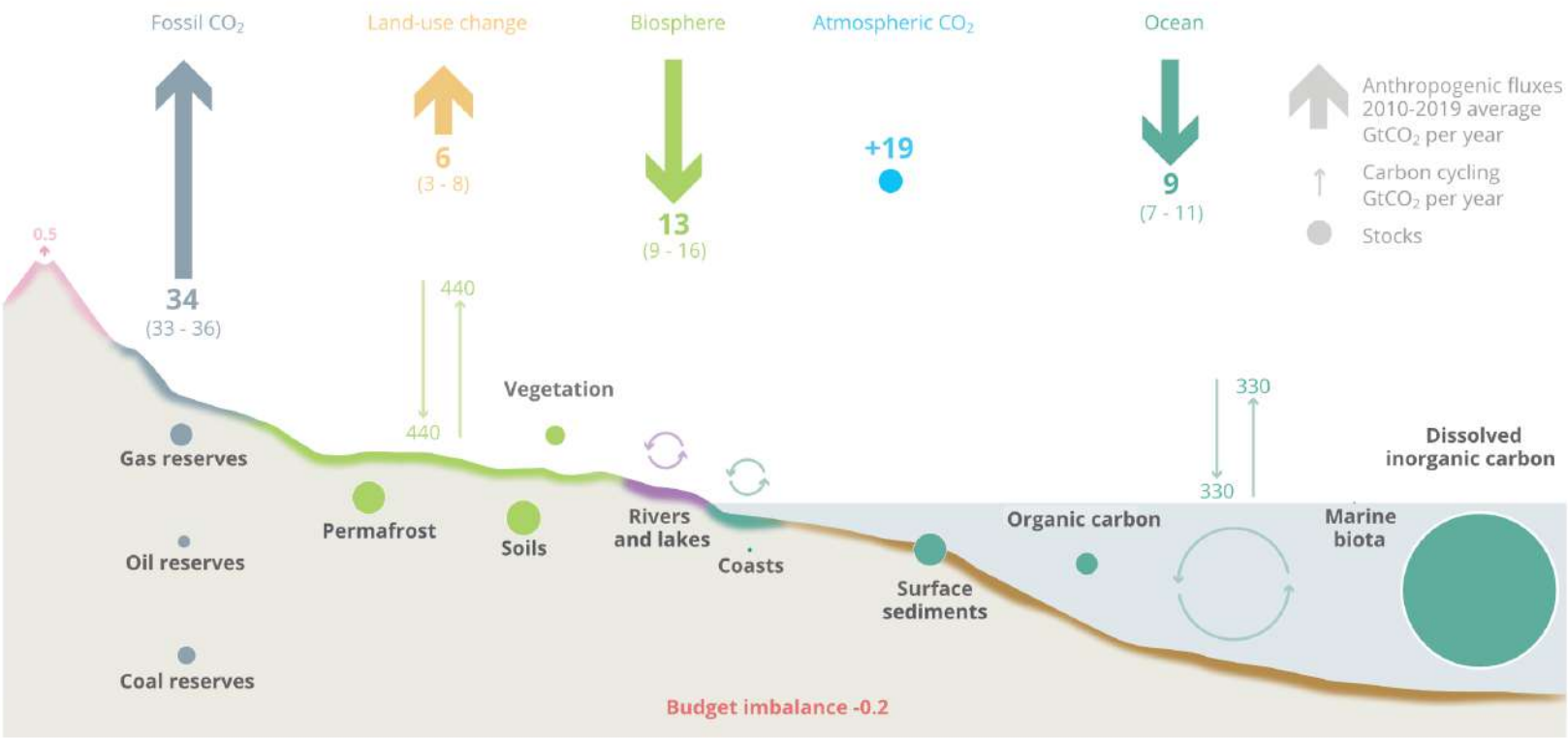

GCP 2020

Global carbon budget

Carbon emissions are partitioned among the atmosphere and carbon sinks on land and in the ocean
The "imbalance" between total emissions and total sinks is an active area of research

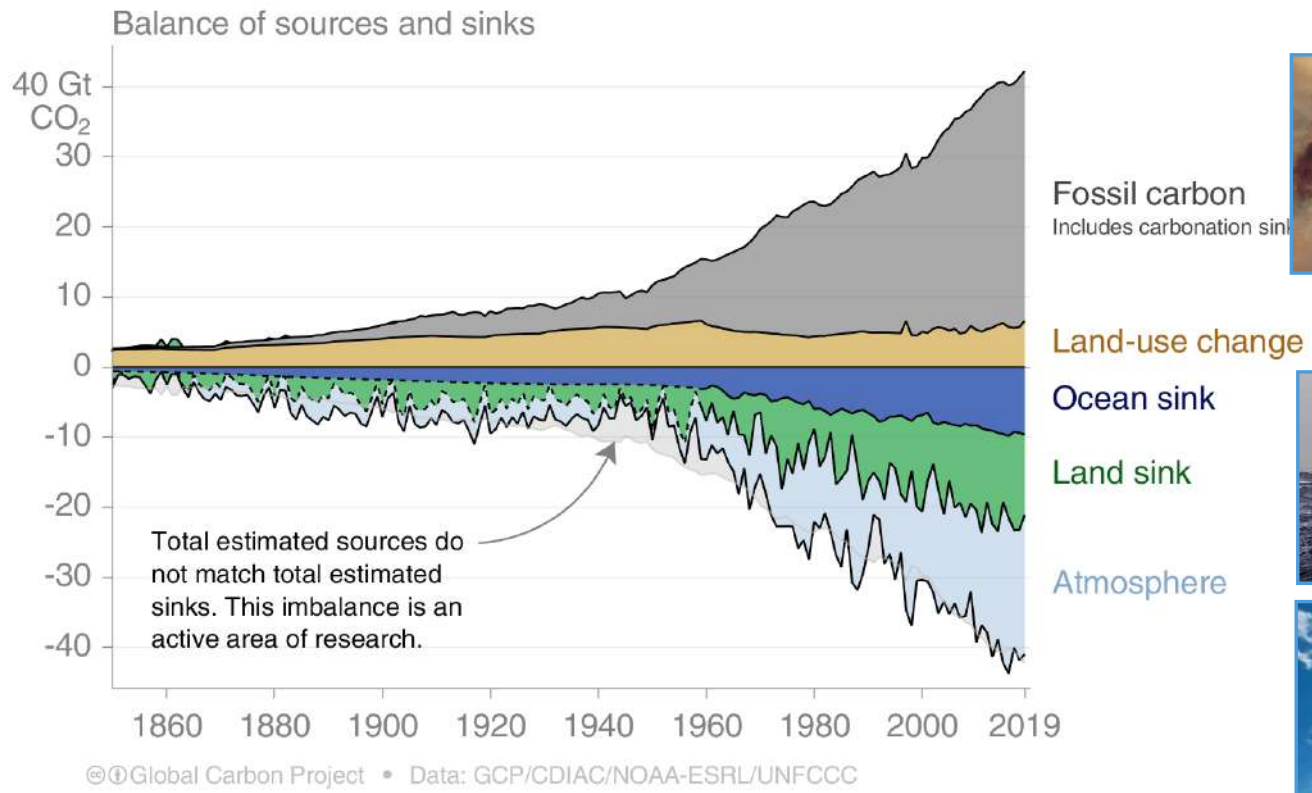

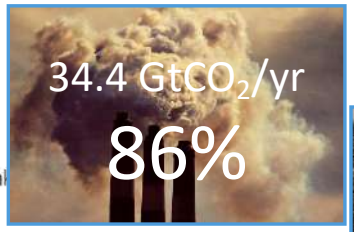

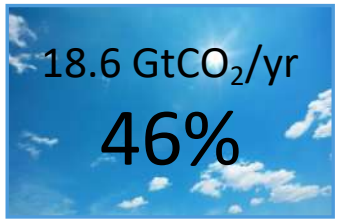

Source: Friedlingstein et al 2020; Global Carbon Budget 2020

Global Fossil CO_2 Emissions

Global fossil CO_2 emissions: 34.8 ± 2 $GtCO_2$ in 2020, 53% over 1990

● Projection for 2021: 36.4 ± 2 $GtCO_2$, 4.9% [4.1%–5.7%] higher than 2020

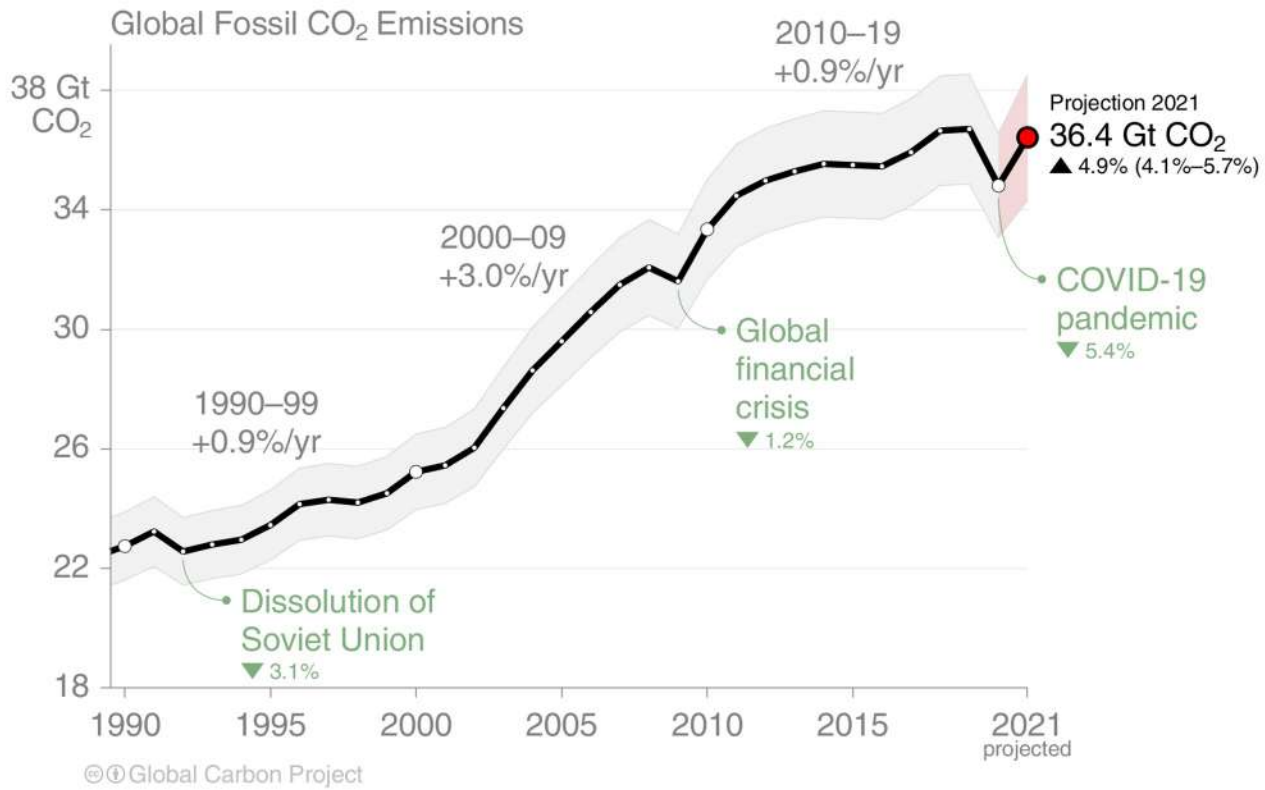

Uncertainty is ±5% for one standard deviation (IPCC "likely" range)

The 2021 projection is based on preliminary data and modelling.
Source: Friedlingstein et al 2021; Global Carbon Project 2021

UEA Projection: Overall impact of COVID-19 on regional emissions

While China's emissions declined strongly during February,
emissions declines in the rest of the world reached their peaks in April.

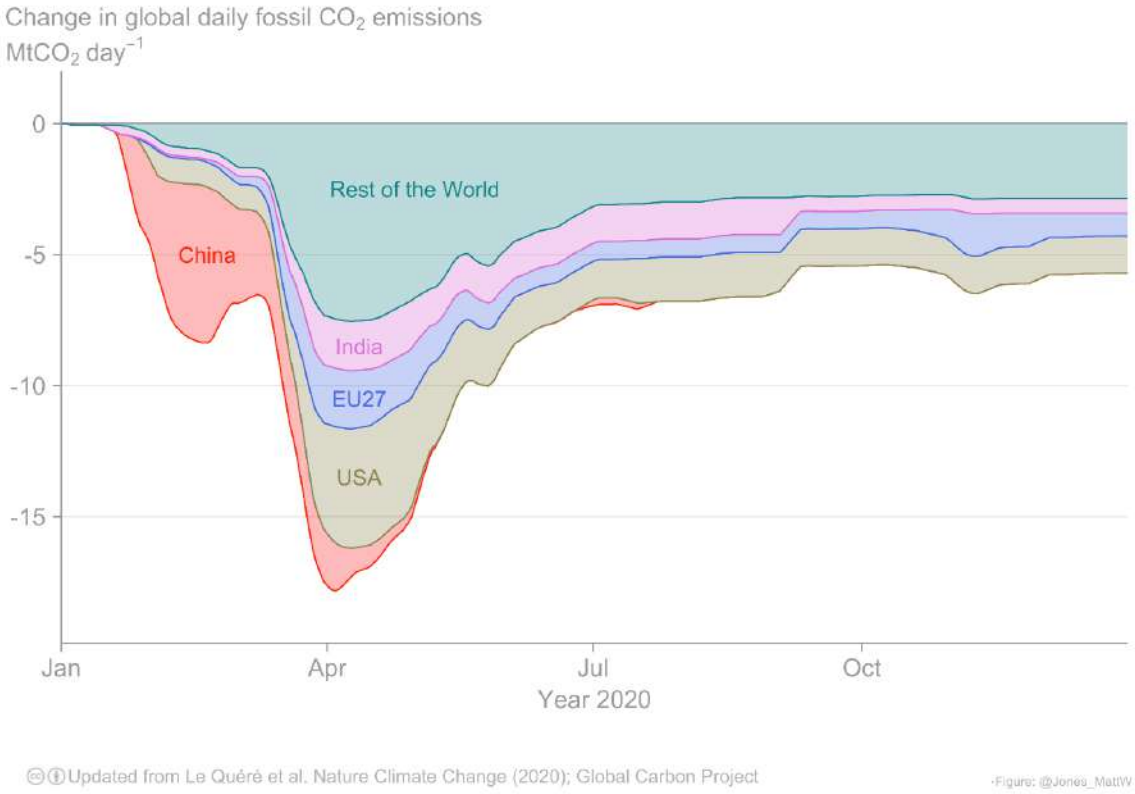

Source: Le Quéré et al 2020; https://www.icos-cp.eu/gcp-covid19

Fossil CO_2 Emissions by source

Share of global fossil CO2 emissions in 2020: coal (40%), oil (32%), gas (21%), cement (5%), flaring and others (2%, not shown)
Projection by fuel type is based on monthly data (GCP analysis)

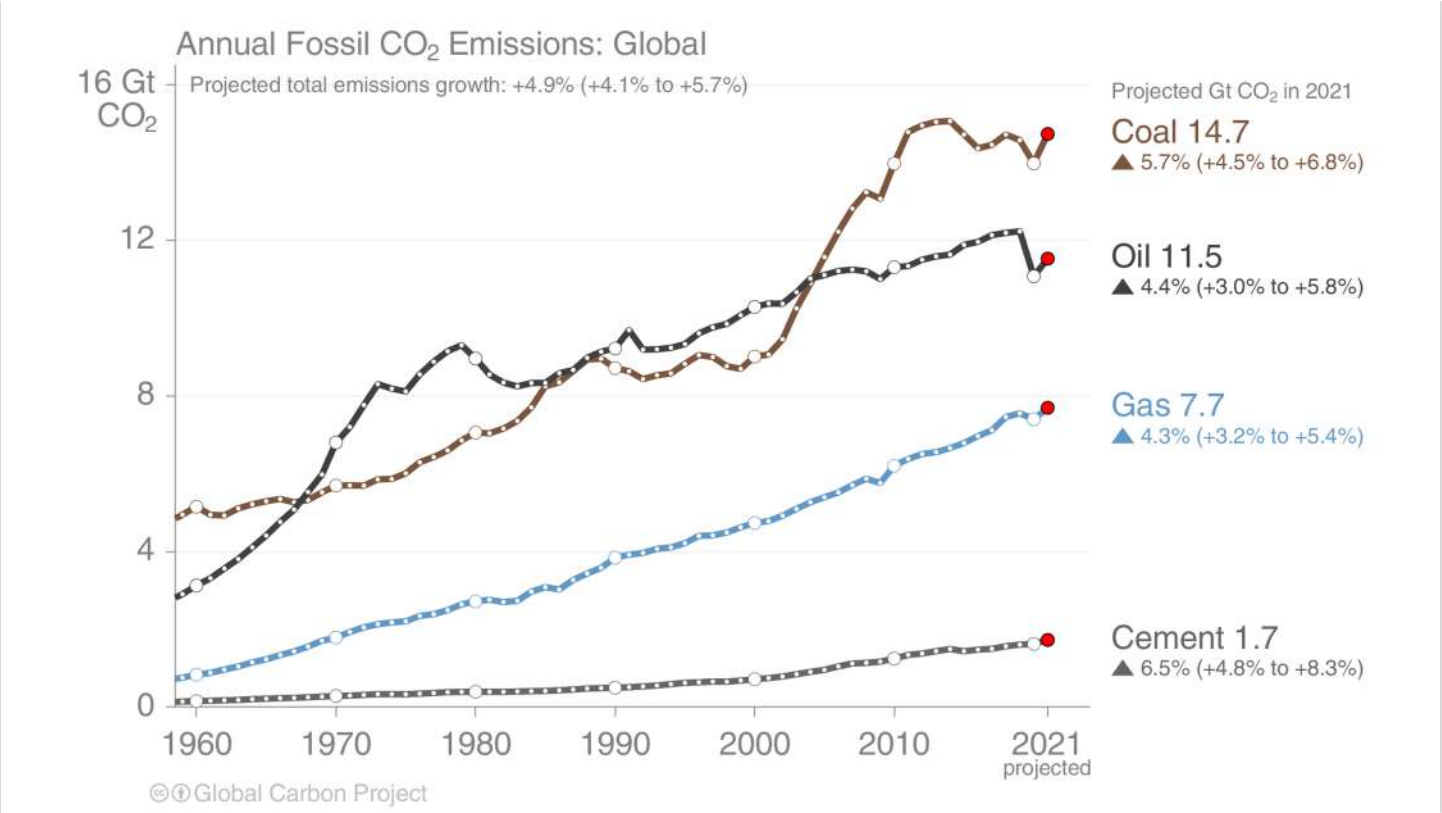

Source: Friedlingstein et al 2021; Global Carbon Project 2021

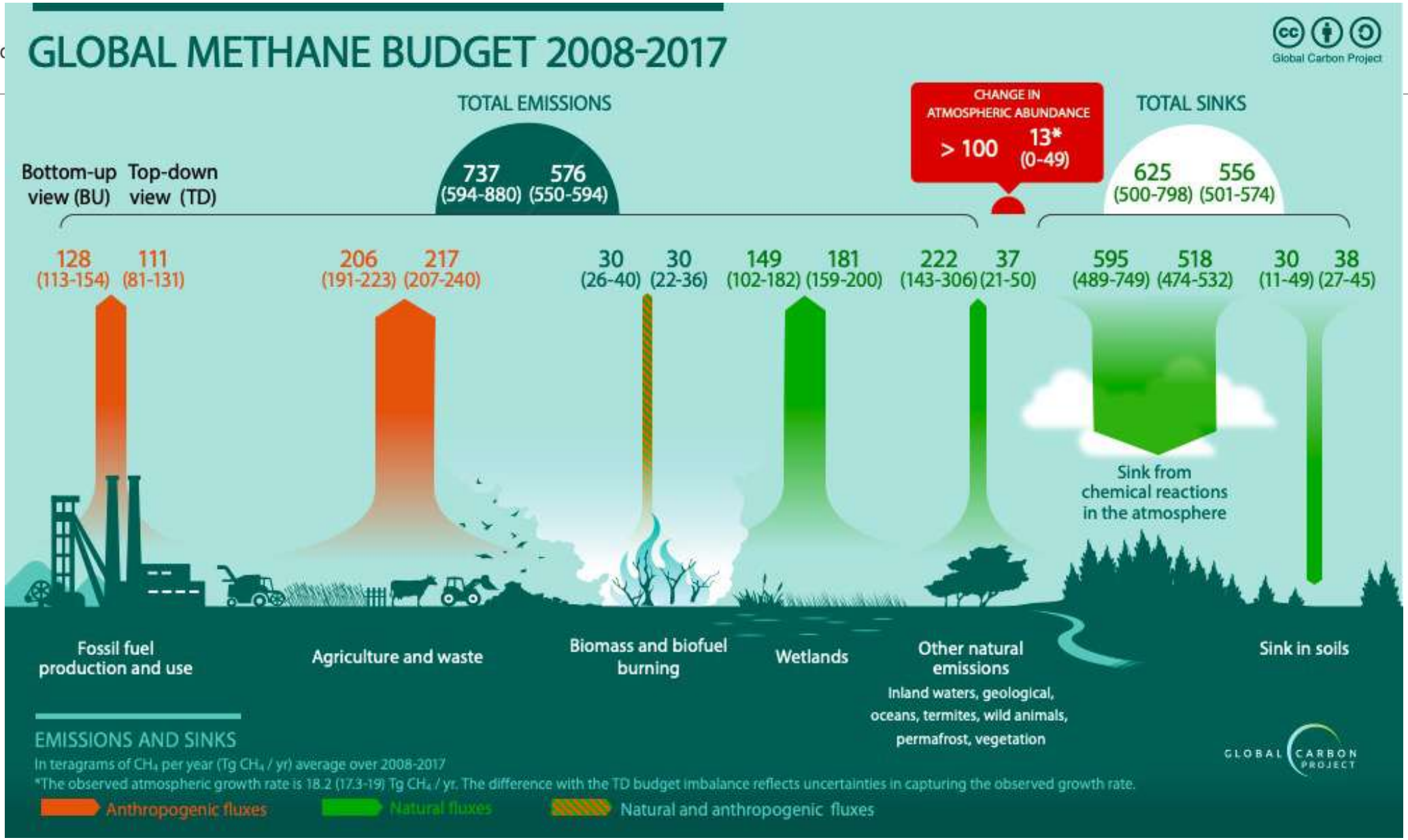
GLOBAL METHANE BUDGET 2008-2017
Global Carbon Project
TOTAL EMISSIONS
Bottom-up view (BU)
Top-down view (TD)
737 (594-880)
576 (550-594)
CHANGE IN ATMOSPHERIC ABUNDANCE
> 100
13* (0-49)
TOTAL SINKS
625 (500-798)
556 (501-574)
128 (113-154)
111 (81-131)
206 (191-223)
217 (207-240)
30 (26-40)
30 (22-36)
149 (102-182)
181 (159-200)
222 (143-306)
37 (21-50)
595 (489-749)
518 (474-532)
30 (11-49)
38 (27-45)
Sink from chemical reactions in the atmosphere
Fossil fuel production and use
Agriculture and waste
Biomass and biofuel burning
Wetlands
Other natural emissions
Inland waters, geological, oceans, termites, wild animals, permafrost, vegetation
Sink in soils
EMISSIONS AND SINKS
In teragrams of CH4 per year (Tg CH4 / yr) average over 2008-2017
*The observed atmospheric growth rate is 18.2 (17.3-19) Tg CH4 / yr. The difference with the TD budget imbalance reflects uncertainties in capturing the observed growth rate.
Anthropogenic fluxes
Natural fluxes
Natural and anthropogenic fluxes
GLOBAL CARBON PROJECT

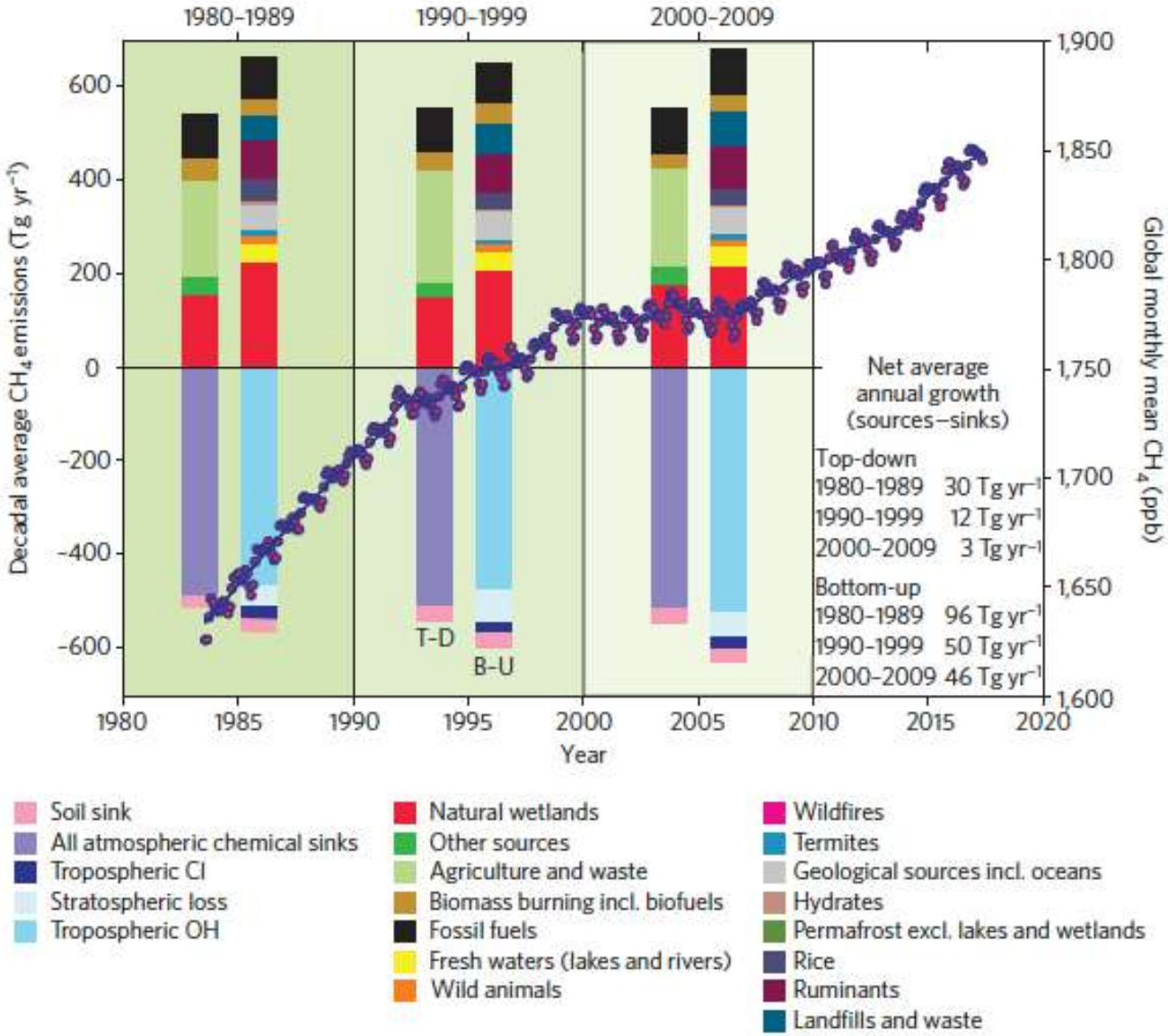

Crill & Thornton 2017

Sector by sector potential for emission reduction

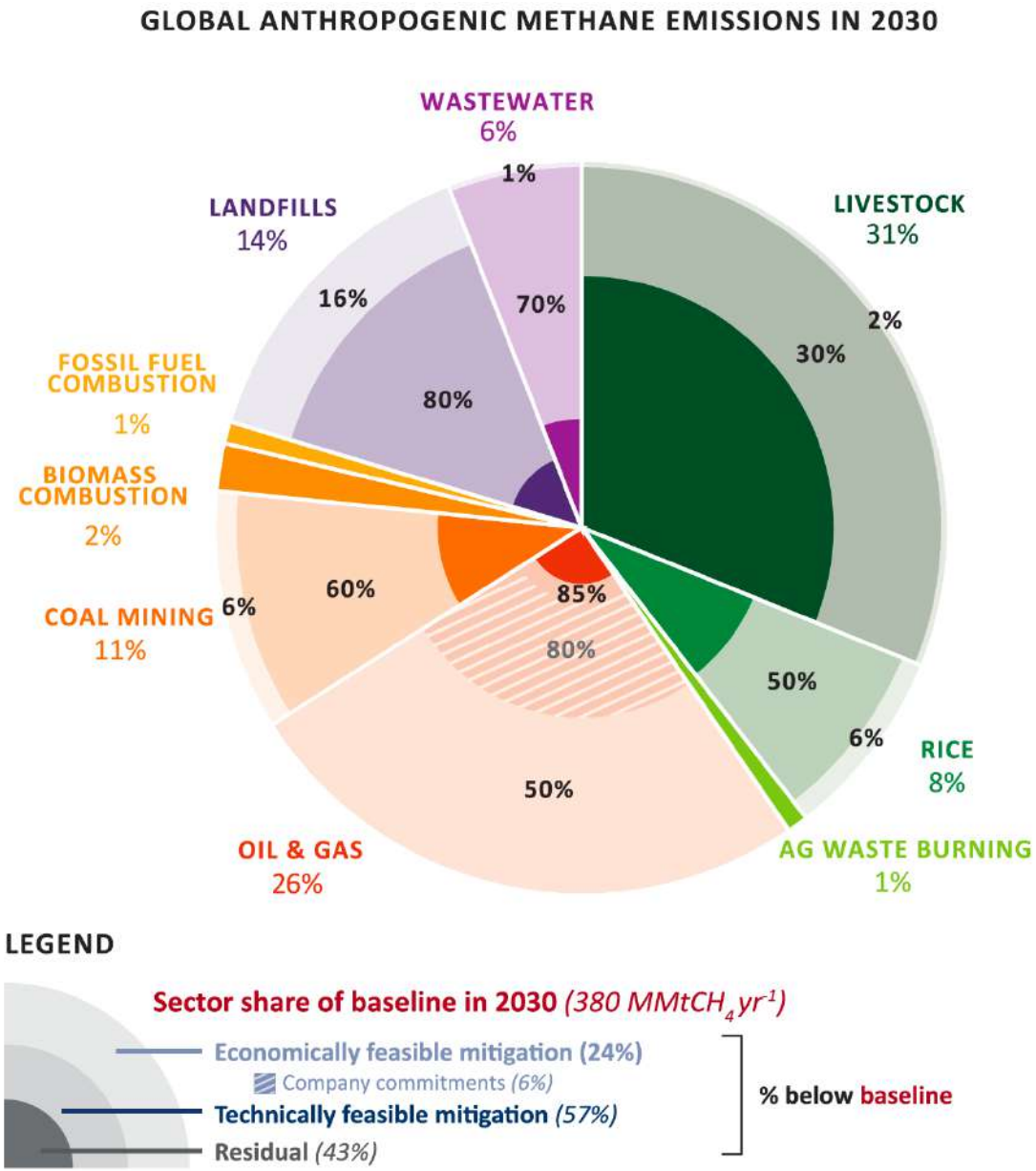

Ocko et al., ERL 2021

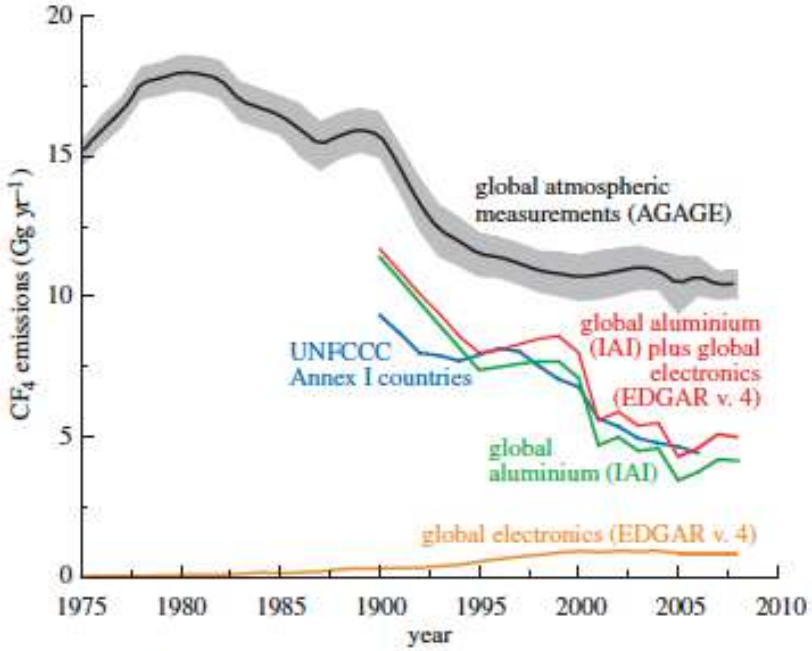

Figure 3. Top-down global emissions of carbon tetrafluoride (CF_4) modelled from global atmospheric measurements in the AGAGE programme [41], with shaded combined modelling and measurement uncertainties (±1 standard deviation), compared with the bottom-up global emissions estimates for the aluminium industry (e.g. [43]), for the electronics industry [44] and for these two sources combined. Also plotted are bottom-up emissions reported to the UNFCCC for the Annex I developed countries [3]. Adapted from Mühle *et al.* [41].

Prinn & Weiss 2011

CFC-11 emissions from atmospheric observations

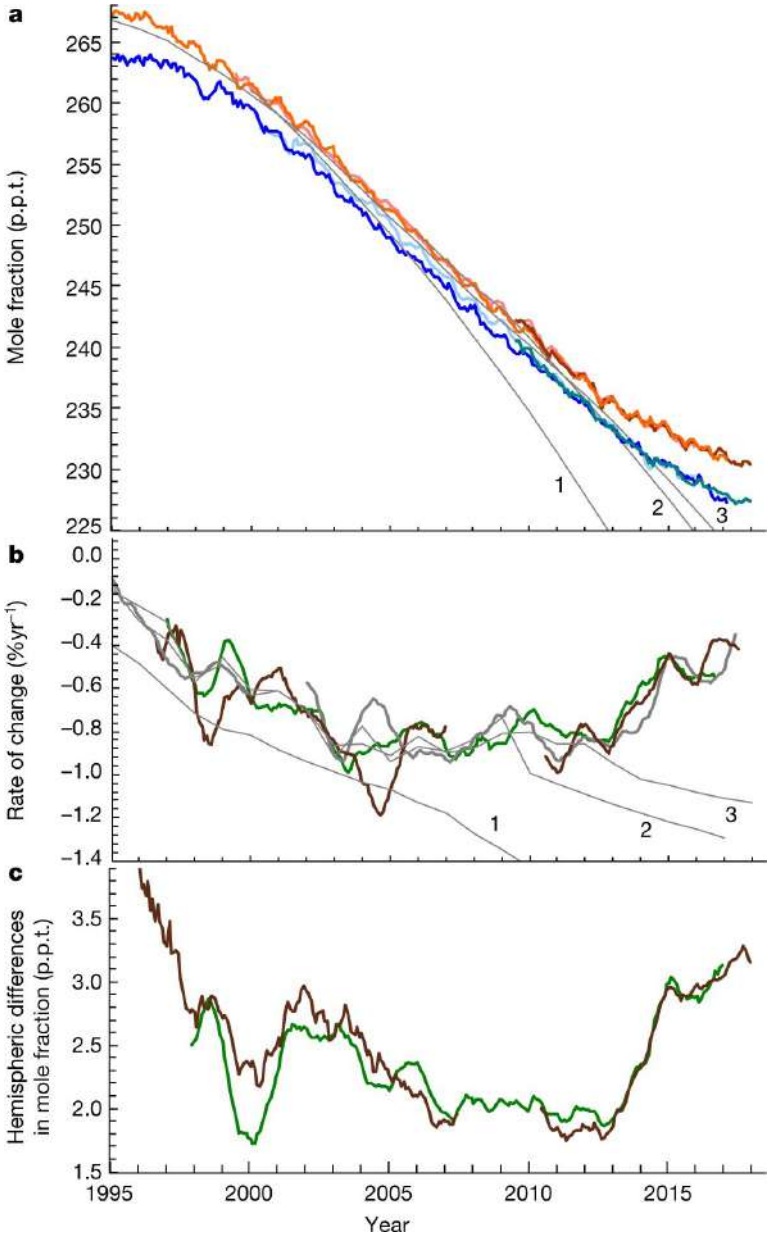

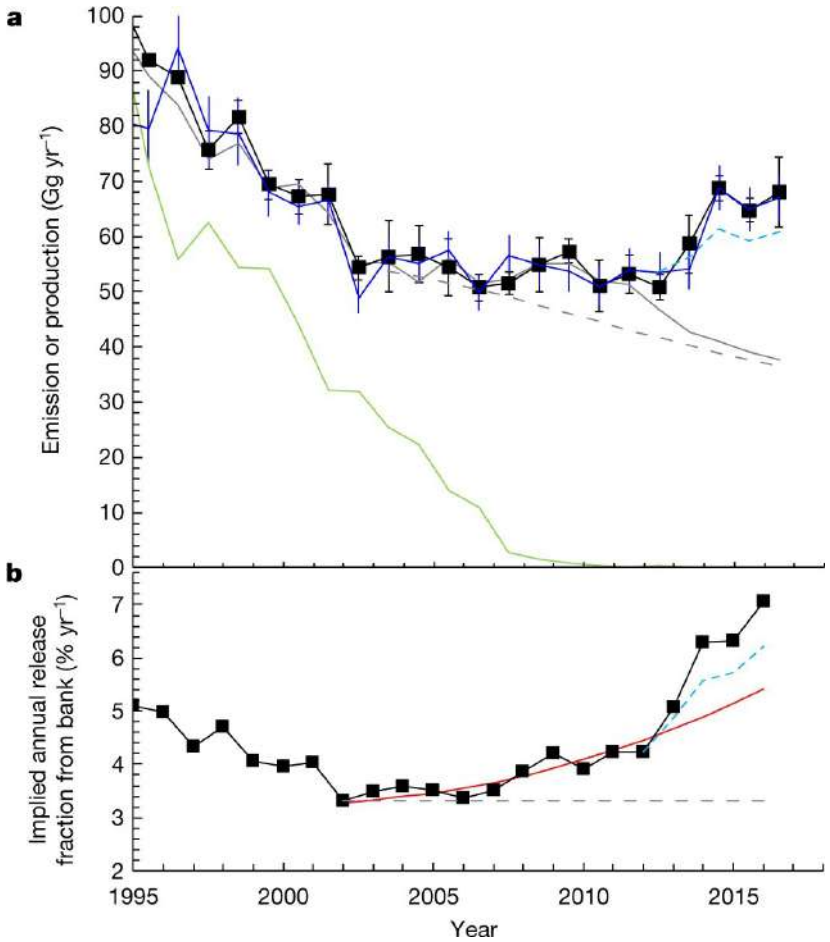

Montzka et al., 2018

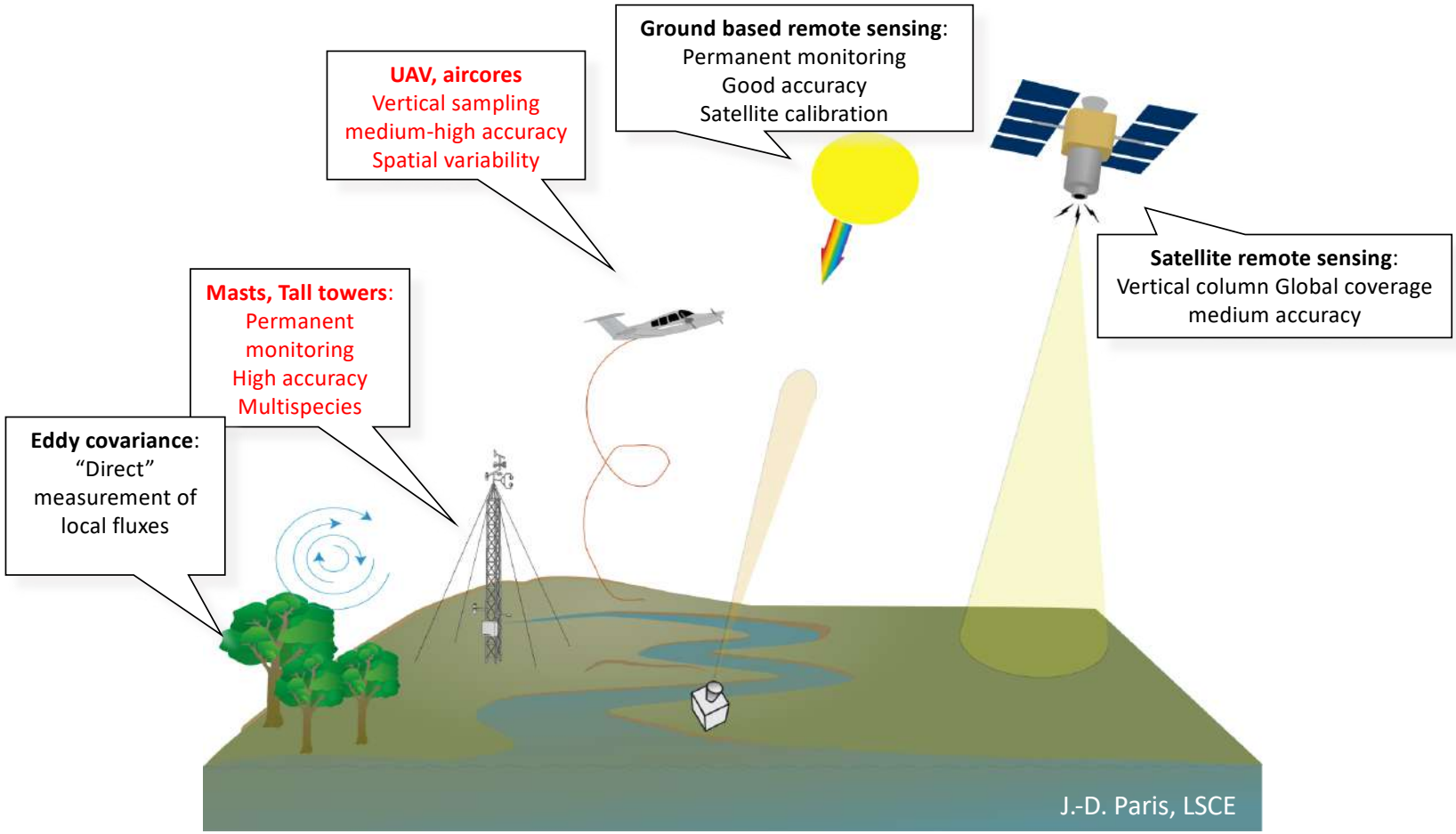
Ground based remote sensing:
Permanent monitoring
Good accuracy
Satellite calibration
UAV, aircores
Vertical sampling
medium-high accuracy
Spatial variability
Satellite remote sensing:
Vertical column Global coverage
medium accuracy
Masts, Tall towers:
Permanent
monitoring
High accuracy
Multispecies
Eddy covariance:
"Direct"
measurement of
local fluxes
J.-D. Paris, LSCE

Atmospheric GHG measurement

- Why measuring atmospheric GHG composition?
- Stable isotopes and tracers
- Ppm vs umolmol-1
- GC/MS
- Optical methods: NDIR, CRDS
- calibration and the WMO scale
- 14C
- Mobile measurements
- Ground base remote sensing

NATURAL ISOTOPES OF CARBON

6 Protons
6 Neutrons

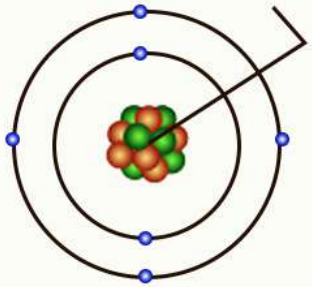

6 Protons
7 Neutrons

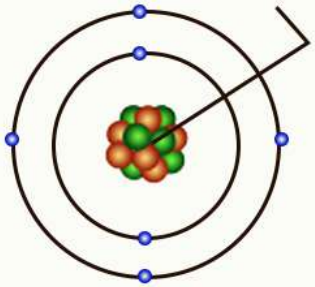

6 Protons
8 Neutrons

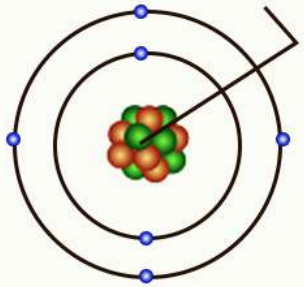

Carbon-12
(6P + 6N)
Atomic Weight = 12
Isotope Mass: 12 u
Abundance: 98.89%

Carbon-13
(6P + 7N)
Atomic Weight = 13
Atomic Mass = 13.00335 u
Abundance: 1.109%

Carbon-14
(6P + 8N)
Atomic Weight = 14
Isotope Mass: 14.003241 u
Abundance: 1 Part Per Trillion
Half-life: 5,730 ± 40 Years

C isotopes of CO_2

CO_2 Pool	$\Delta^{14}C$ Value (‰)	$\delta^{13}C$ Value (‰)
Fossil Fuels	-1,000	-28
Terrestrial Biosphere	+45	-26
Ocean	+45	-10
Atmosphere	+45	-8

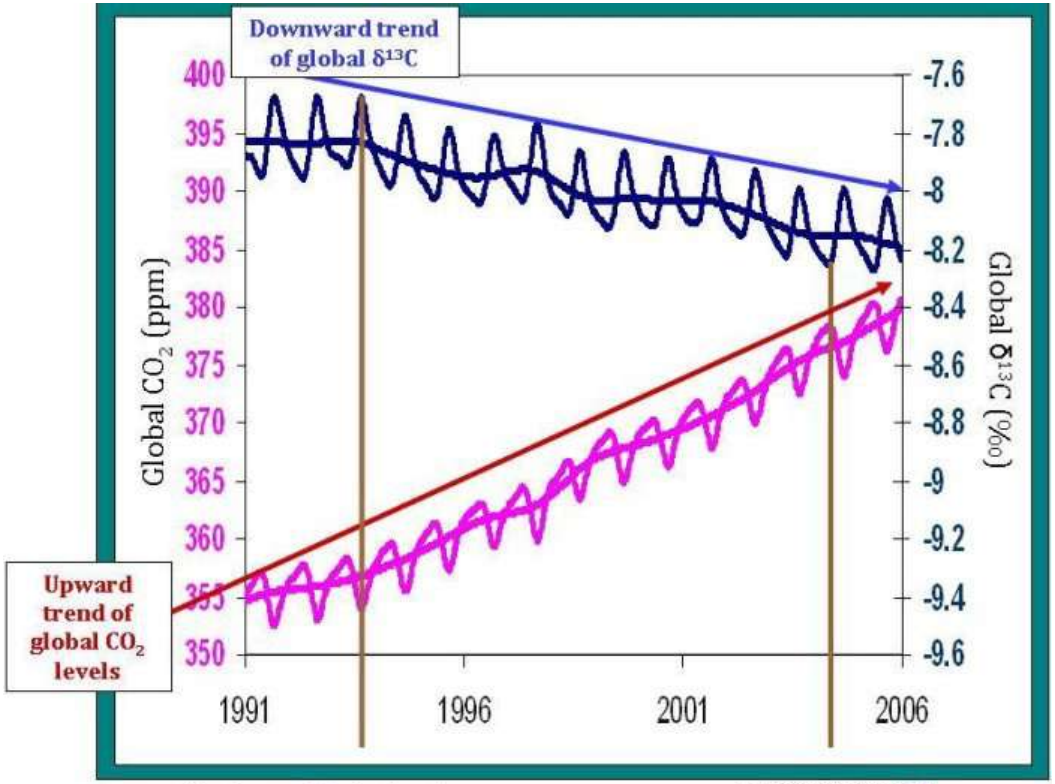

The lowest CO_2 level each year is when the $\delta^{13}C$ value is highest...

...and the highest CO_2 level each year is when the $\delta^{13}C$ value is lowest.

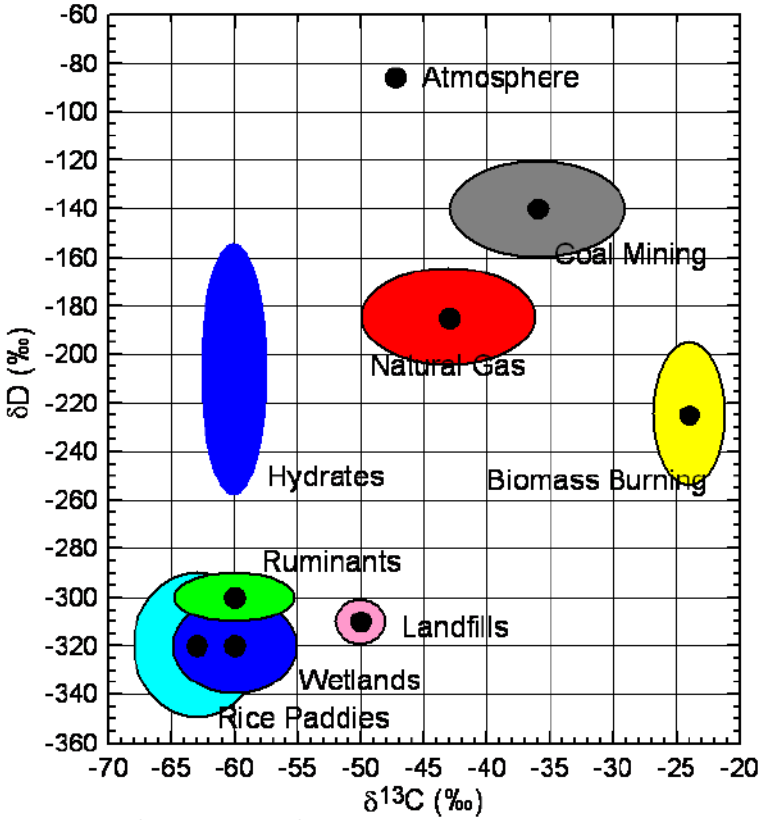

Quay et al., 1999; Whiiticar 2019

Ethane measurements - context

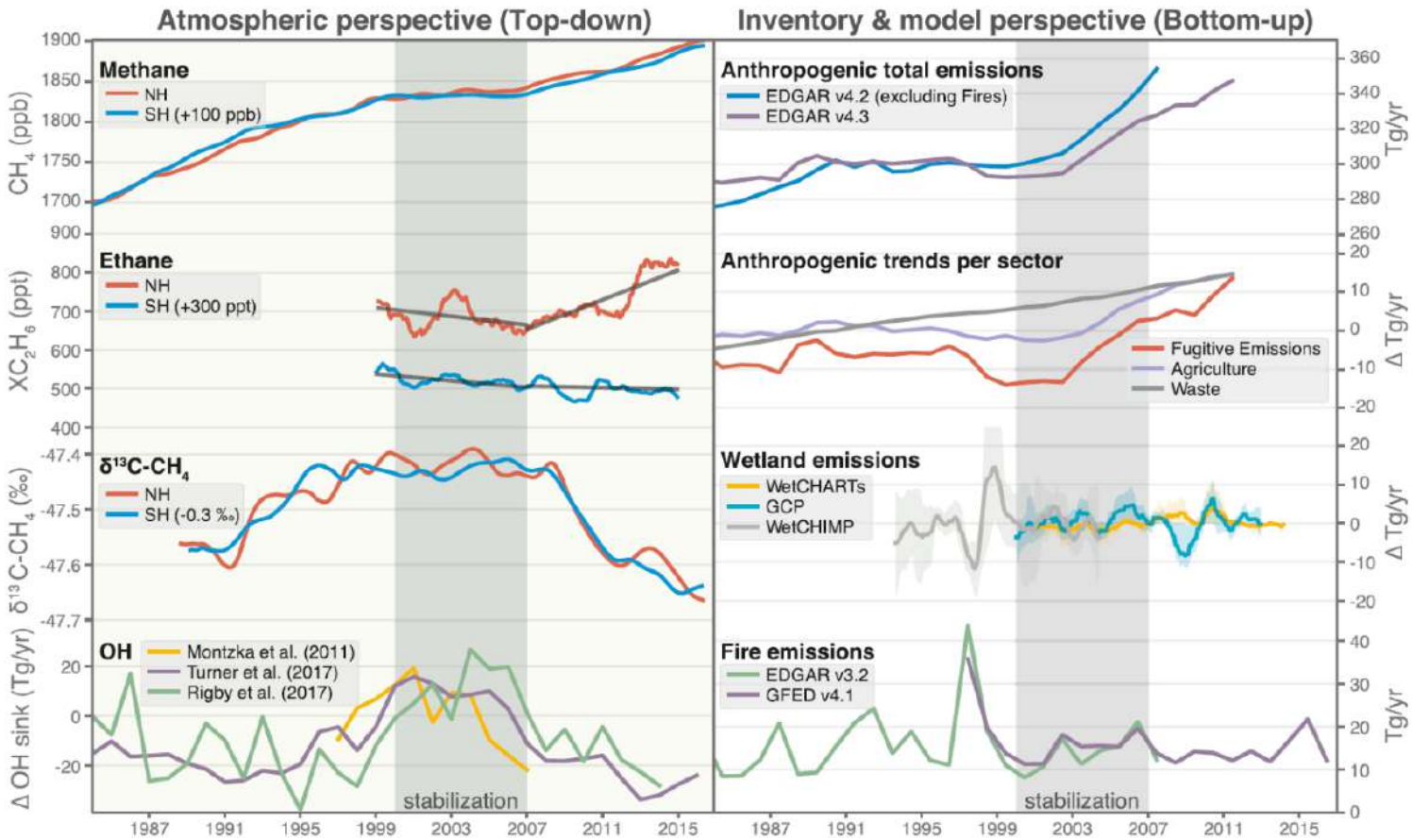

Turner et al., 2018

C_2H_6/CH_4 mole ratio

- 0.1 raw natural gas
- 0.04 processed/refined natural gas

Lopez et al.,2017

Atmospheric GHG measurement

- Why measuring atmospheric GHG composition?
- Stable isotopes
- Ppm vs umolmol-1
- GC/MS
- Optical methods: NDIR, CRDS
- calibration and the WMO scale
- 14C
- Vertical measurements
- Mobile measurements
- Ground base remote sensing

Units and conventions

- ‘ppm’ is more rigorously expressed as ‘µmol mol^{-1}’
- ‘concentration’ vs ‘mole fraction’
- 1 ppb = 10^{-3} ppm
- 1 ppm of atmosphere CO_2 = 2.13 Gt C
  - (Uses atmospheric mass (M_a) = 5.137×10^{18} kg)
- 1 mole CO_2 = 44.009 g CO_2 = 12.011 g C
- 1 g C = 0.083 mole CO_2 = 3.664 g CO_2
- 1 GtC = 1 PgC = 10^{15}gC

Atmospheric GHG measurement

- Why measuring atmospheric GHG composition?
- Stable isotopes
- Ppm vs umolmol-1
- GC/MS
- Optical methods: NDIR, CRDS
- calibration and the WMO scale
- 14C
- Vertical measurements
- Mobile measurements
- Ground base remote sensing

Flask samplers

Gas chromatography

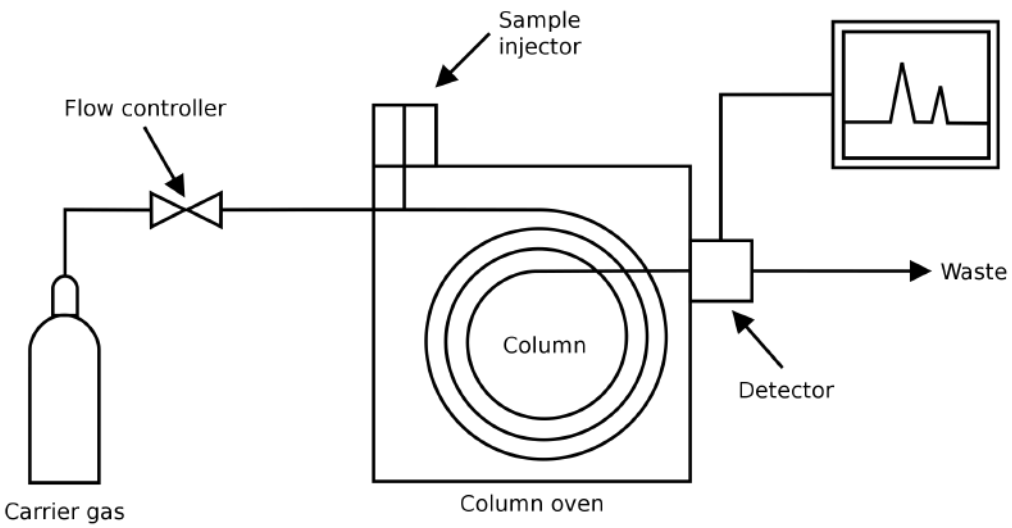

Vaporized sample passes through a column, carried along by a continuous flow of nonreactive gas.
Components of the sample pass through the column at different rates, depending on their chemical and physical properties and the resulting interactions with the column lining or filling, called the *stationary phase*.
As the chemicals exit the end of the column, they are detected and identified electronically.

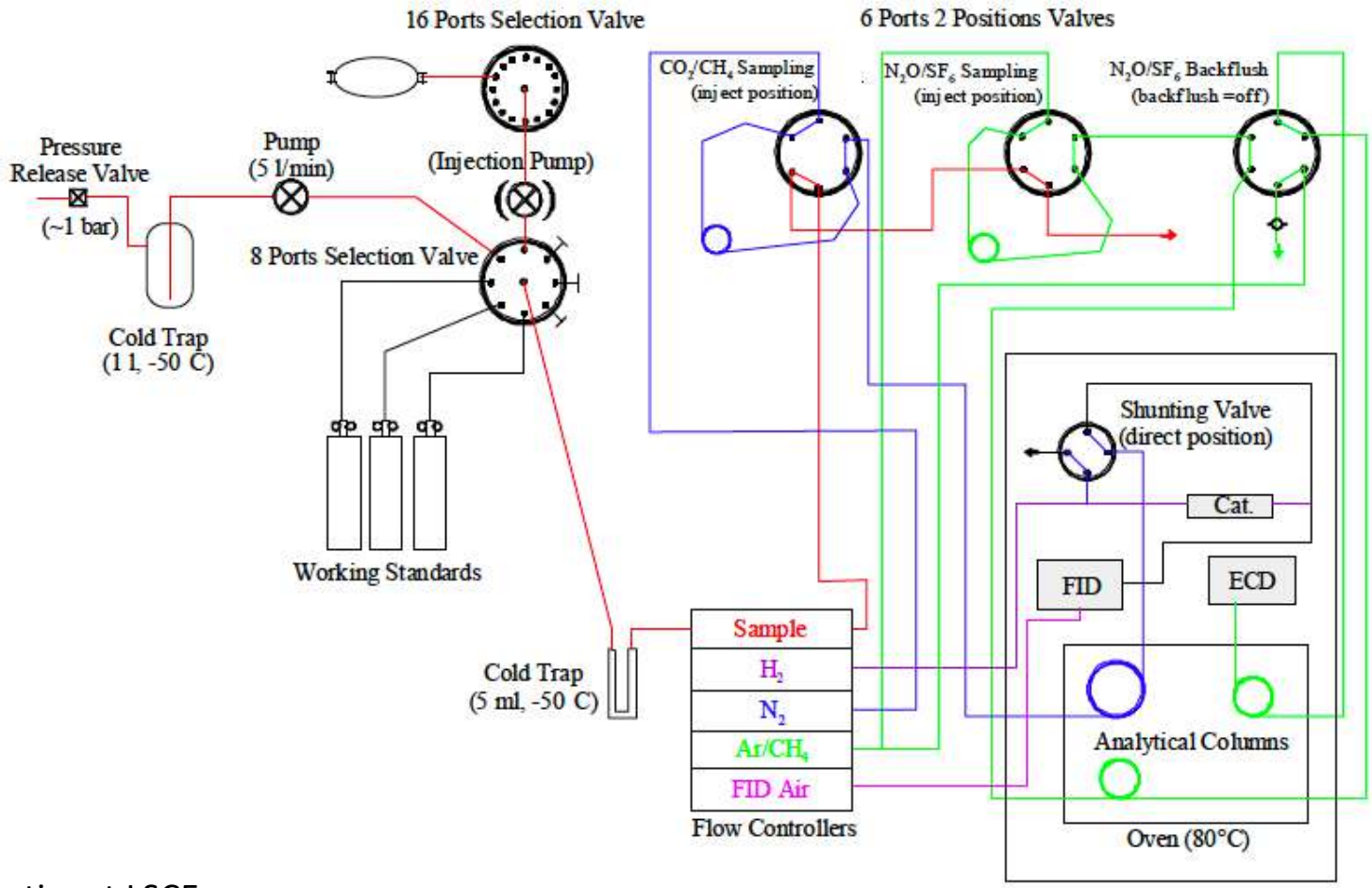

GC schematics at LSCE

Pepin et al., 2001

Mass spectrometry

- MS converts molecules to ions and accelerates them by external electric a magnetic fields. The three essential functions of a mass spectrometer, and the associated components, are:

- 1. Ionize a small sample. graphite targets are bombarded with cesium atoms to produce negatively charged ions of carbon.
- 2. Sort and separate ions according to their mass and charge. A magnet deflects the ions on a different trajectory, depending on their mass
- 3. Measure the separated ions

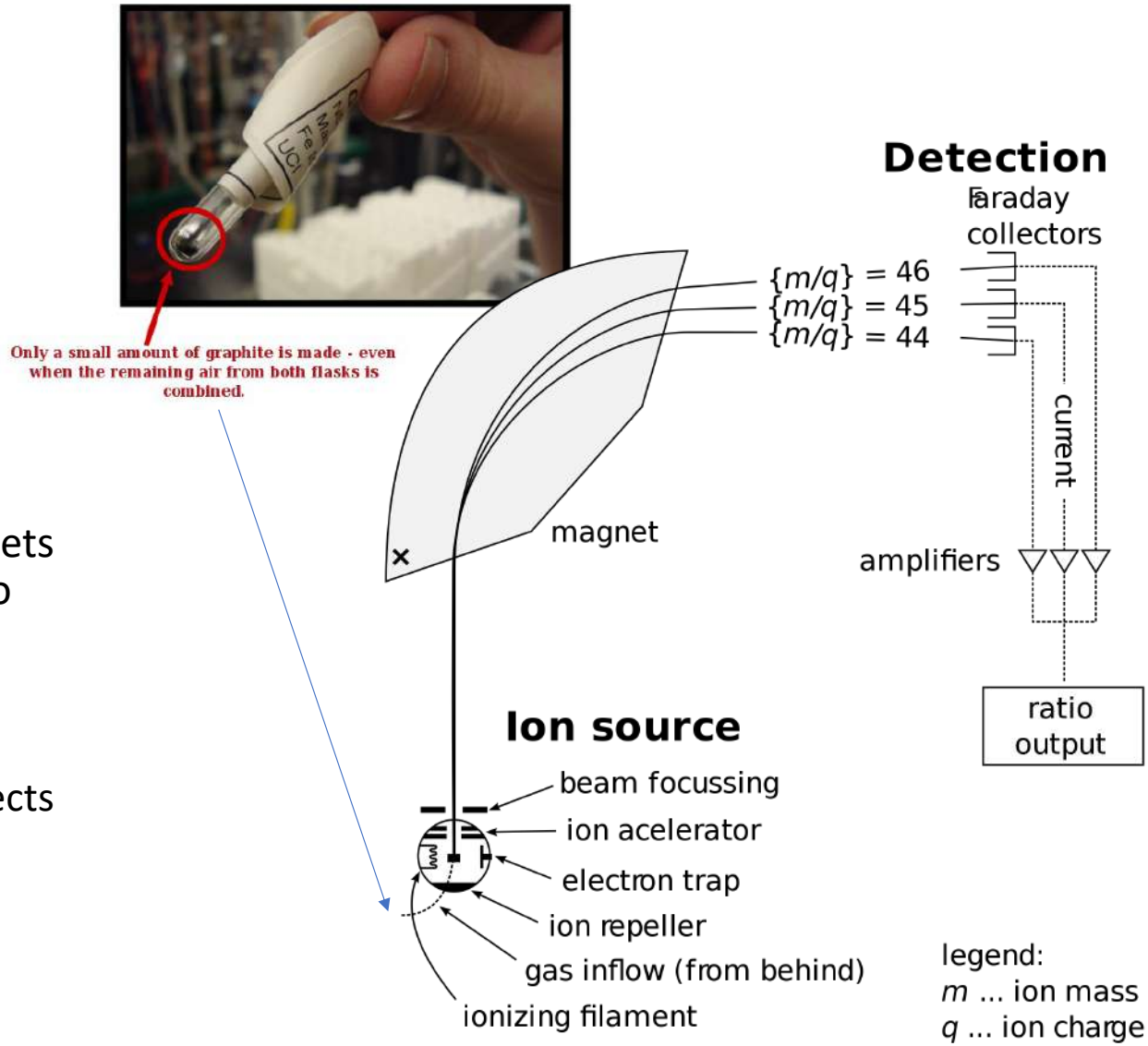

Atmospheric GHG measurement

- Why measuring atmospheric GHG composition?
- Stable isotopes
- Ppm vs umolmol-1
- GC/MS
- Optical methods: NDIR, CRDS
- calibration and the WMO scale
- 14C
- Vertical measurements
- Mobile measurements
- Ground base remote sensing

GHG absorption bands in the EM spectrum

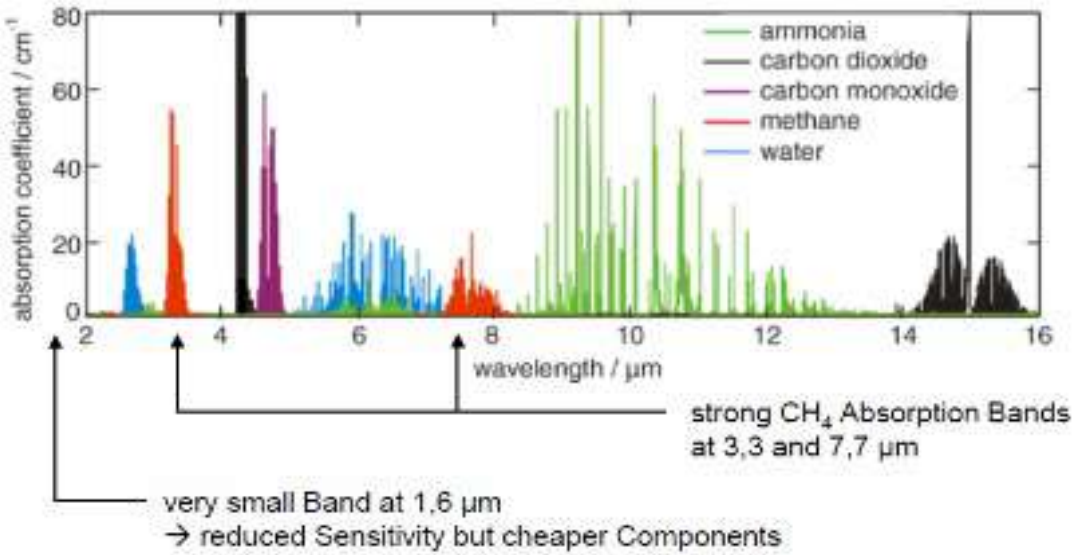

- Fourier Transform IR (FTIR): Infrared light from the light source passes through a Michelson interferometer along the optical path. The Michelson interferometer comprises a beam splitter, moving mirror, and fixed mirror. The light beam split into two by the beam splitter is reflected from both mirrors, before being recombined by the beam splitter. The intensity of the interference light is recorded in an interferogram, with the optical path difference recorded along the horizontal axis.

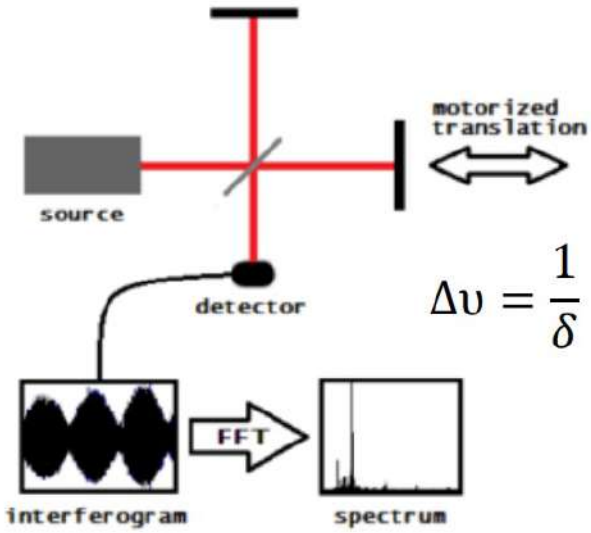

$$\Delta\upsilon = \frac{1}{\delta}$$

- Tunable Diode Laser Spectroscopy (TDLAS): The laser source comes from a diode, which induces a low spectral width, stability, compactness and ability to operate at ambient temperature. In addition to concentration, the device is also able to determine the temperature, pressure, velocity and mass flow of the observed gas

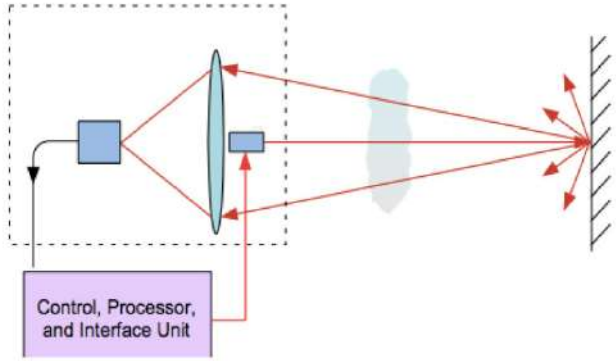

- **Cavity Ring-Down Spectroscopy (CRDS)**: two or three highly reflective mirrors trap a light beam in the optical vessel/cavity, allowing light to resonate. After obtaining the resonance in the cavity, the laser is switched off to allow for the measurement of the time of exponential decay of the light intensity exiting the cavity, which provides information on the concentration of the gas to be measured. This principle of loading and then unloading the cavity is that of the PICARRO instruments

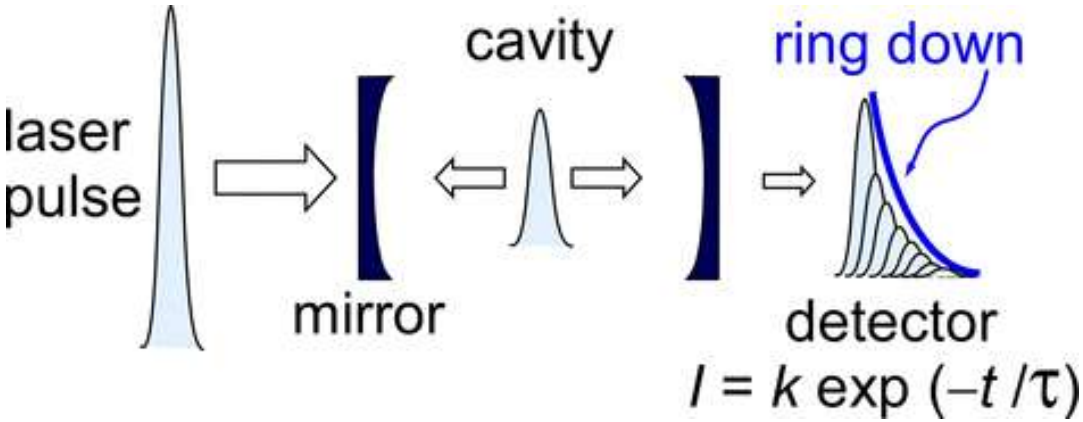

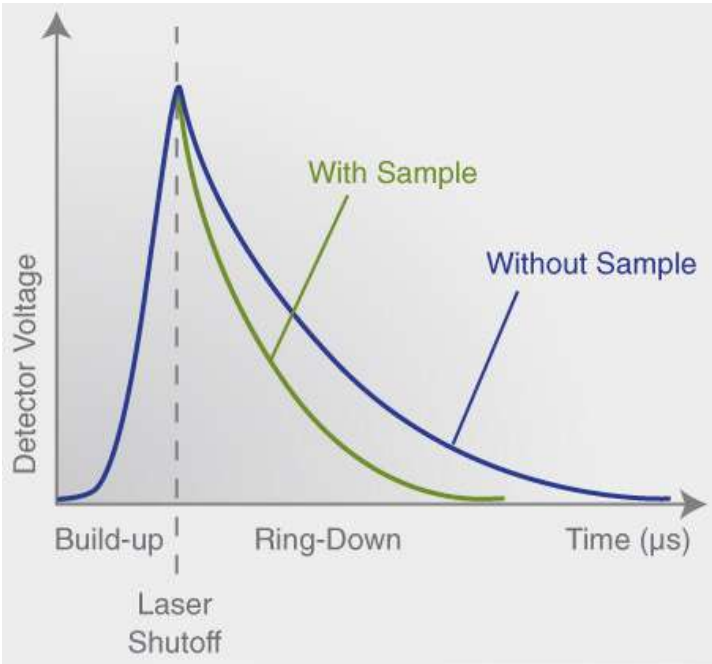

- **Off-Axis Integrated Cavity Output Spectroscopy (OA–ICOS)**: technology patented by ABB (formerly Los Gatos Research) based on CRDS. In this case, the laser penetrates the optical cavity (measurement cell) at an off-axis eliminates limitations of previou (extreme alignment stability and locking) based on the resonance laser, but maintains the long opt (thousands of meters) for ultra-h detection accuracy

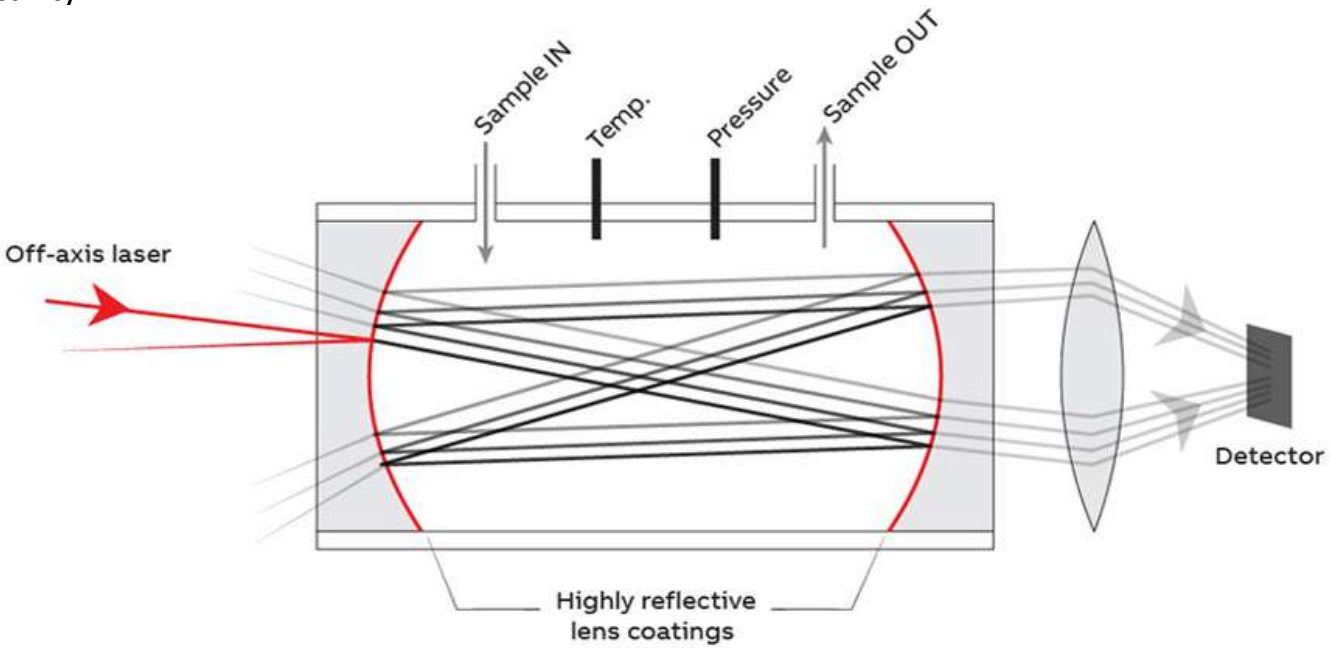

Atmospheric GHG measurement

- Why measuring atmospheric GHG composition?
- Stable isotopes
- Ppm vs umolmol-1
- GC/MS
- Optical methods: NDIR, CRDS
- Networks, calibration and the WMO scale
- 14C
- Vertical measurements
- Mobile measurements
- Ground base remote sensing

Integrated Carbon Observation System

- ❑ European Flagship Research Infrastructure - ICOS ERIC created 2015
  - 16 European member countries
- ❑ ICOS Atmospheric Thematic Center at LSCE
  - Internationally recognized metrology lab for GHG measurements
  - Reference protocols for ICOS Atmosphere
- ❑ NRT data provision to Copernicus Atmosphere
- ❑ First ICOS data release (atm) in summer 2018: 11 sites contributing,
  - 26 sites in R2020-1 (septembre)
- ❑ France/LSCE : One of the largest national atmospheric network in Europe

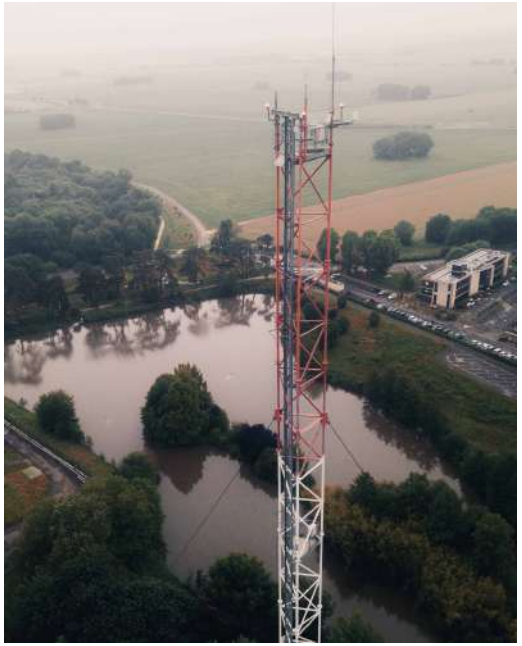

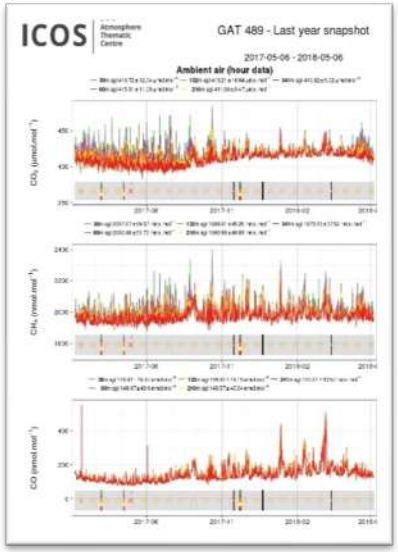

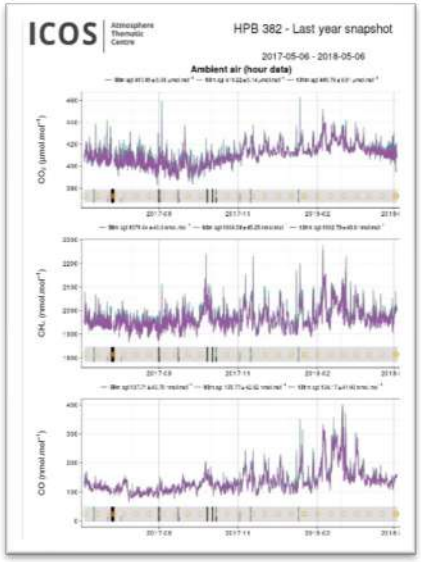

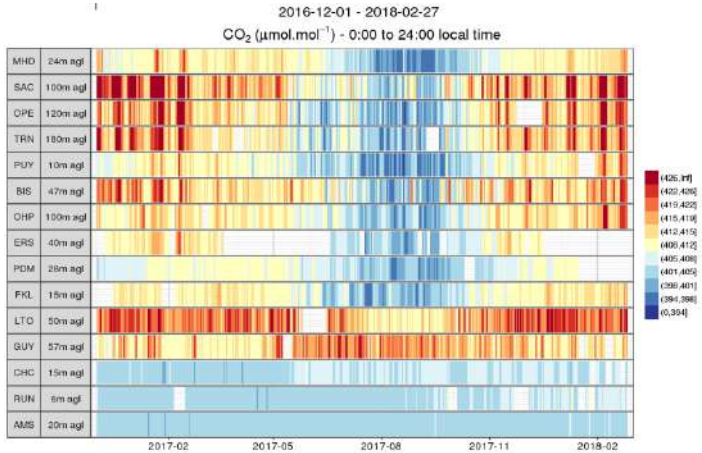

ICOS Atmospheric station:
Mandatory and optional parameters

Category	Gases, continuous	Gases, flask sampling	Meteorology	Eddy fluxes
Class 1 mandatory parameters	CO_2, CH_4, CO: at each sampling height	CO_2, CH_4, N_2O, SF_6, CO, H_2, CO_2 ^{13}C, ^{18}O and ^{14}C: sampled weekly at highest sampling height* ^{14}C (radiocarbon integrated samples): at highest sampling height	Air temperature, relative humidity, wind direction, wind speed: at highest and lowest sampling heights; atmospheric pressure at the surface; planetary boundary layer height*	
Class 2 mandatory parameters	CO_2, CH_4: at each sampling height		Air temperature, relative humidity, wind direction, wind speed: at highest and lowest sampling heights; atmospheric pressure at the surface	
Recommended parameters	^{222}Rn, N_2O, O_2 / N_2 ratio; CO for Class 2 stations	CH_4 stable isotopes, O_2 / N_2 ratio for Class 1 stations: sampled weekly at highest sampling height		CO_2: at one sampling height

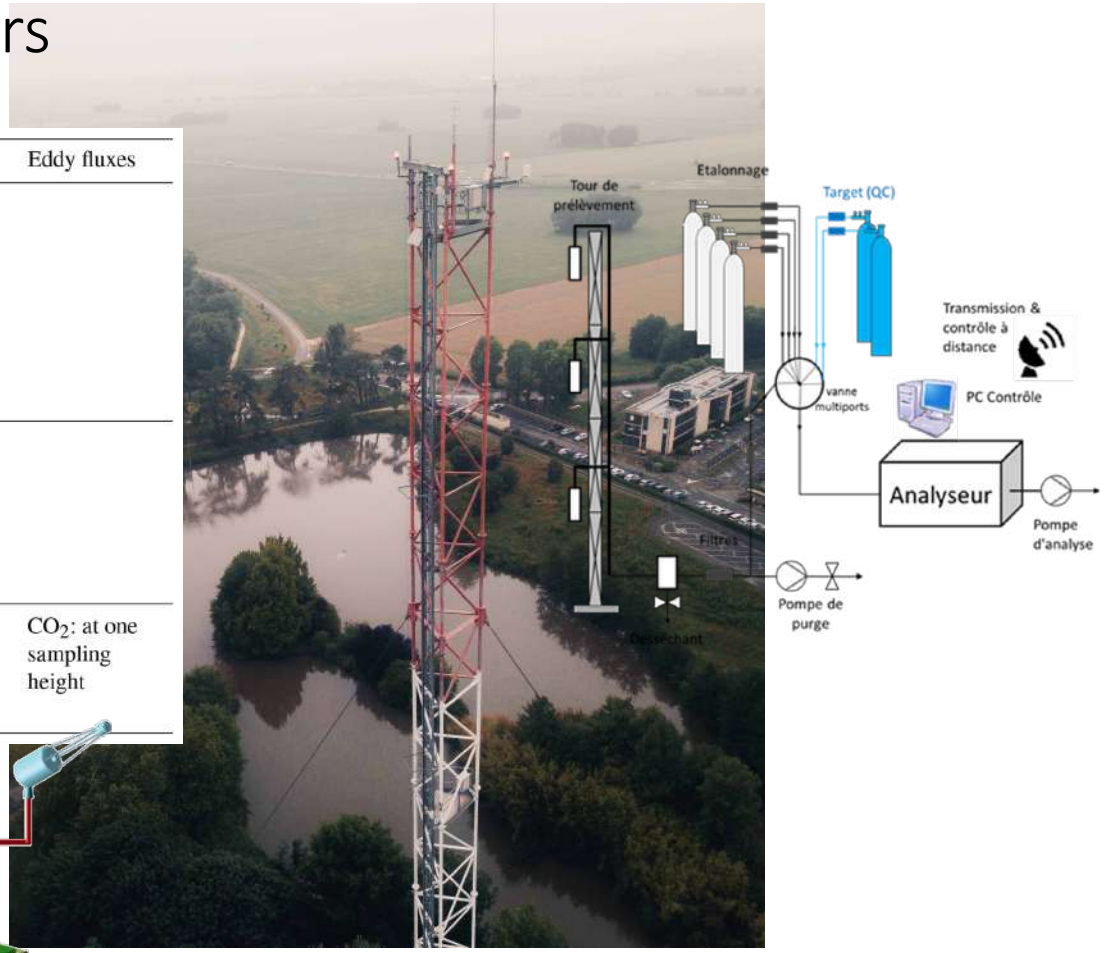

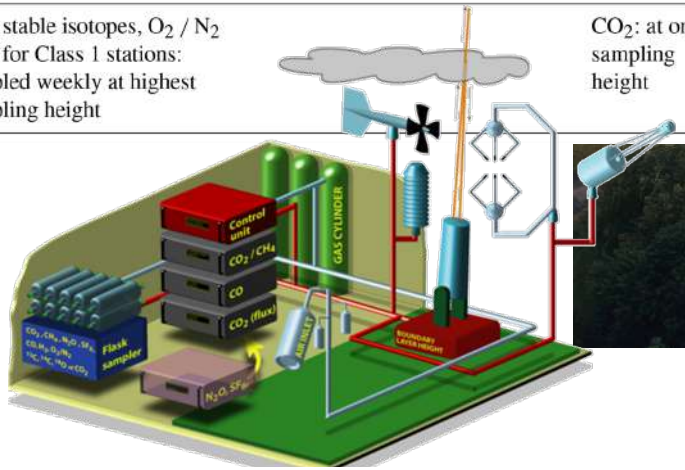

Yver et al., 2020

Near real time concentrations

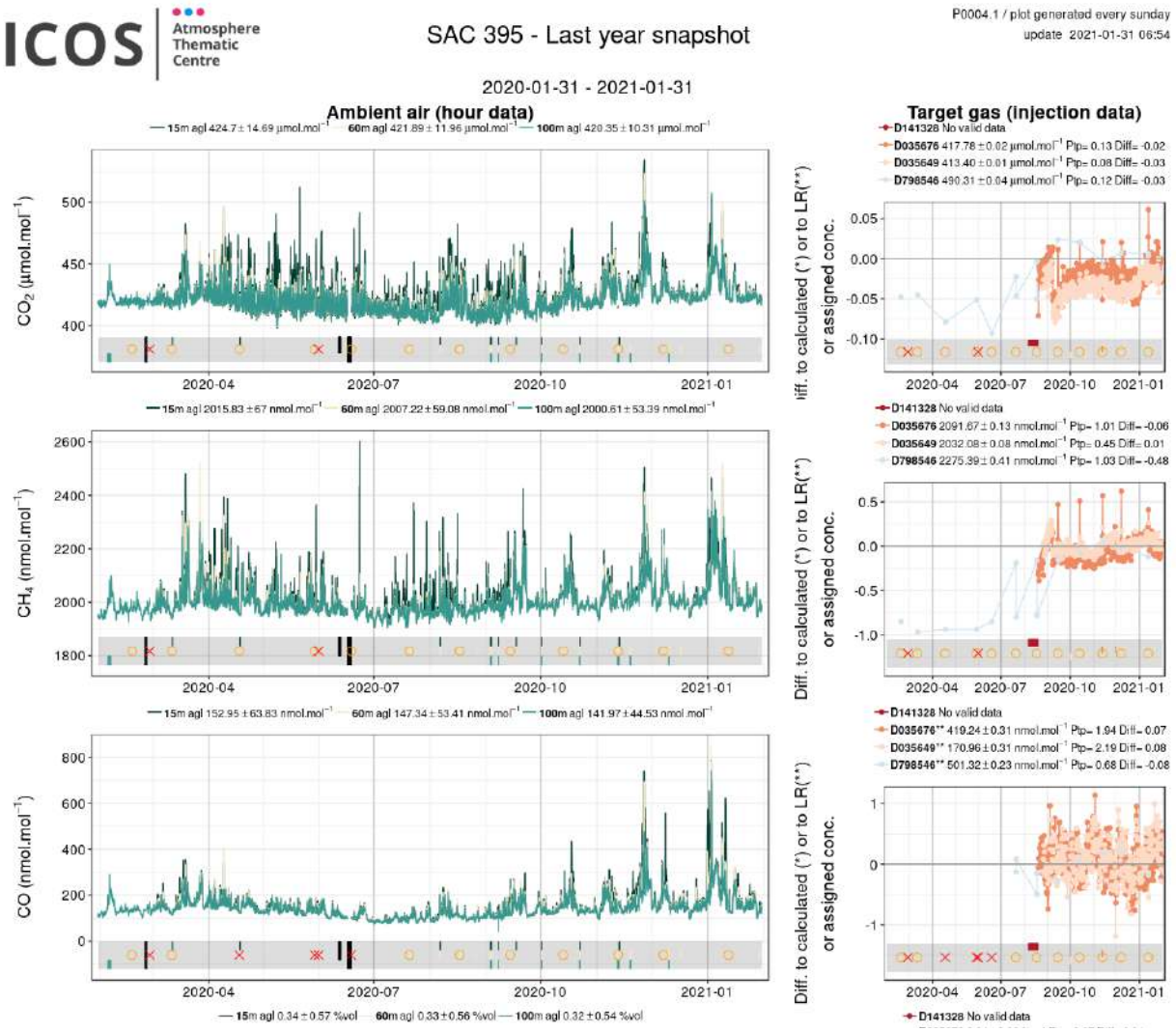

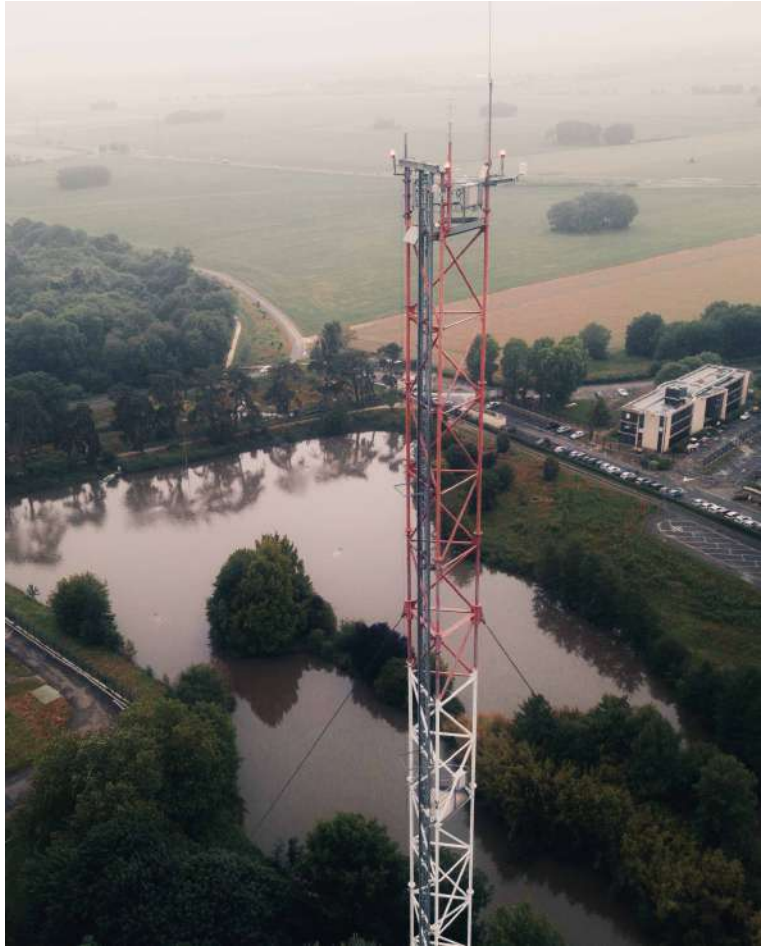

ICOS Atmosphere Thematic Centre

P0004.5 / plot generated every sunday
update 2021-01-31 07:00

Network concentration evolution

2014-01-01 - 2021-01-31

CO_2 ($\mu mol.mol^{-1}$) - 12:00 to 16:00 local time

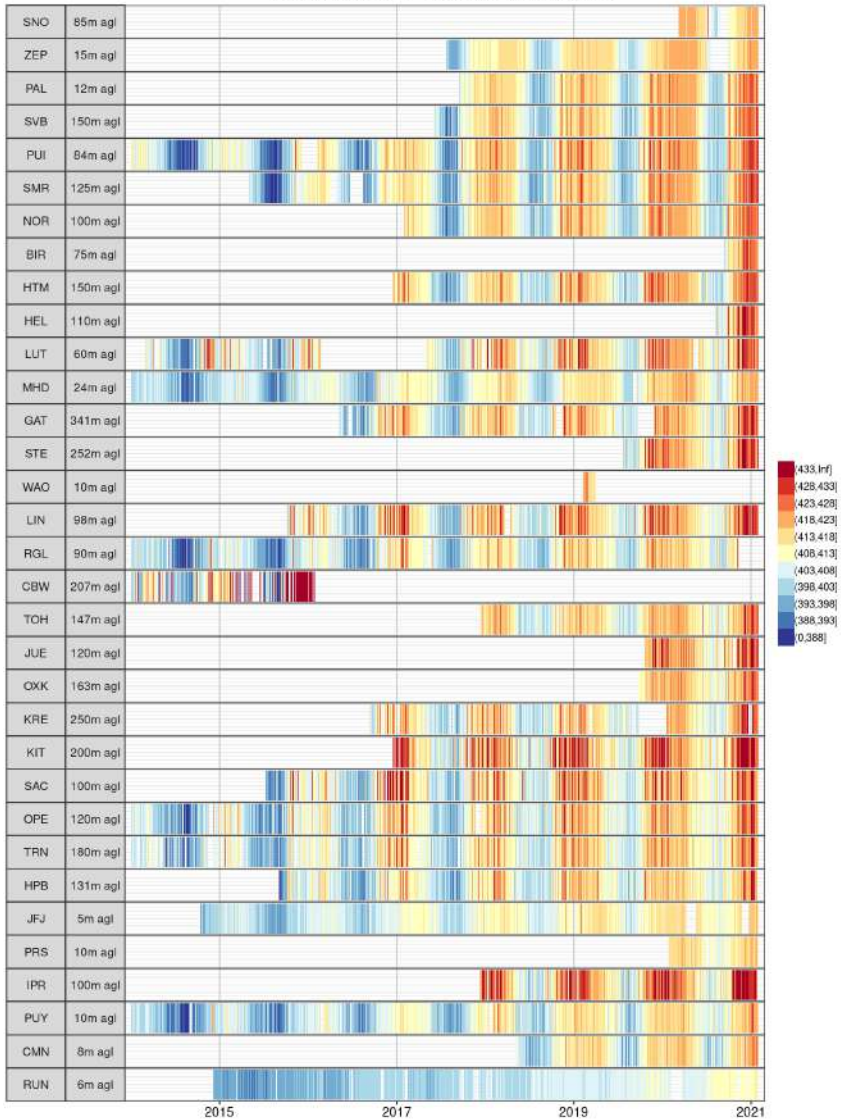

ICOS Atmosphere Thematic Centre

P0004.5 / plot generated every sunday
update 2021-01-31 07:06

Network concentration evolution

2014-01-01 - 2021-01-31

CH_4 ($nmol.mol^{-1}$) - 12:00 to 16:00 local time

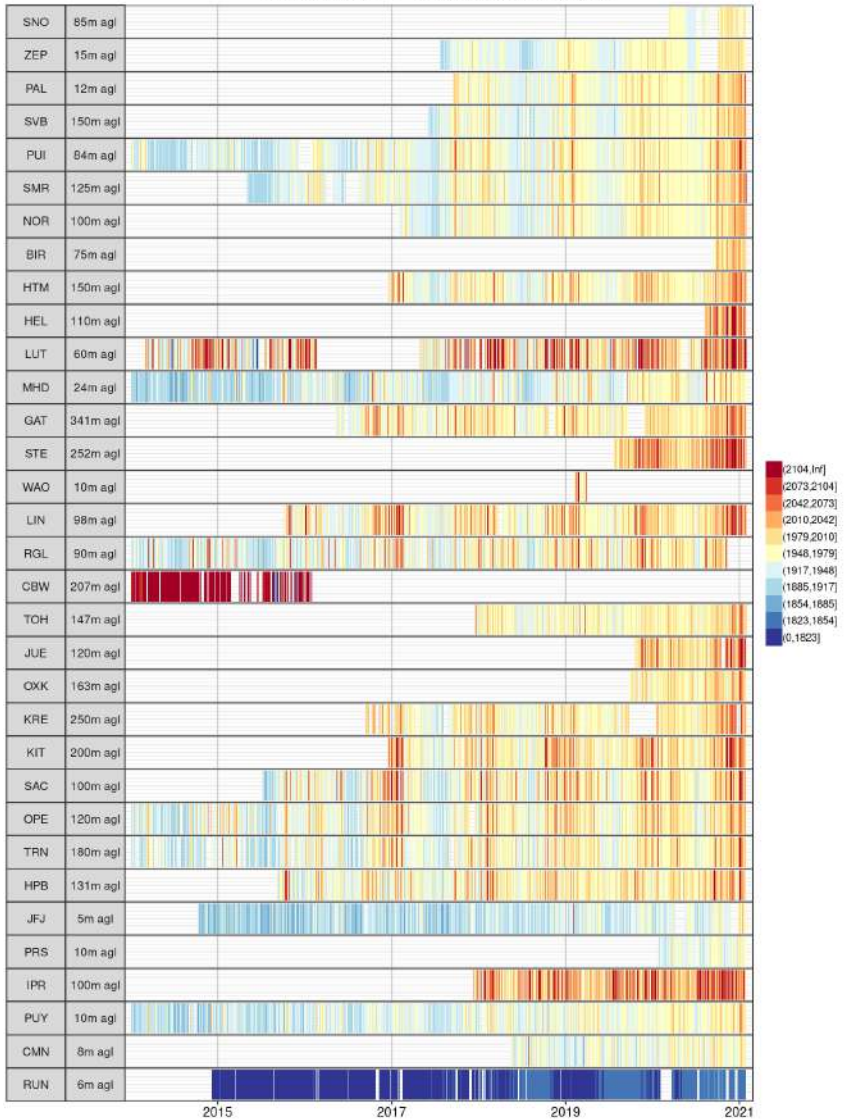

Precision vs accuracy

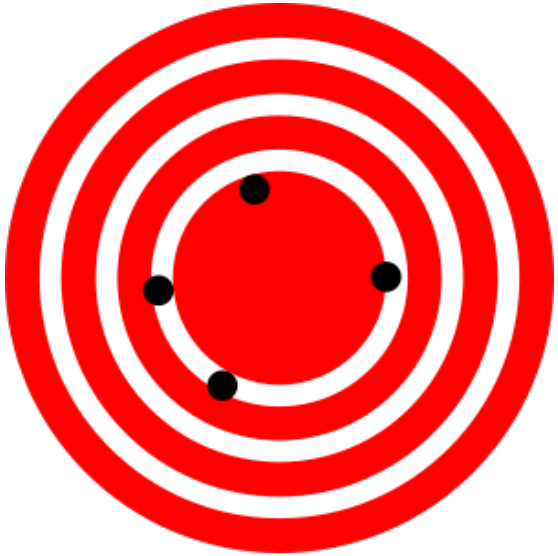

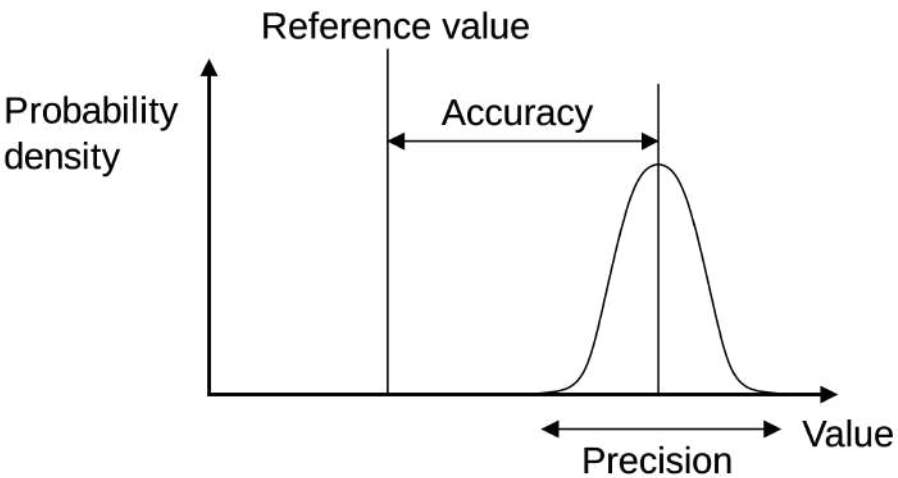

Wikipedia

What matters most when comparing measurements made by different laboratories?

Why ensure international standards for measurements?

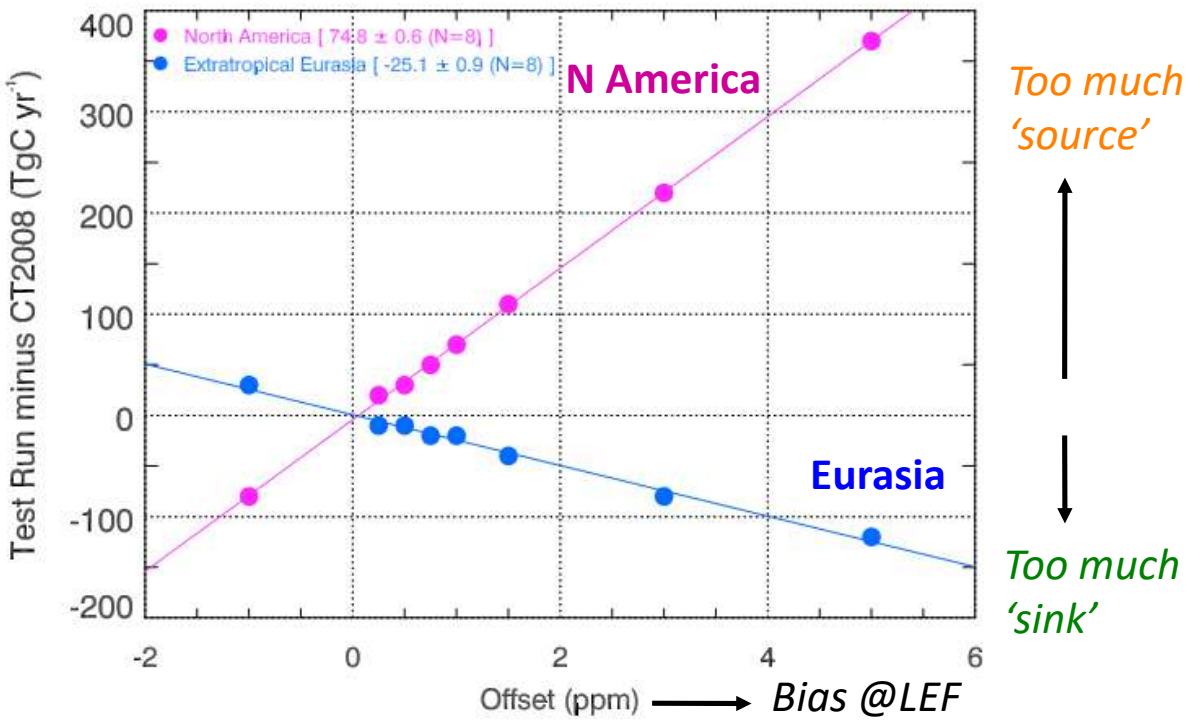

Example: Using globally available atmos. data, **estimated CO2 exchange** erroneously increase for N America and **decrease for Eurasia** when adding a positive hypothetical **measurement bias in Wisconsin** at LEF

K. A. Masarie et al. (2011), J. Geophys. Res., 116, D17305.

Atmospheric GHG measurement

- Why measuring atmospheric GHG composition?
- Stable isotopes
- Ppm vs umolmol-1
- GC/MS
- Optical methods: NDIR, CRDS
- calibration and the WMO scale
- 14C
- Vertical measurements
- Mobile measurements
- Ground base remote sensing

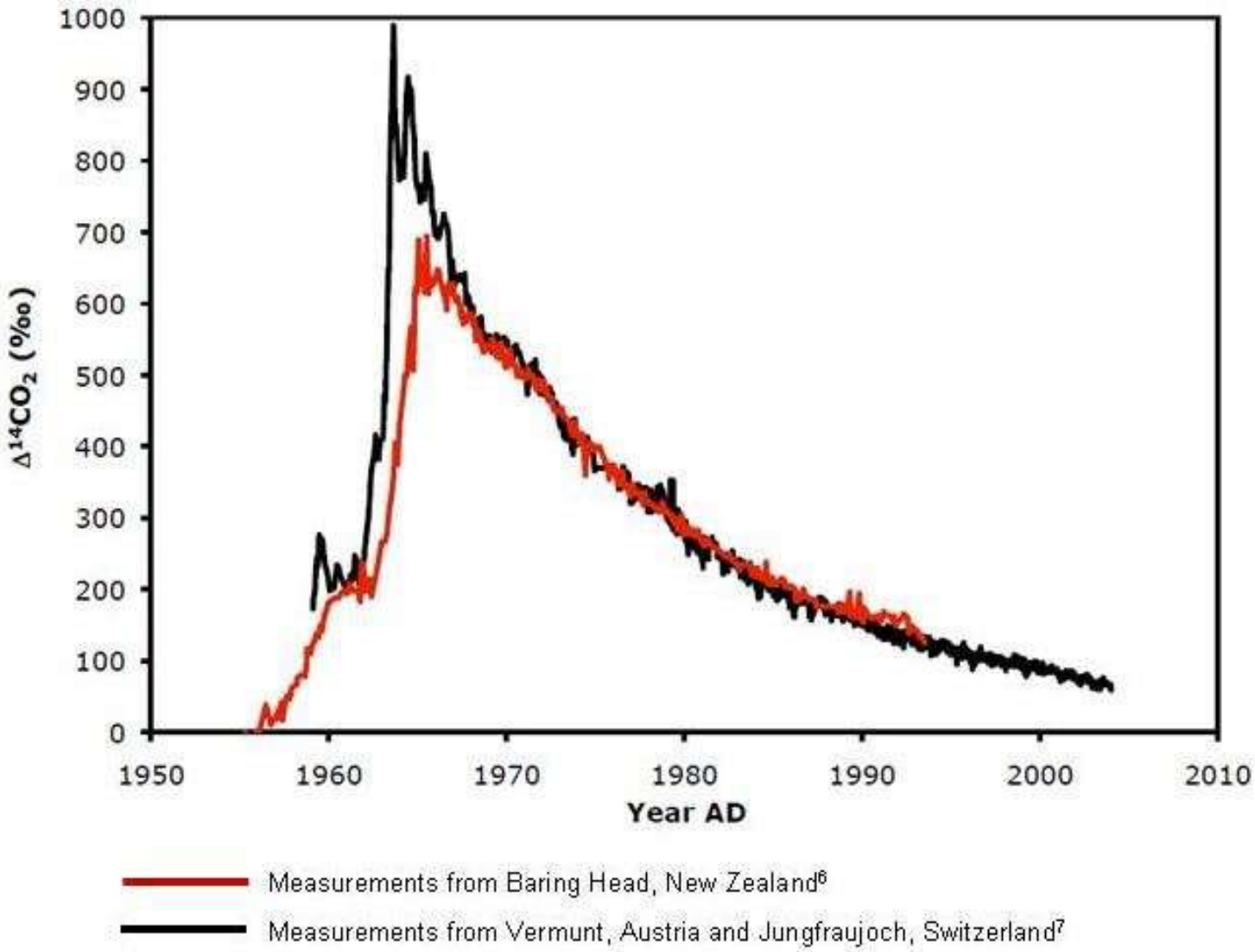
1000
900
800
700
600
500
400
300
200
100
0
$\Delta^{14}CO_2$ (‰)
1950
1960
1970
1980
1990
2000
2010
Year AD
Measurements from Baring Head, New Zealand[6]
Measurements from Vermunt, Austria and Jungfraujoch, Switzerland[7]

Measured $\Delta^{14}CO_2$ in East Asia and Colorado

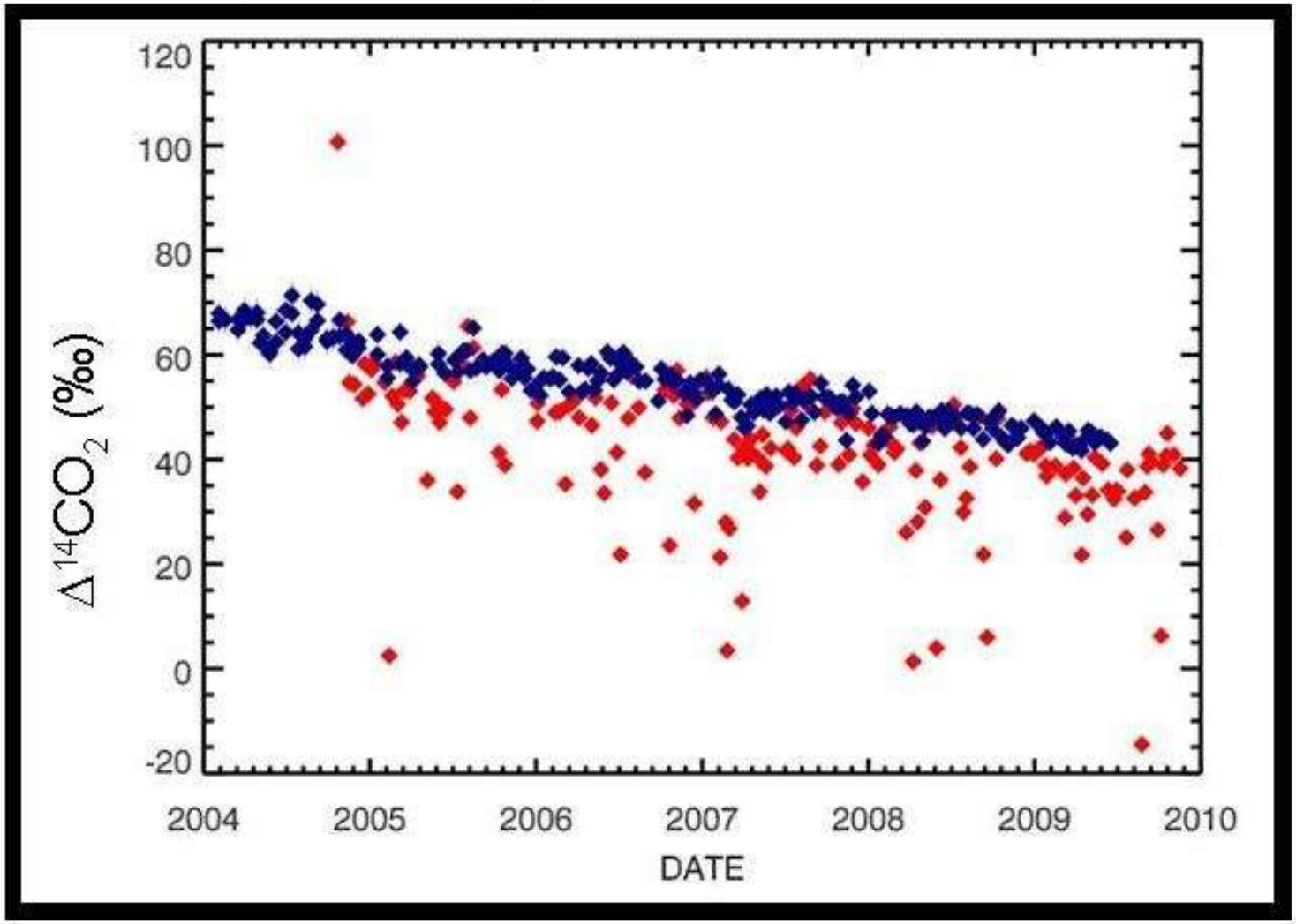

https://www.esrl.noaa.gov/gmd/outreach/isotopes/c14tellsus.html

Atmospheric GHG measurement

- Why measuring atmospheric GHG composition?
- Stable isotopes
- Ppm vs umolmol-1
- GC/MS
- Optical methods: NDIR, CRDS
- calibration and the WMO scale
- 14C
- Vertical measurements
- Mobile measurements
- Ground base remote sensing

Aircore sampling principles

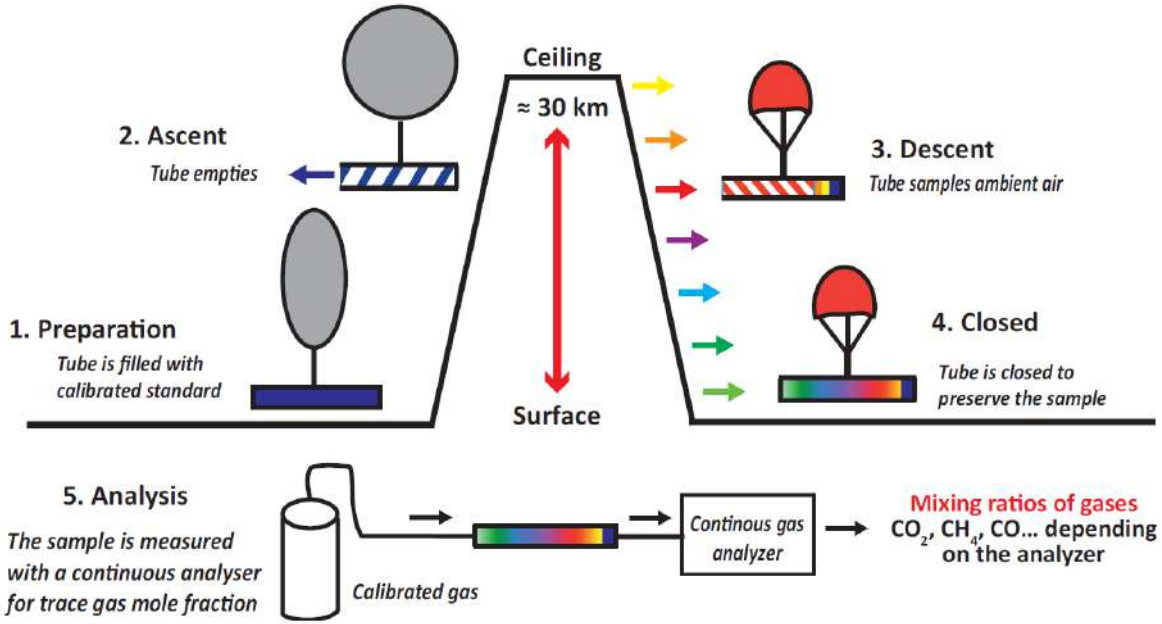

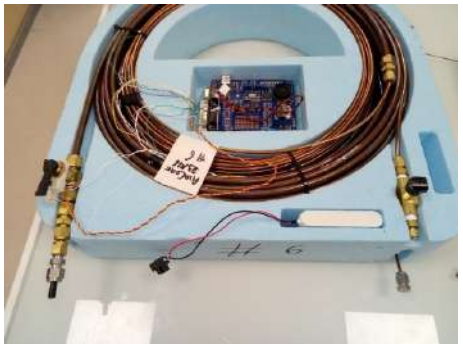

Membrive et al., 2017 (AMT)

Mesure des profils verticaux de concentration de GES : le programme AirCore-France

AirCore sous ballons météo.

- **AirCore = échantillonneur atmosphérique sous ballon** (Membrive et al., 2017)
- **2014**: démarrage du projet au LMD (Crevoisier et al.)
- **Depuis 2018** : lâchers depuis 4 sites en France coordonnés et analysés au LMD.
- **Fev. 2020 :** 100e vol AirCore-Fr !
- **Dès 2021**: lachers mensuels au passage de satellites à ASA et Reims

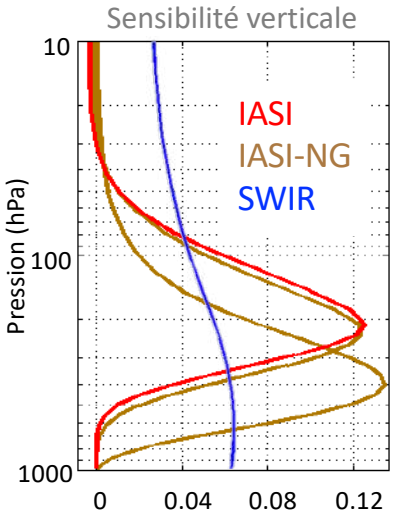

Validation des colonnes mesurées depuis l'espace

IASI-AirCore = 2,8±8,5 ppb
(18 colocalisations 2014-2019)

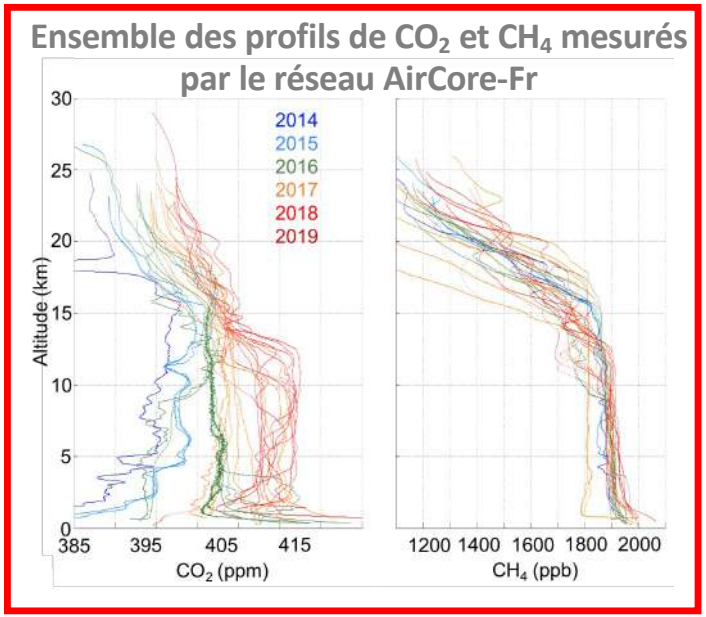

https://aircore.aeris-data.fr

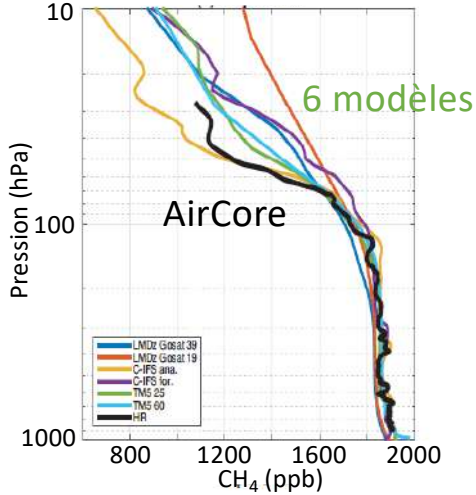

Evaluation des modèles de chimie-transport atmosphérique

→ Mise en évidence d'une sur-estimation systématique du CH_4 dans la stratosphère

Atmospheric GHG measurement

- Why measuring atmospheric GHG composition?
- Stable isotopes
- Ppm vs umolmol-1
- GC/MS
- Optical methods: NDIR, CRDS
- calibration and the WMO scale
- 14C
- Vertical measurements
- Mobile measurements
- Ground base remote sensing

LSCE aircraft measurement

- Piper Aztec ~monthly candle profiles up to 3km over ORL tall tower (forest)
- Flask sampling + in situ (CONDOR, Picarro)

YAK-AEROSIB aircraft campaigns in Siberia

https://yak.aeris-data.fr

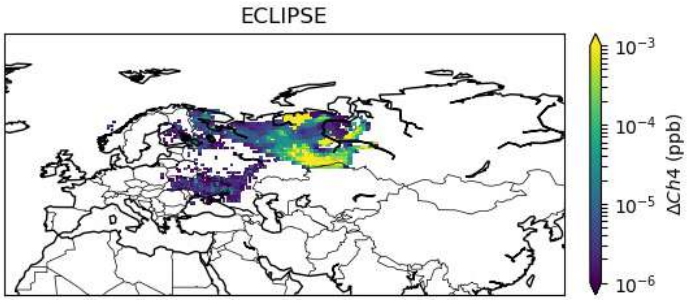

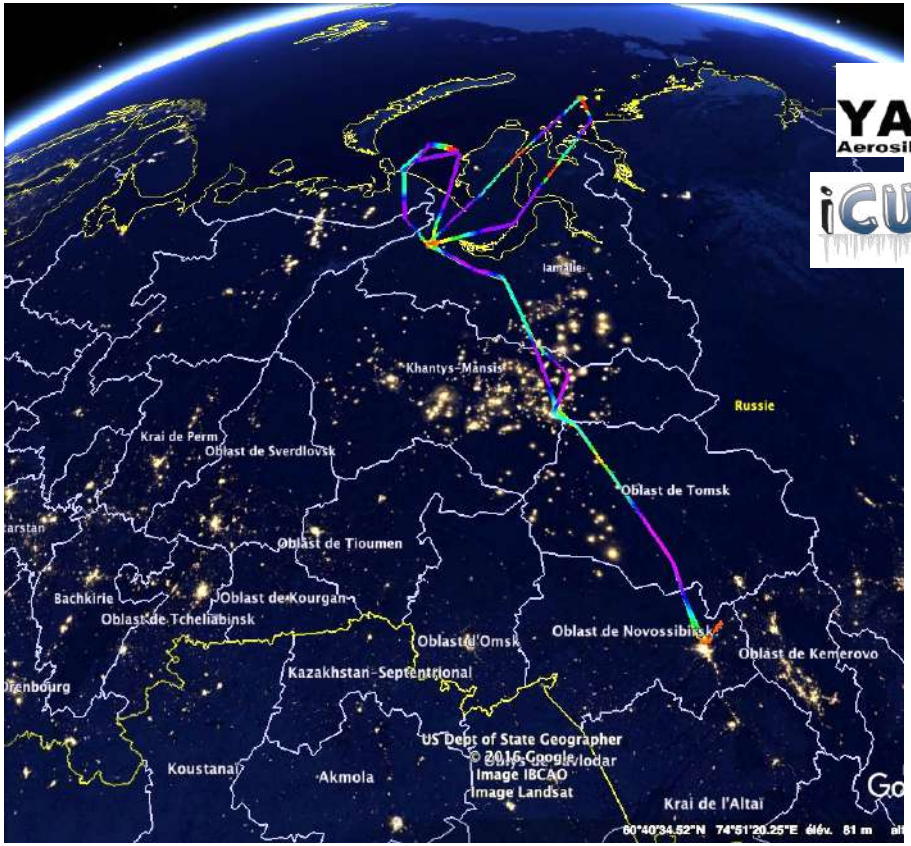

Paris et al., Petaja et al., 2020

Extreme pollutants and GHG concentrations in wildfire plumes

Tomsk->Mirny
31/07/2012

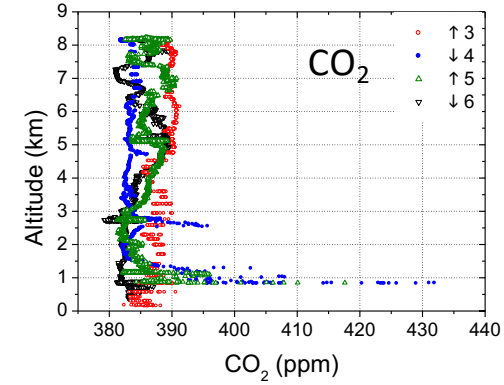

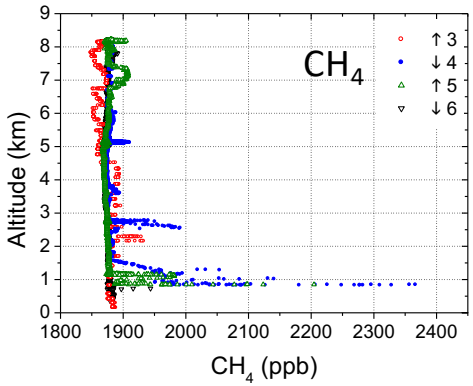

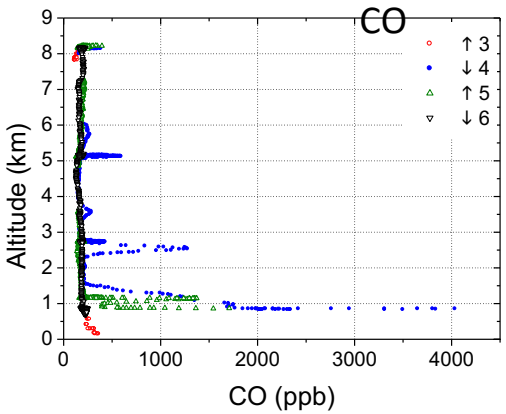

Tomsk-Mirny 31.07.2012

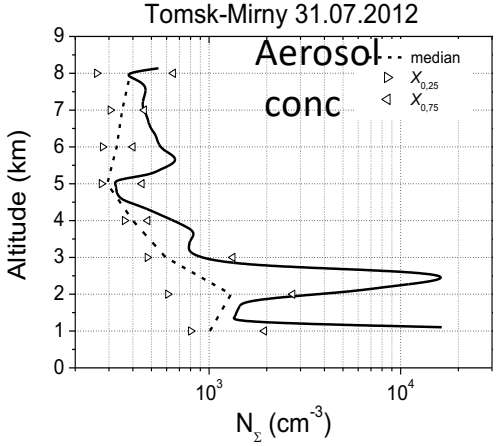

M. Yu. Arshinov et al., EGU, 2013

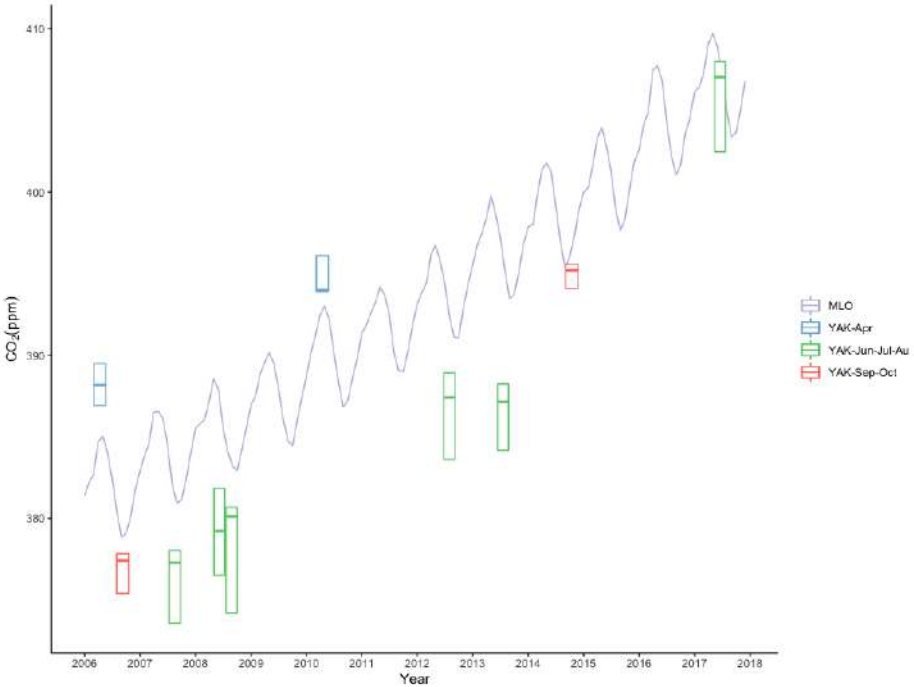

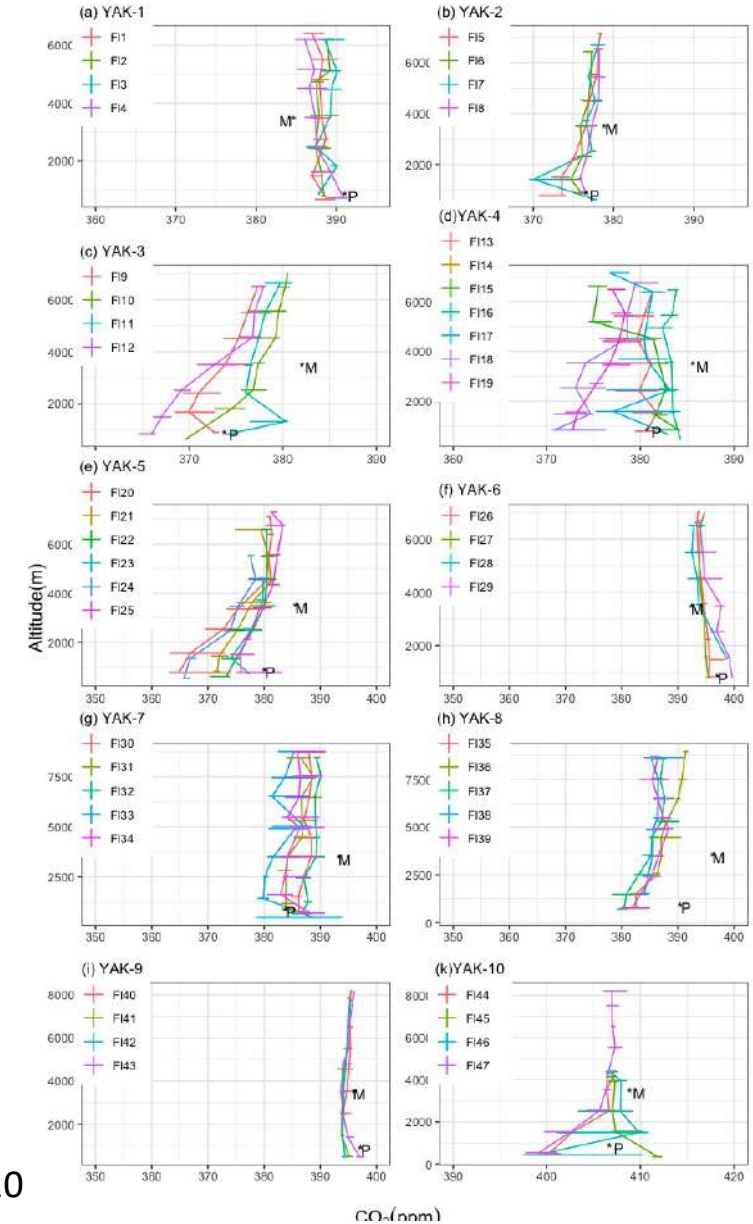

T. Huyen Vu & JD Paris, 2020

Biogenic vs anthropogenic CH4 in the Arctic: longitudinal gradient

Sept. 2020 campaign

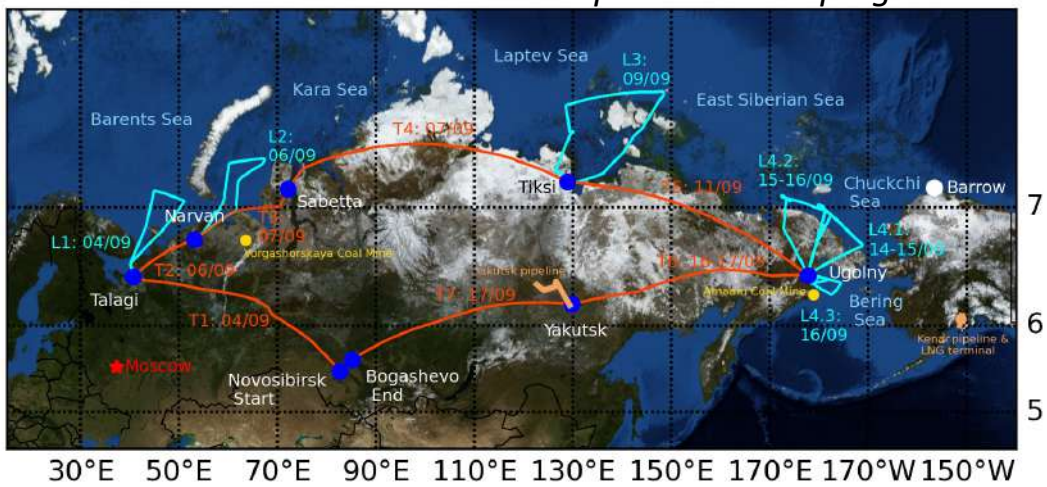

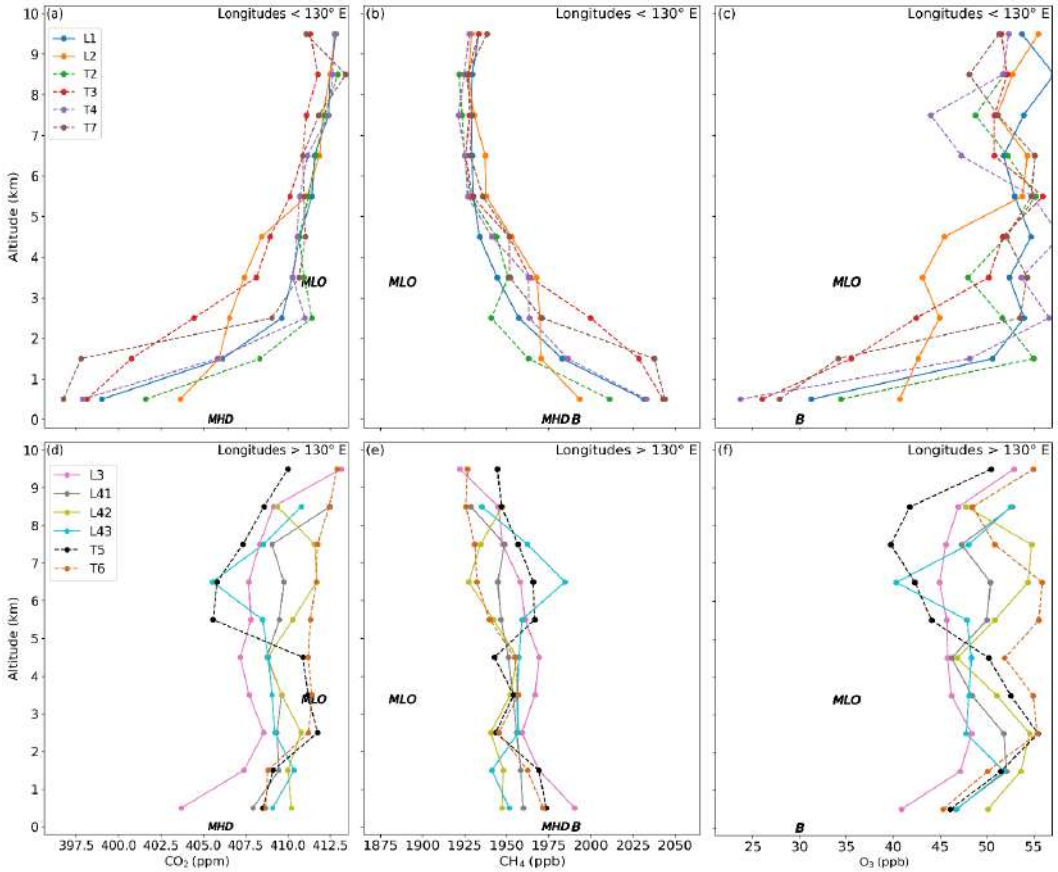

Narbaud et al., ACPD 2022

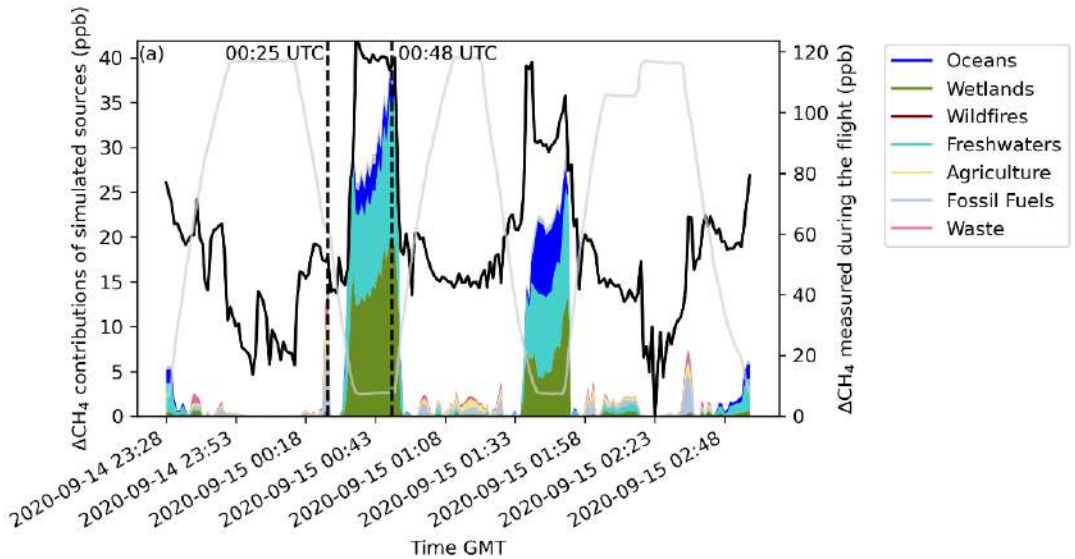

Shipborne & airborne measurements.

- **The Middle East region is poorly covered by current networks**
- **What is the contribution from oil and gas sources?**

Paris et al., 2019

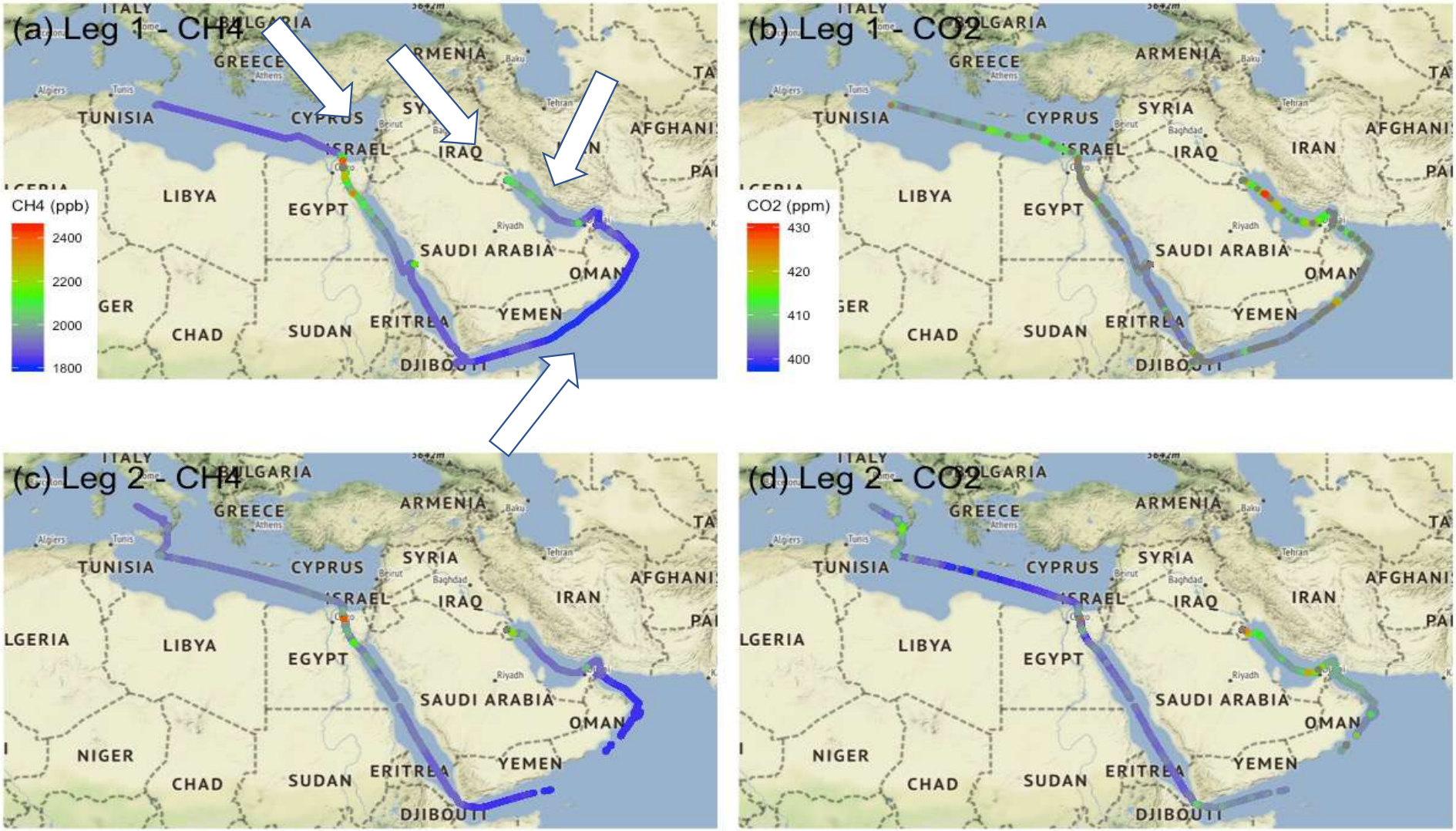
(a) Leg 1 - CH4
CH4 (ppb)
2400
2200
2000
1800
(b) Leg 1 - CO2
CO2 (ppm)
430
420
410
400
(c) Leg 2 - CH4
(d) Leg 2 - CO2
TUNISIA
LIBYA
EGYPT
SAUDI ARABIA
OMAN
YEMEN
ERITREA
DJIBOUTI
SUDAN
CHAD
NIGER
LGERIA
CYPRUS
ISRAEL
IRAQ
SYRIA
IRAN
ARMENIA
GREECE
BULGARIA
ITALY
AFGHANI

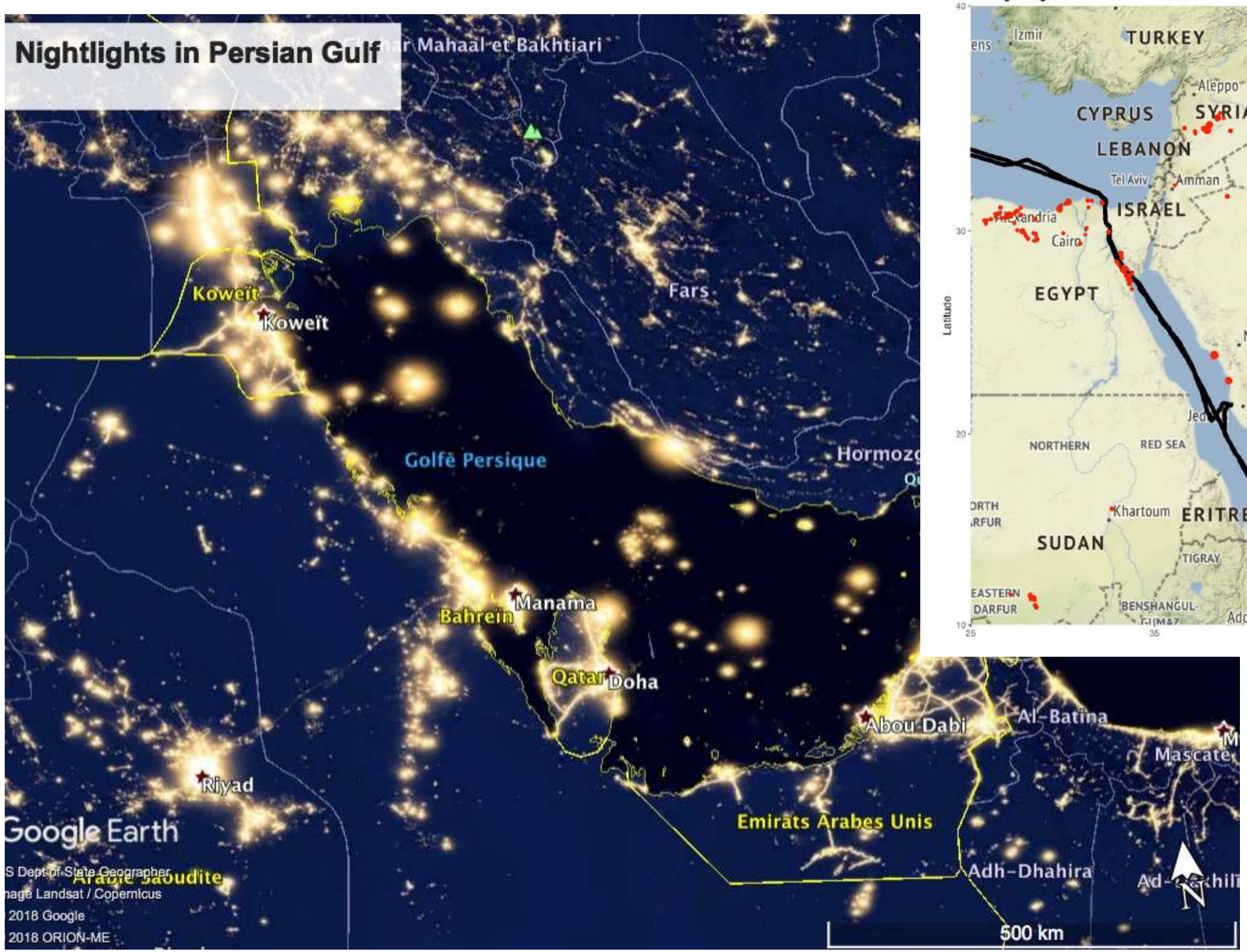
Nightlights in Persian Gulf
Mahaal et Bakhtiari
Koweit
Koweït
Fars
Golfe Persique
Hormoz
Bahrein
Manama
Qatar
Doha
Abou Dabi
Al-Batina
Mascate
Riyad
Emirats Arabes Unis
Adh-Dhahira
Arabie Saoudite
Google Earth
S Dept of State Geographer
nage Landsat / Copernicus
2018 Google
2018 ORION-ME
500 km
N

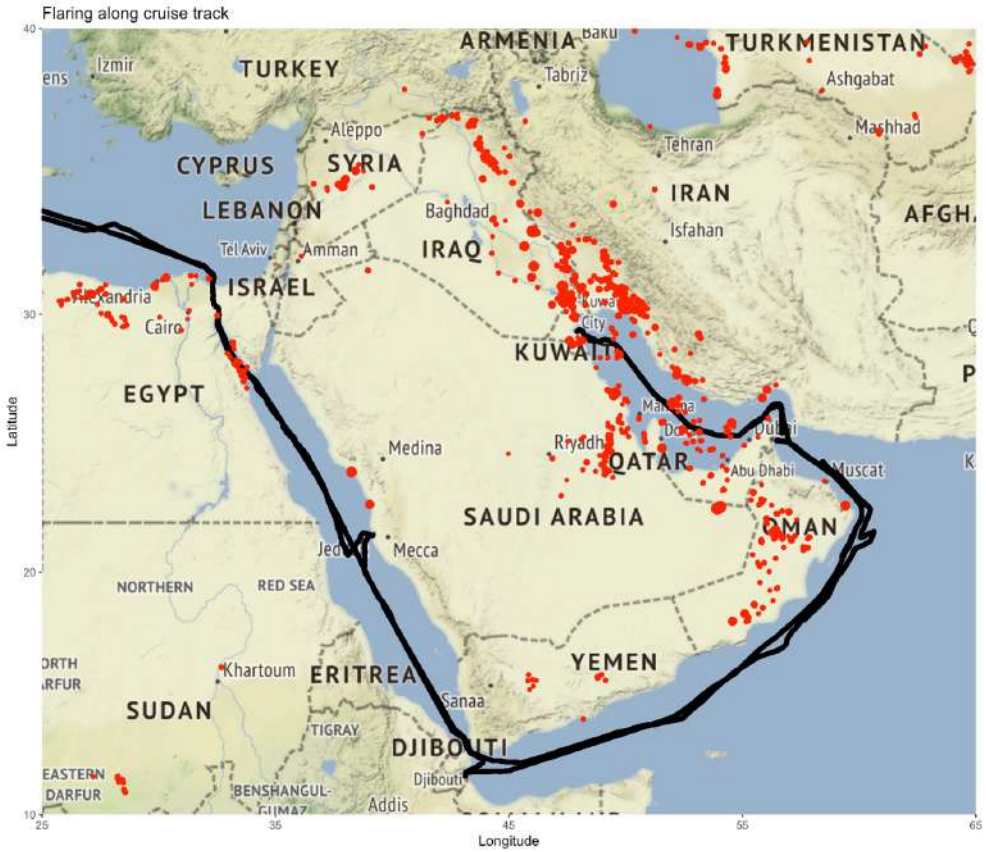
Flaring along cruise track
ARMENIA
TURKMENISTAN
TURKEY
Izmir
Tabriz
Ashgabat
Aleppo
Mashhad
Tehran
CYPRUS
SYRIA
IRAN
LEBANON
Baghdad
Isfahan
Tel Aviv
Amman
IRAQ
ISRAEL
Alexandria
Cairo
KUWAIT
EGYPT
Medina
Riyadh
QATAR
Abu Dhabi
Muscat
SAUDI ARABIA
OMAN
Jeddah
Mecca
NORTHERN
RED SEA
YEMEN
Khartoum
ERITREA
SUDAN
Sanaa
TIGRAY
DJIBOUTI
Djibouti
EASTERN
DARFUR
Addis
Latitude
Longitude

Excess methane mainly from oil and gas in the Middle East

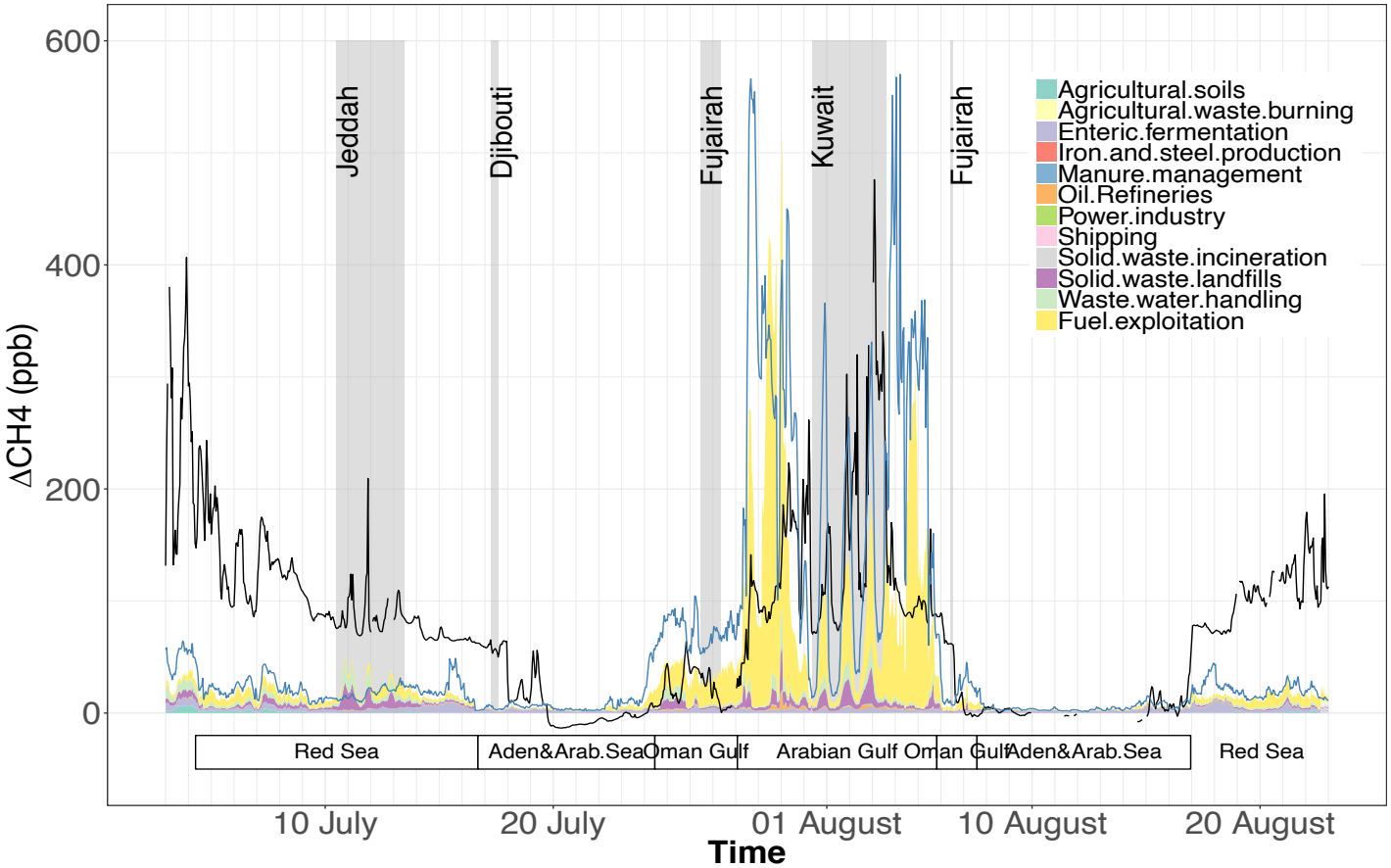

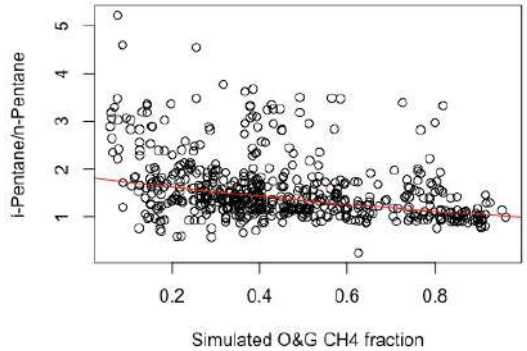

Pilot applications in urban landscapes (PAUL)

A response to the Green Deal H2020-LC-GD-2020

Lead: ICOS-ERIC

Observational approaches

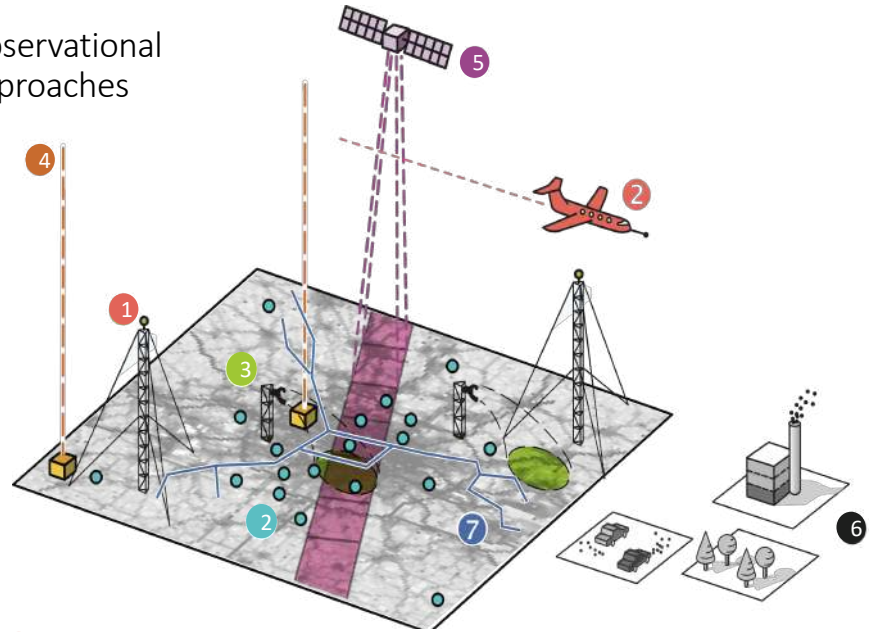

1. High-precision tall tower network & $^{14}CO_2$
2. Roof- and street-level network
3. Tall eddy covariance towers
4. Ground-based total column network
5. Satellite-based total column observations
6. Biogenic process studies

Paris

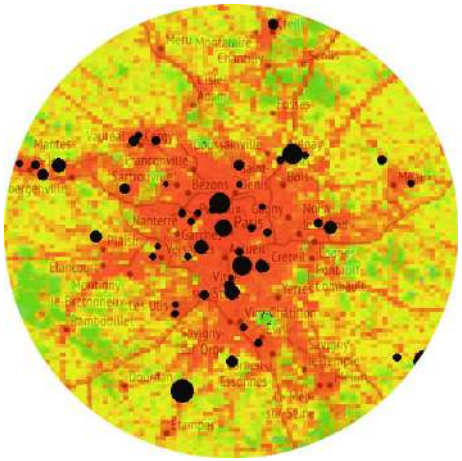

10 high-precision sites
30 roof-level sensors

Munich

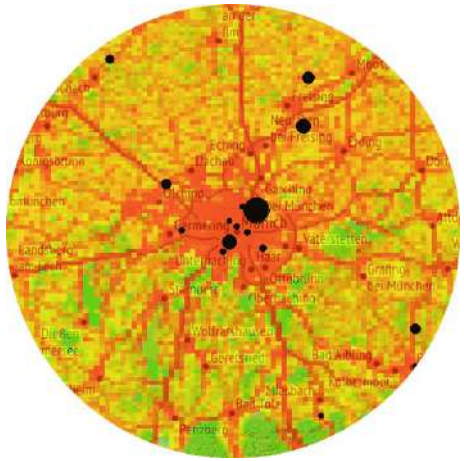

20 roof-level sensors
100 street-level sensors

Zurich

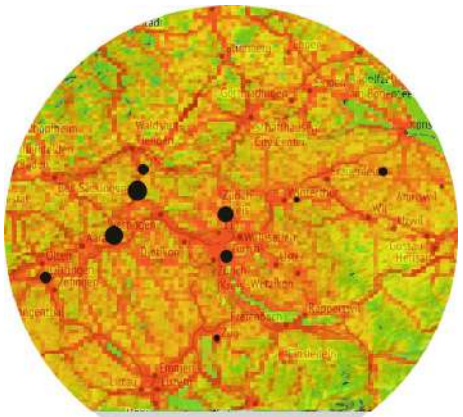

20 roof-level sensors
60 street-level sensors

$ffCO_2$ Emissions
kg yr^{-1} m^{-2}

1e+08
1e+06
1e+04
1e+02

$ffCO_2$ Point sources
kg yr^{-1}

1e+06
1e+07
1e+08
1e+09

Impact of lockdown on measured emissions in Paris, France

Atmospheric CO_2 monitoring over the Greater Paris region + near-real-time emission inventory + atmospheric Bayesian inverse model.
$FFCO_2$ emissions : decreases by 42–53% during the first lockdown with stringent measures and by only 20% during the second lockdown.
Both reductions are mainly due to decreases in traffic.
Atmospheric CO_2 monitoring makes it possible to identify significant emission changes (>20%) at subannual time scales over an urban region.

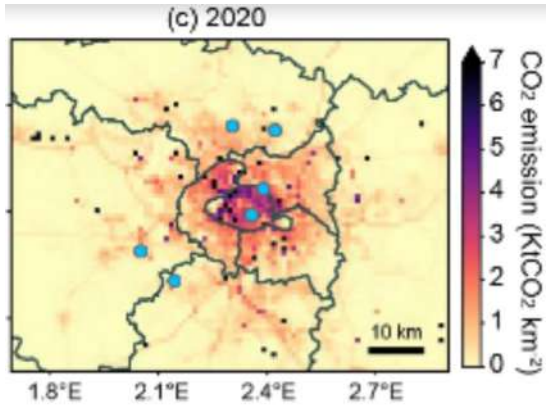

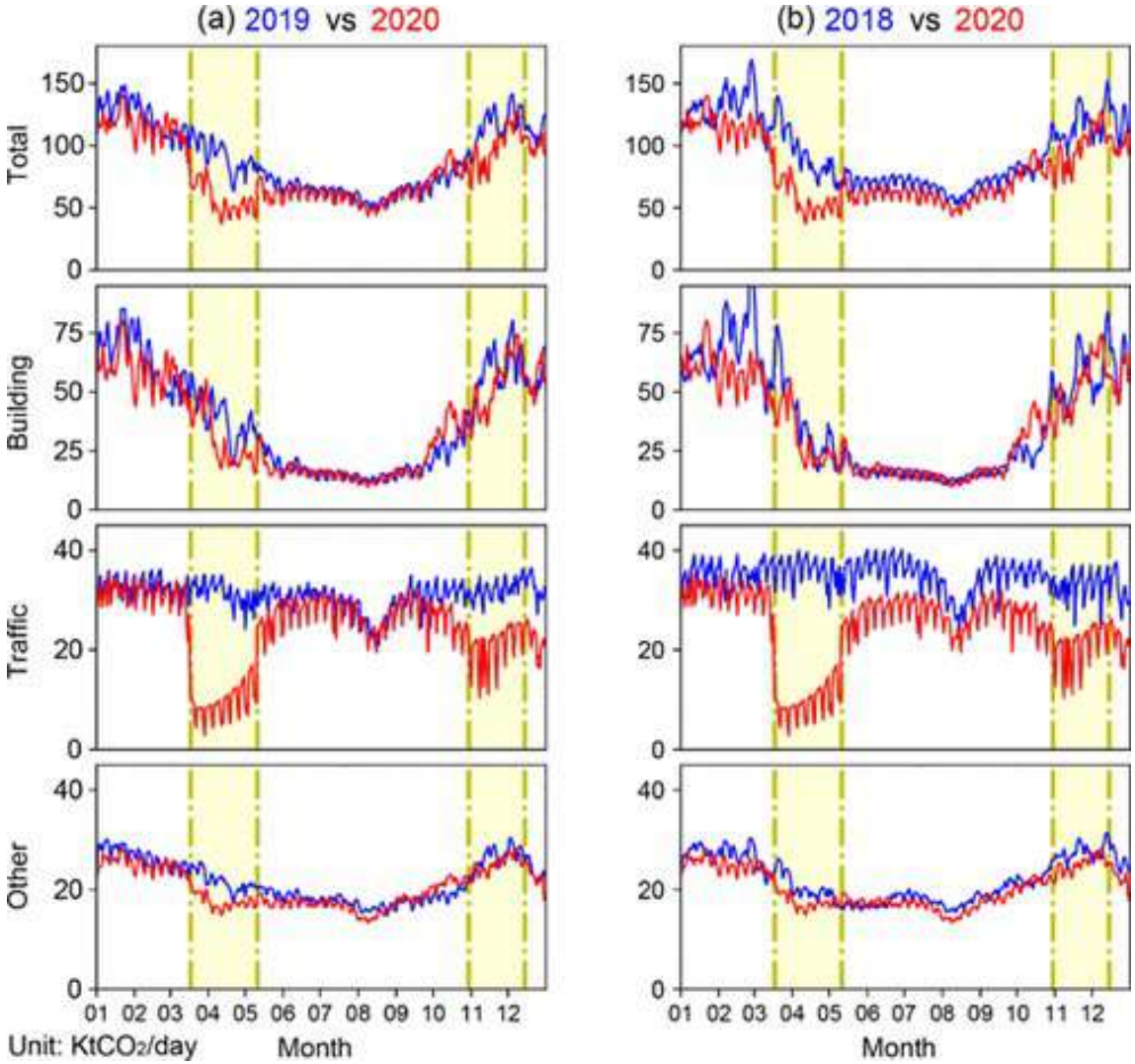

Lian et al., 2022

Verifying national emission inventories: the case of Cyprus

Liu et al. submitted to ERL

- In Cyprus, 98% methane emissions are from waste and agriculture.
- Mobile measurements account for about 28% of total CH_4 emission in Cyprus.
- Landfills: 160% higher than inventory .
- closed landfills may be a significant, underestimated CH_4 emission source.
- Livestock (cattle): 40% higher than inventory.
- 21% uncertainty for mobile emission estimates,

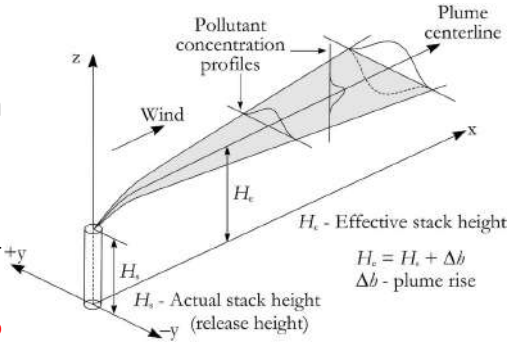

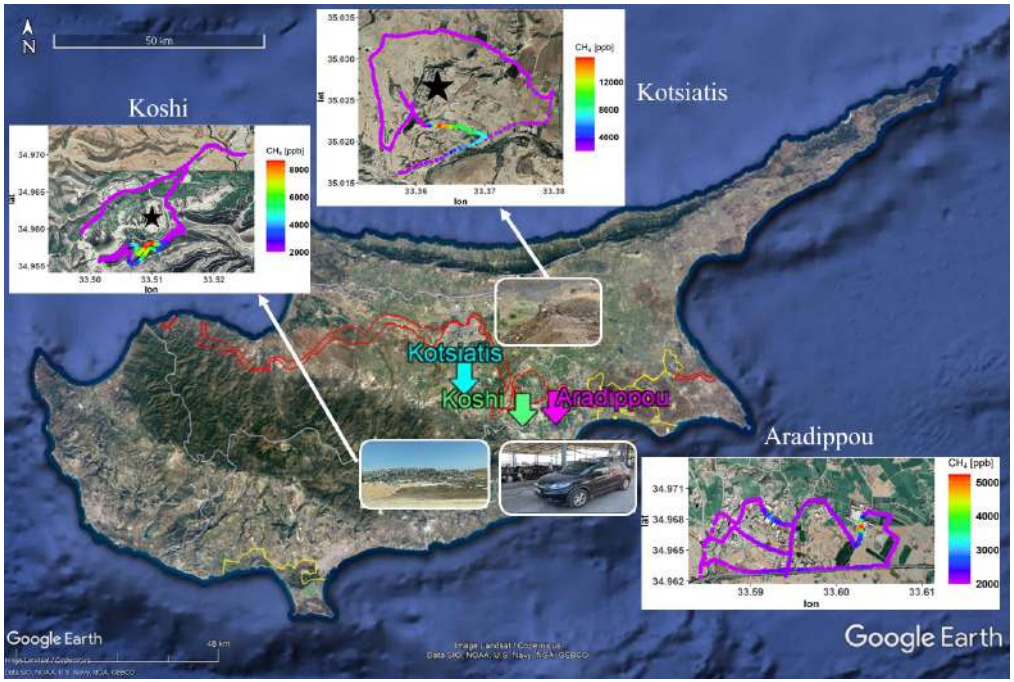

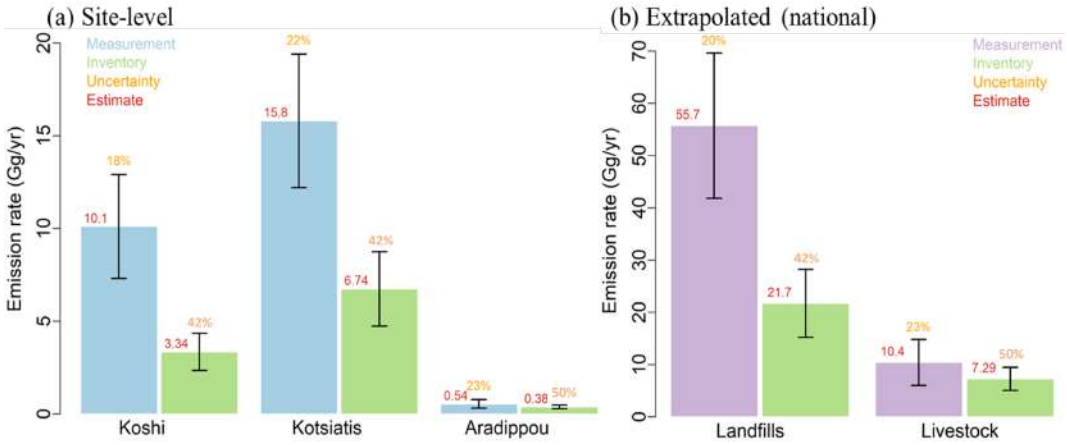

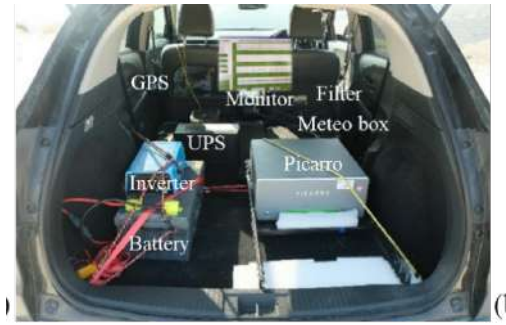

Imaging methane in the infrared

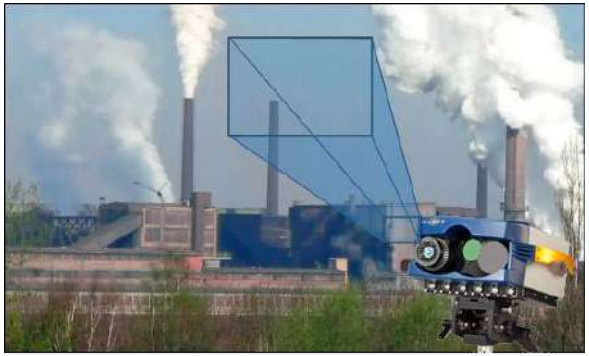

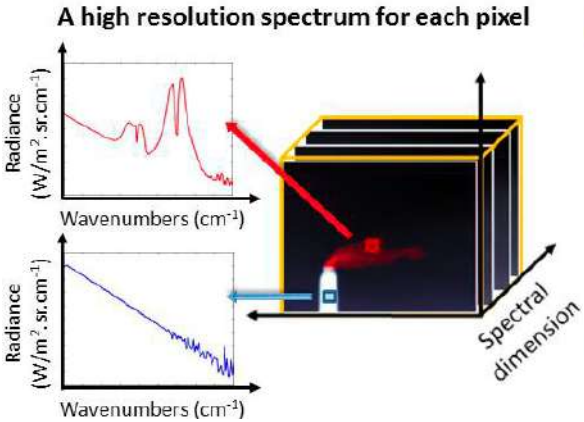

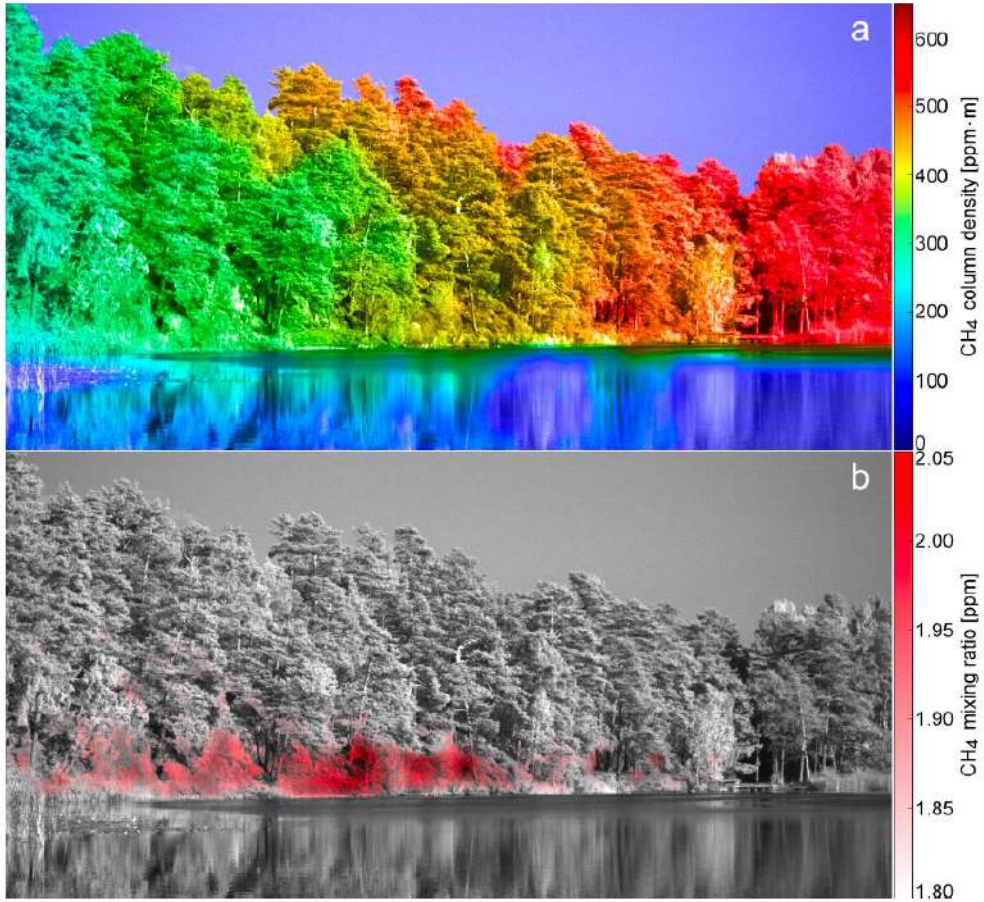

Galfalk et al., 2015

Mesure des sources de methane à l'echelle du site industriel

Shah et al.

MEMO2

Defratyka et al., subm.

Joly et al. (GSMA, Total)
AMULSE/AUSEA

Emission calculation – tracer diespersion method

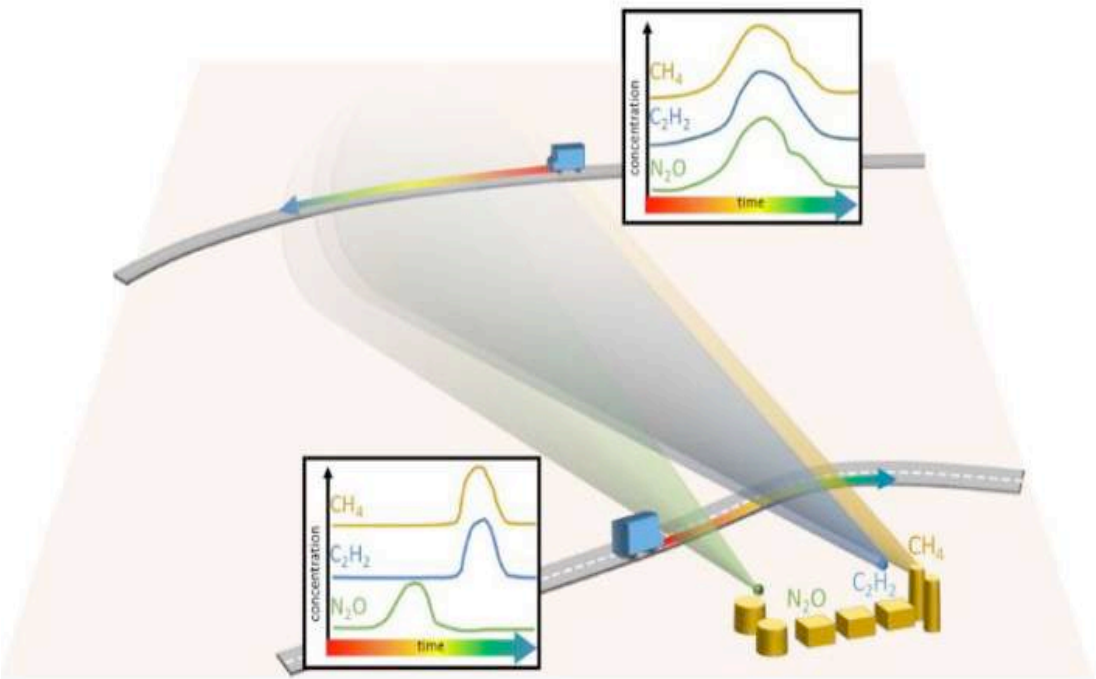

- Mobile platform **measures CH_4 and tracer gas** in the same time (e.g. C_2H_2)
- **Release tracer gas with known emission** rate
- Assumption: **the same emission way** of the tracer gas as CH_4 (e.g. dispersion, chemical reaction)

The **tracer ratio equation** for CH_4 source emission $E_{gas} = E_{tracer} \frac{C_{gas}}{C_{tracer}}$

Disadvantages ---

- dependence on **weather conditions** & **road access**,
- a **snapshot in time** – no temporal variation
- Required access to the measured site

Advantages +++

+ measurements of **whole plume**
+ information about site's **total emssions**
+ visible **wind influence** for emission
+ data can be used as **improving input for models**

S. Ars et al 2017

S. Defratyka et al., 2020

Emission calculation Gaussian plume model

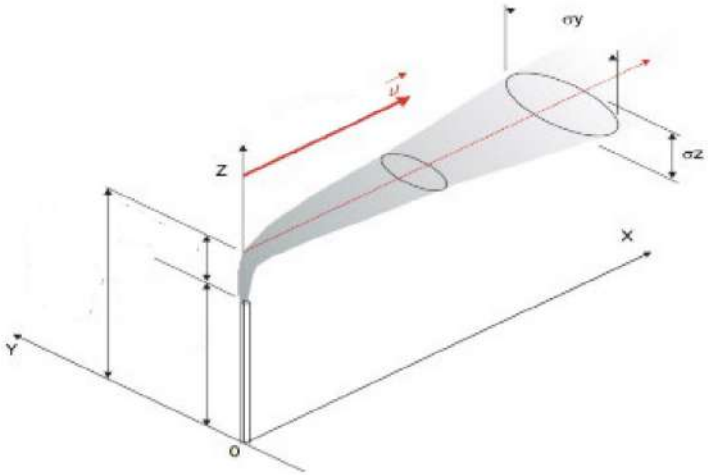

Example of modelled CH_4 concentration

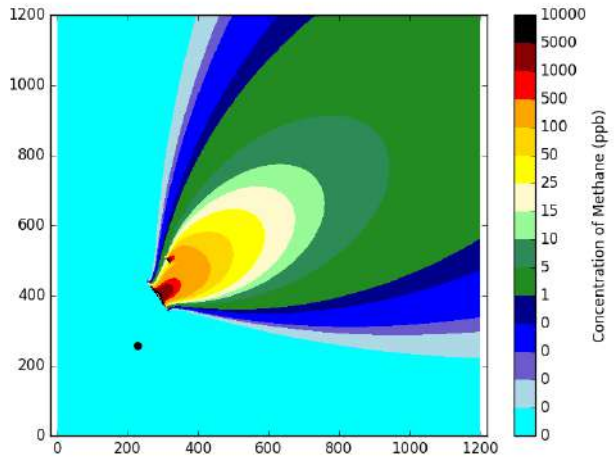

Examples of modelled and observed CH_4 – one plume crossing

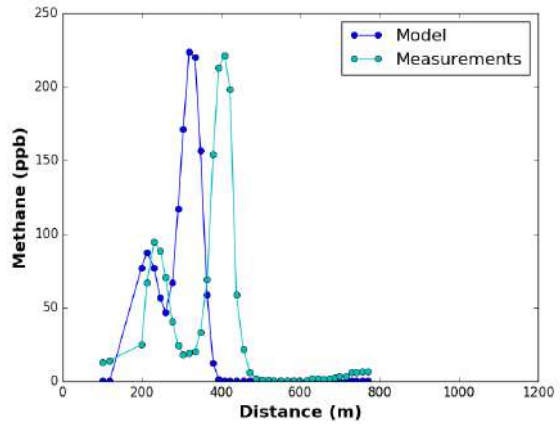

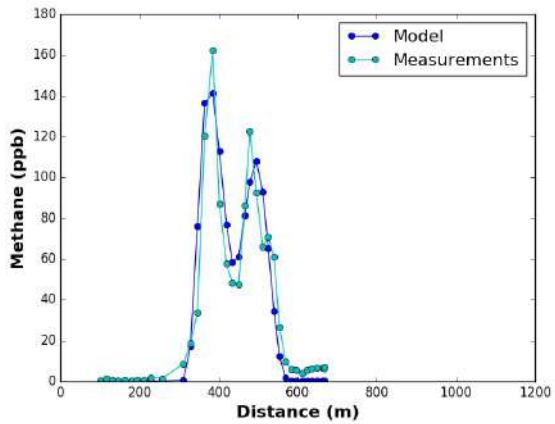

Model input: meteo data + known emission rate (e.g 1 g/s)

↓

Compare model results with observed concentration

↓

Calculation emission rate from the source

Mapping methane sources in Paris

- Driving 720km in Paris and suburbs with in-situ optical analyzers
- Peak-based approach + isotopic signatures + hand-held sensor
- Identification of previously unquantified sources in Paris : sewage, furnaces
- Paris is in the lower range of known cities CH_4 emission intensity
- But Paris CH_4 represents mitigation options.

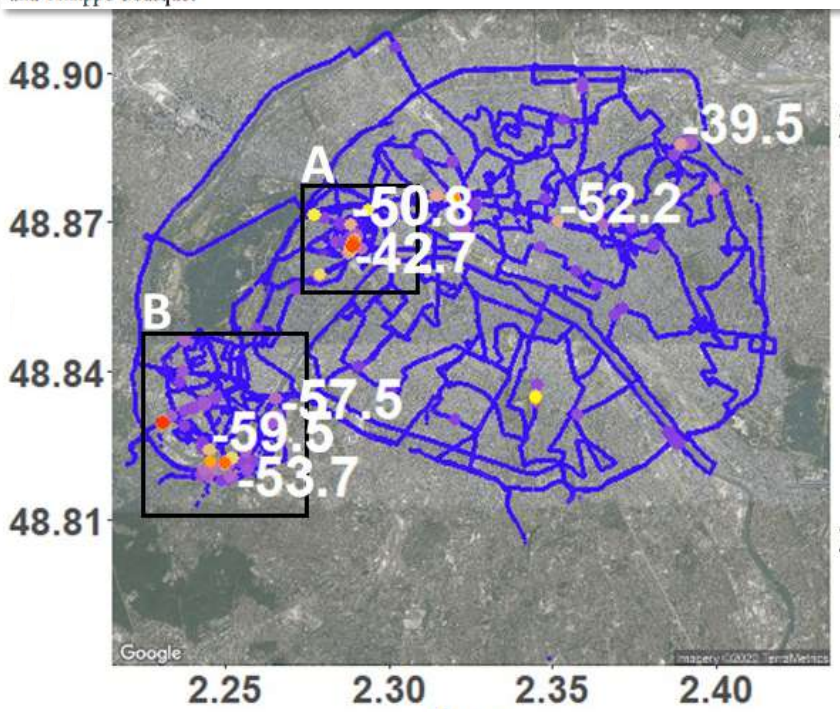

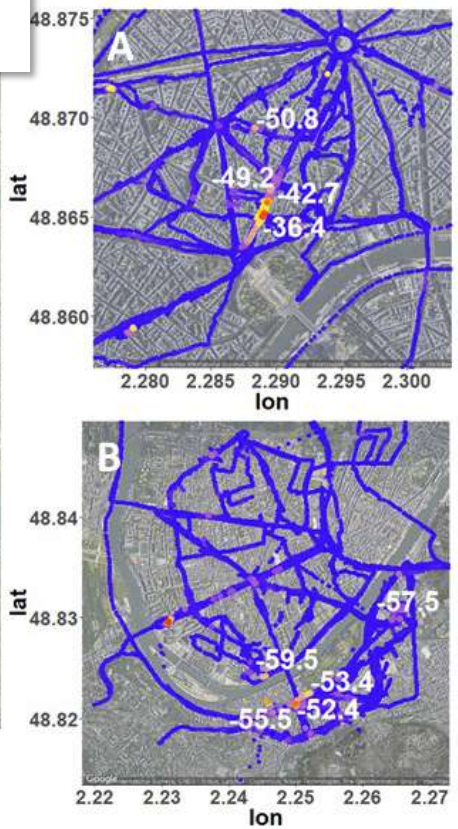

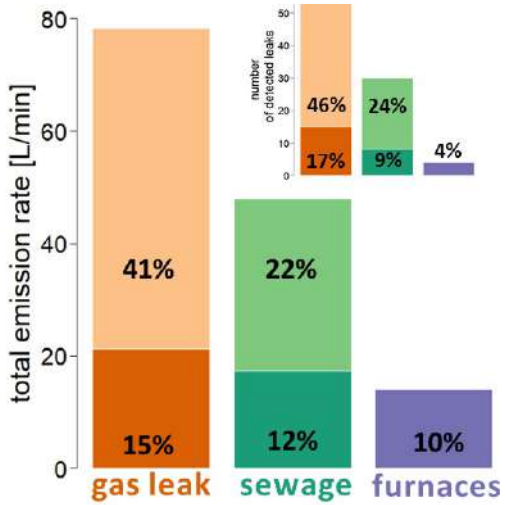

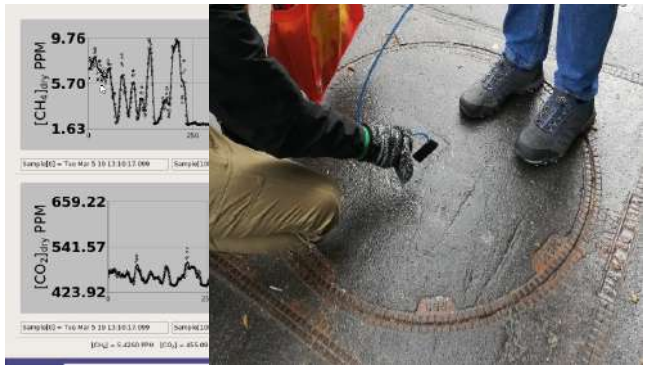

Defratyka et al., 2021

Mapped Ethane to Methane Ratios

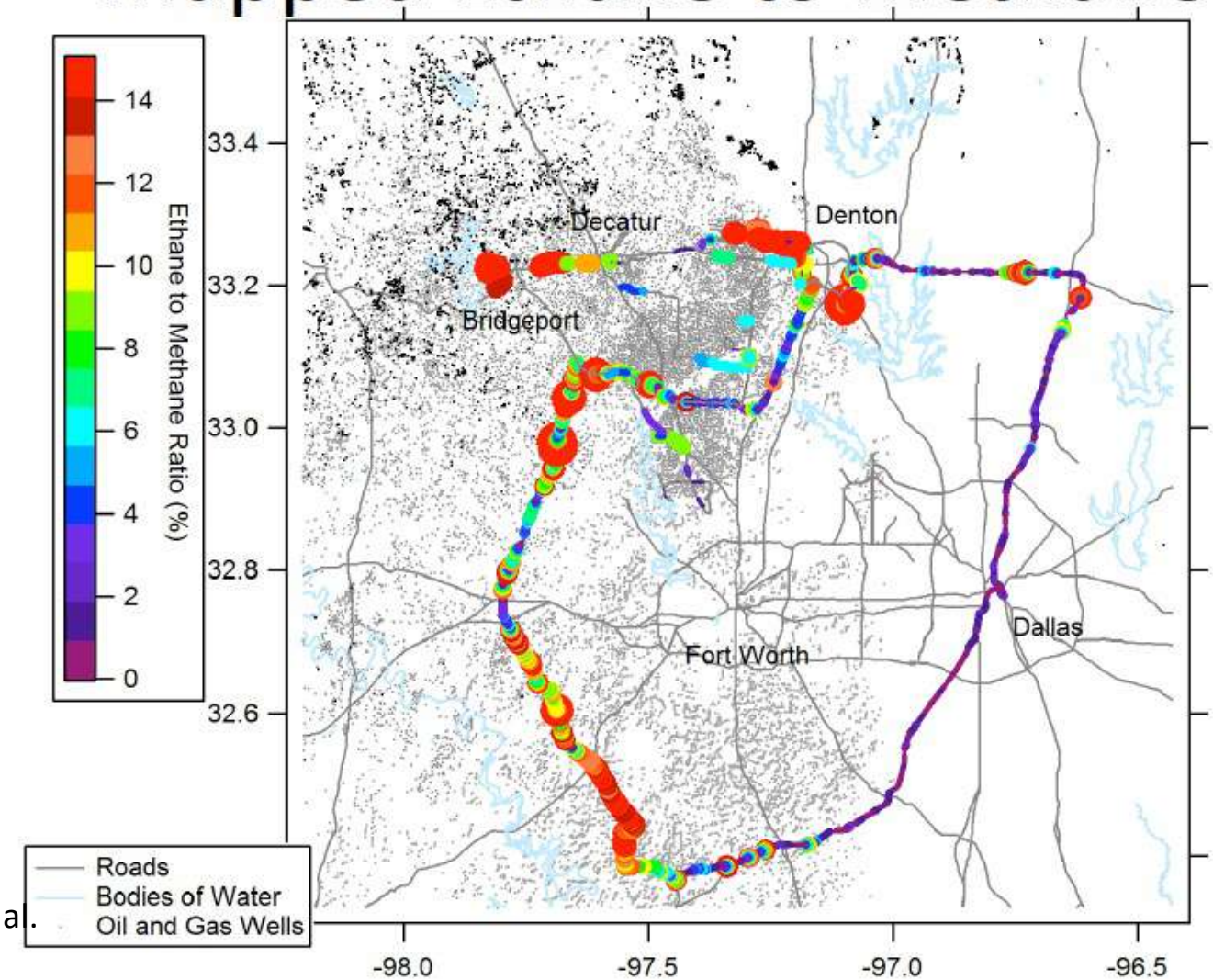

Ratio:
-composition of the gas
-exact emission vector (leak, tank…)

Yacovitch et al.

Ethane to methane ratio

Biogenic Sources

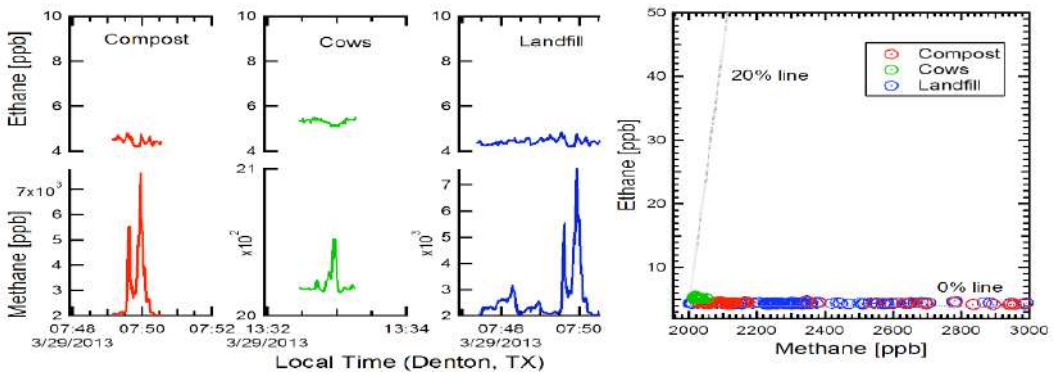

Yacovitch et al.

Oil and Gas Sources

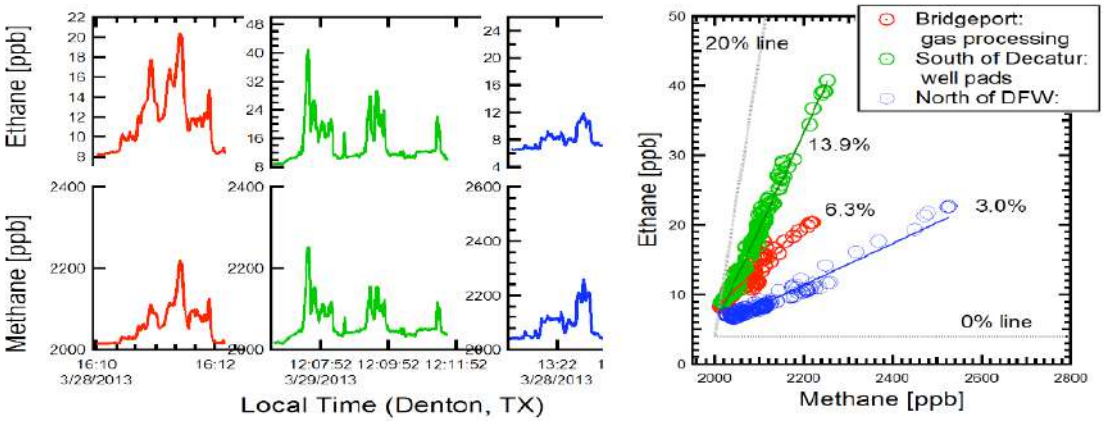

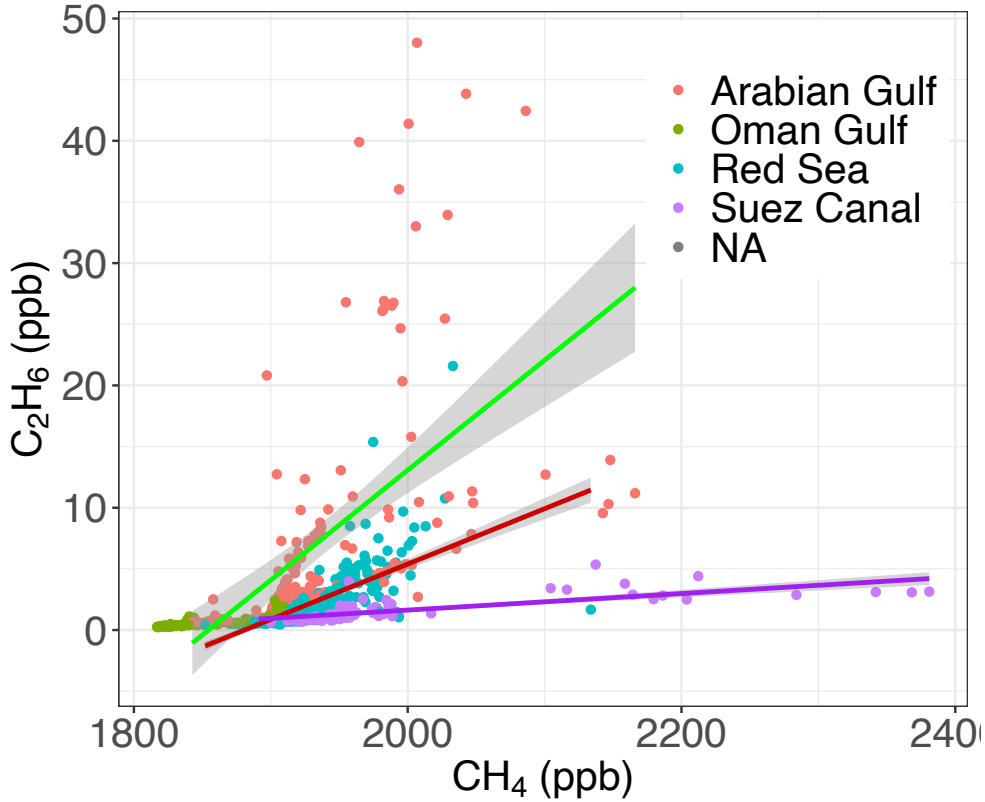

Paris et al. 2021

CH4 leak from the Nordstream pipelines

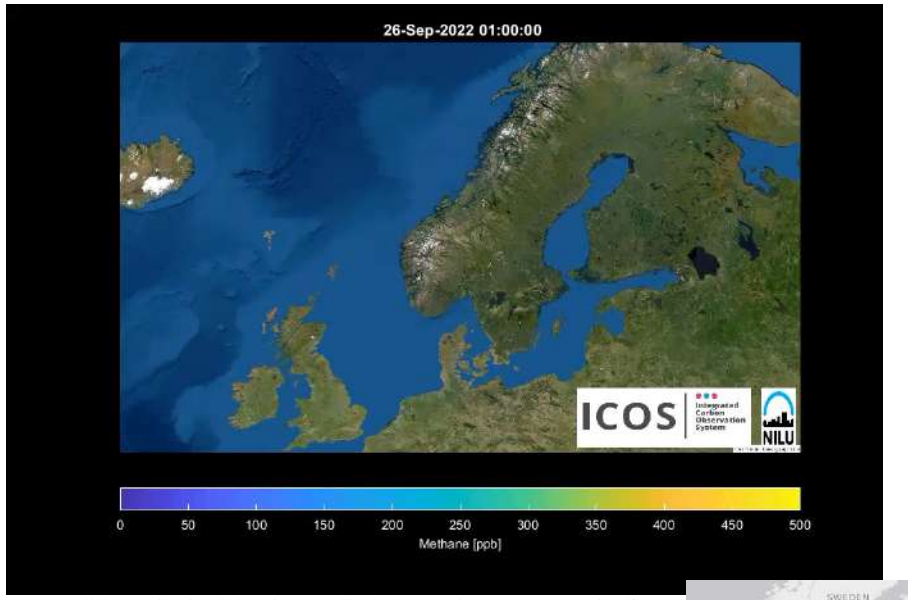

Water depth: 55m
NS2 had 300Mm3 pressurized gas
Pressure drop in pipe from 105 to 7 bars
Ebullition diameter: up to 100m

Initial assessment (without atmospheric measurements):
300-500ktCH4

Atmospheric data compatible with release of
55-155 kt CH4

Largest single leak ever recorded

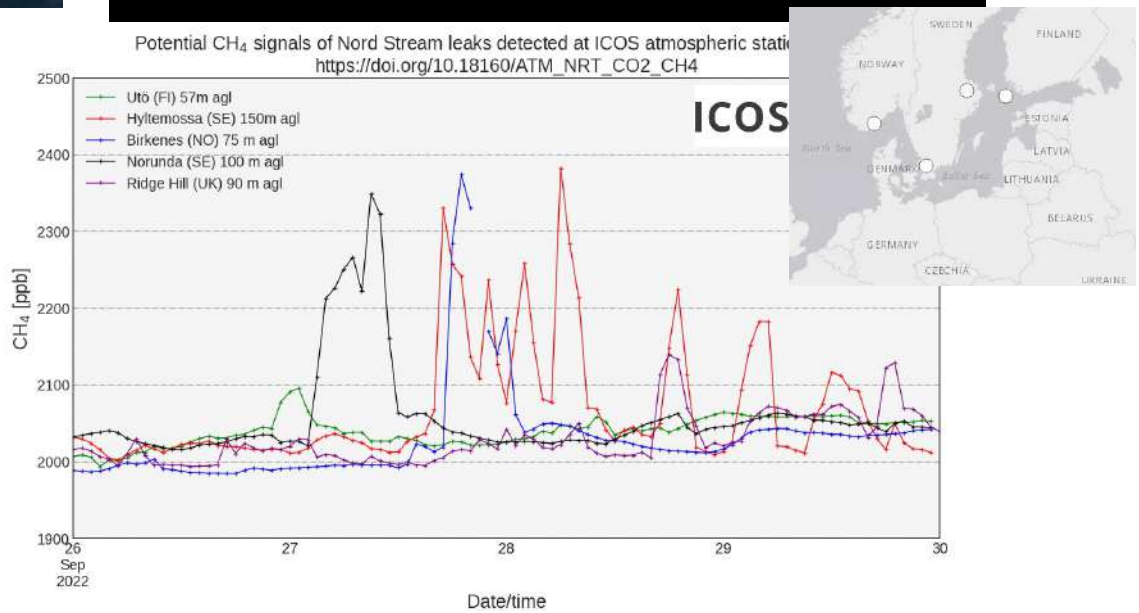

Large uncertainties on (natural) marine methane fluxes

Marine seepages emit **~65 Tg of CH_4/ yr** in the water column

Marine sources release ~6 to 12 Tg of CH_4/ yr (in a total source of 600 Tg CH4/yr, see e.g. Saunois et al., 2020)

Do we have sufficiently reliable measurements to ensure confidence in global estimates? How robust are basin-scale estimates?

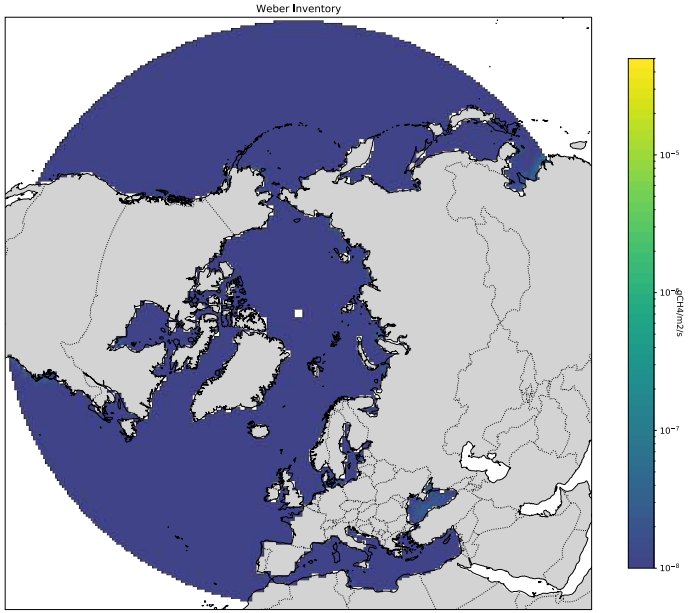

Lambert & Schmidt 1993
Diffusive fluxes
3.5 Tg CH4 yr^{-1}

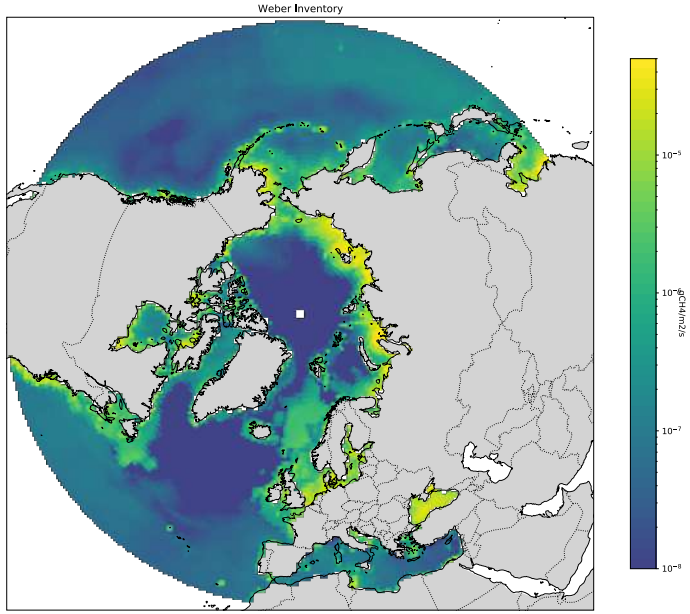

Weber et al., 2019
Diffusive+bubbles fluxes
6-12 Tg CH4 yr^{-1}

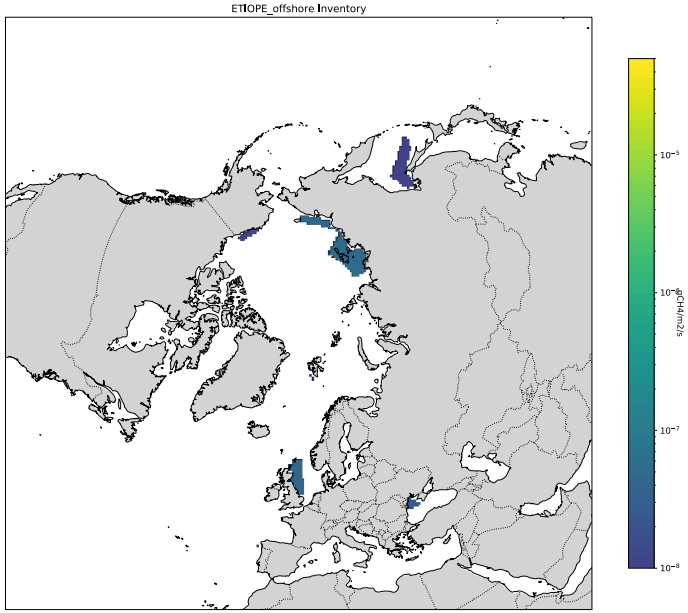

Etiope et al., 2019
Geological fluxes
3.9-9 Tg CH4 yr^{-1}

Marine methane emissions: main drivers

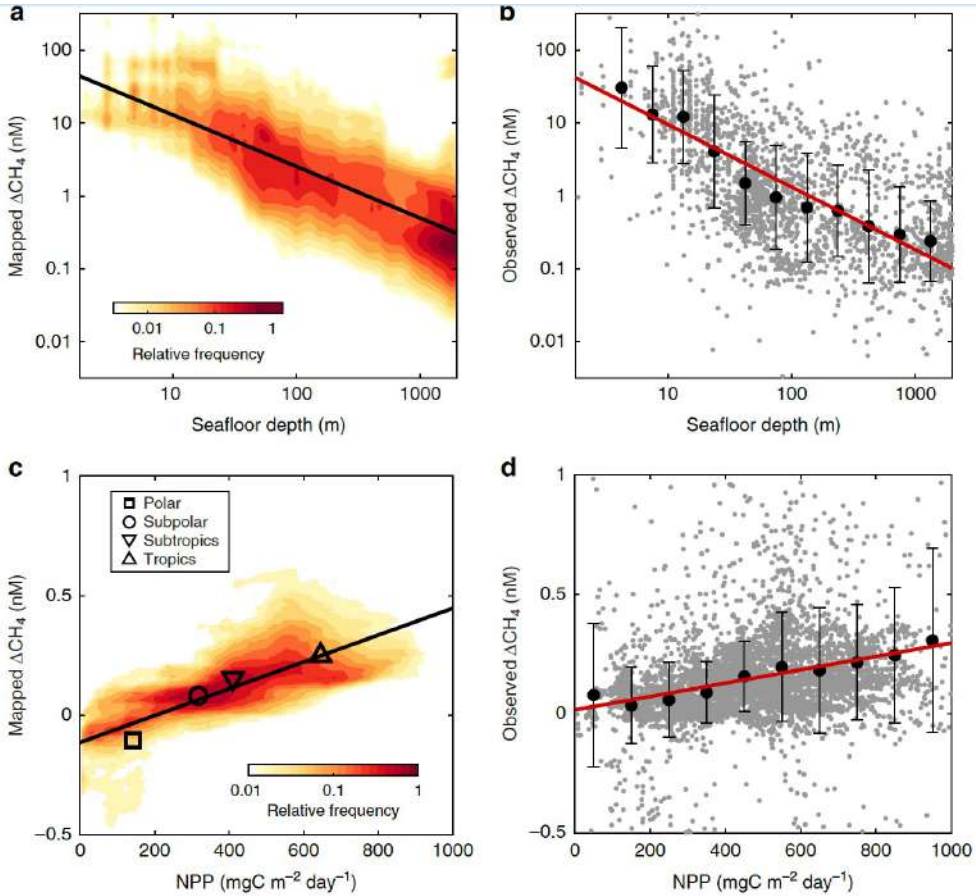

Fig. 6 Controls on surface ocean ΔCH_4. **a** Joint probability distribution for mapped ΔCH_4 and seafloor depth (z_{sf}) in coastal ocean regions (<2000 m depth). Color scale represents the frequency of gridcells with a given combination of $\log_{10}$(depth) and $\log_{10}(\Delta CH_4)$, after averaging together all 200,000 machine-learning maps. Black line is the best fit for the mapped data ($\Delta CH_4 = 67 z_{sf}^{-0.7}$, $R^2 = 0.55$). **b** Scatter plot of observed ΔCH_4 versus depth. Gray points show raw data; black circles with errorbars show mean ± s.d. ΔCH_4 within depth bins. Red line is best fit to the binned data ($CH_4 = 69 z_{sf}^{-0.8}$, $R^2 = 0.94$). **c**, **d** Same as **a** and **b**, but for the relationship of mapped **c** and observed **d** ΔCH_4 to net primary production (NPP) in open ocean (>2000 m depth) environments. In **c**, black line is the best fit for mapped data ($\Delta CH_4 = (0.5\text{NPP} - 62)/10^3$, $R^2 = 0.30$), and symbols represent large-scale averages (Supplementary Fig. S8). In **d**, black circles show mean ± s.d. ΔCH_4 within NPP bins, and red line is best fit to the binned data ($\Delta CH_4 = (0.3\text{NPP} + 14)/10^3$, $R^2 = 0.91$)

Weber et al., 2019

Revising East Siberian Arctic Shelf (ESAS) fluxes

- Subsea permafrost and hydrates in the ESAS constitute a large C pool, and a potentially large source of CH4 to the atmosphere. Previous studies based on oceanographic campaigns estimated ESAS emissions at 8–17 TgCH4 yr−1.
- Statistical analysis of high-resolution simulations of atmospheric CH4 and continuous observations during 2012. indicates annual CH4 emissions from ESAS range from 0.0 to 4.5 TgCH4 yr−1.

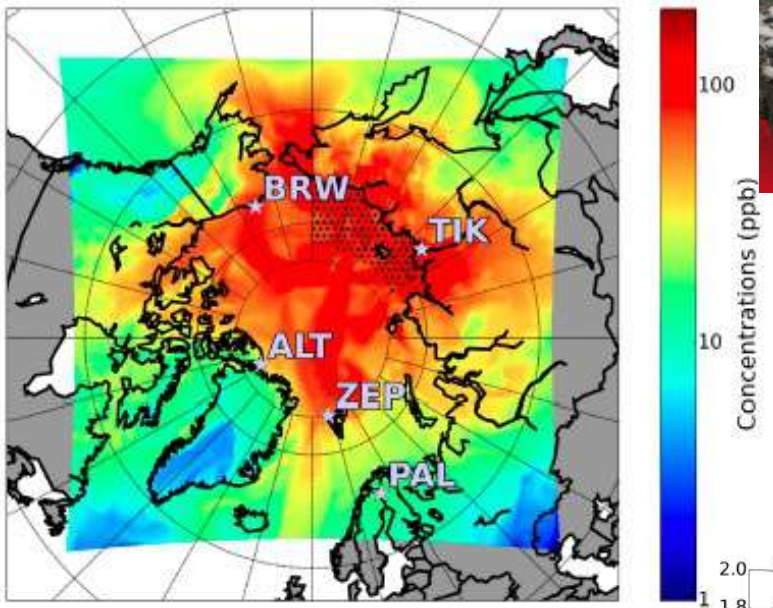

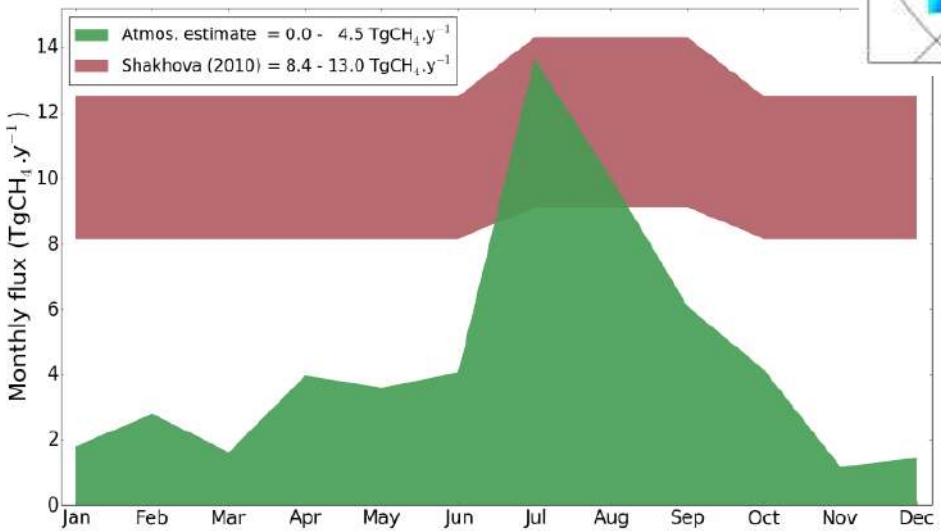

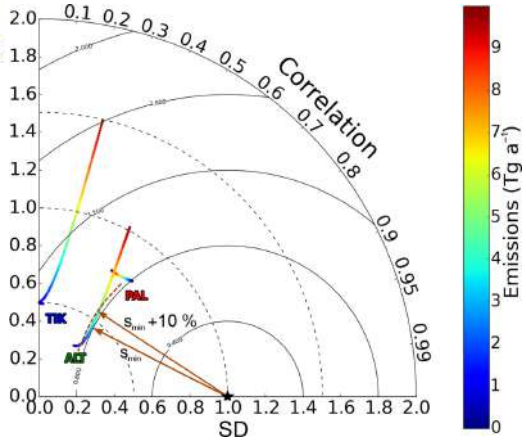

Berchet et al., ACP 2016